Josip Juraj Strossmayer University of Osijek

University of Dubrovnik

Ruđer Bošković Institute, Zagreb

Postgraduate Interdisciplinary University Study Program in Molecular Biosciences

Mateja Ćosić

ROLE OF OVERLAP MICROTUBULE BUNDLES IN CHROMOSOME PASSENGER COMPLEX LOCALIZATION AND CORRECTION OF CHROMOSOME SEGREGATION ERROR

Doctoral dissertation

Osijek, 2025.

This doctoral dissertation was done in the Laboratory of Cell Biophysics, Department of Molecular Biology, at the Ruđer Bošković Institute, under the supervision of dr. sc. Iva Marija Tolić. This work was founded by Croatian Science Foundation (PZS-2019-02-7653, Mechanisms of microtubule bundle formation required for spindle maturation) and European Research Council (ERC Synergy Grant Molecular origins of aneuploidies in healthy and diseased human tissues).

TEMELJNA DOKUMENTACIJSKA KARTICA

Sveučilište Josipa Jurja Strossmayera u Osijeku **Doktorski rad**
Sveučilište u Dubrovniku
Institut Ruđer Bošković

Doktorski studij Molekularne bioznanosti

Znanstveno područje: Interdisciplinarno područje znanosti
Znanstvena polja: Biologija i Temeljne medicinske znanosti

ULOGA PREKLAPAJUĆIH SNOPOVA MIKROTUBULA U LOKALIZACIJI KROMOSOMSKOG PUTNIČKOG KOMPLEKSA I ISPRAVLJANJU POGREŠAKA U PODIJELI KROMOSOMA

Mateja Ćosić

Doktorski rad je izrađen u: Laboratorij za biofiziku stanice, Zavod za molekularnu biologiju, Institut Ruđer Bošković, Zagreb

Mentor: dr. sc. Iva M. Tolić, voditeljica laboratorija i znanstvena savjetnica u trajnom zvanju

Kratki sažetak doktorskog rada:
Diobeno vreteno, čija formacija ovisi o preklapajućim snopovima mikrotubula, osigurava pravilnu raspodjelu kromosoma. U ovom istraživanju pokazali smo da Aurora B i Borealin lokaliziraju uz preklapajuće snopove u ranoj mitozi te da utišavanje PRC1 smanjuje njihovu kolokalizaciju. To dovodi do smanjenog nakupljanja CPC-a na centromernom području, slabije fosforilacije kinetohora i češćih pogrešaka u segregaciji kromosoma. Rezultati ukazuju na ključnu ulogu preklapajućih snopova u regulaciji CPC-a i očuvanju genomske stabilnosti.

Broj stranica: 77 stranica
Broj slika: 29 slika
Broj tablica: 0 tablica
Broj literaturnih navoda: 200 literaturnih navoda
Jezik izvornika: engleski jezik
Ključne riječi: preklapajući snopovi, Aurora B, Borealin, fosforilacija kinetohora, pogrešna vezanja mikrotubula

Datum javne obrane:

Povjerenstvo za javnu obranu:
1. dr. sc. Ana Čipak Gašparović, voditeljica laboratorija i znanstvena savjetnica (predsjednica komisije)
2. dr. sc. Andreja Ambriović Ristov, voditeljica laboratorija i znanstvena savjetnica u trajnom zvanju (članica komisije)
3. doc. dr. sc. Ivana Škrlec, docentica (članica komisije)
4. doc. dr. sc. Lidija Milković, viša znanstvena suradnica (zamjenska članica)

Doktorski rad je pohranjen u: Nacionalnoj i sveučilišnoj knjižnici Zagreb, Ul. Hrvatske bratske zajednice 4, Zagreb; Gradskoj i sveučilišnoj knjižnici Osijek, Europska avenija 24, Osijek; Sveučilištu Josipa Jurja Strossmayera u Osijeku, Trg sv. Trojstva 3, Osijek

BASIC DOCUMENTATION CARD

Josip Juraj Strossmayer University of Osijek **PhD thesis**
University of Dubrovnik
Ruđer Bošković Institute

Doctoral Study of Molecular Biosciences

Scientific Area: Interdisciplinary area of science
Scientific Fields: Biology and Basic medical sciences

ROLE OF OVERLAP MICROTUBULE BUNDLES IN CHROMOSOME PASSENGER COMPLEX LOCALIZATION AND CORRECTION OF CHROMOSOME SEGREGATION ERROR

Mateja Ćosić

Thesis performed at: Laboratory of Cell Biophysics, Department of Molecular Biology, Ruđer Bošković Institute, Zagreb

Supervisor: dr. sc. Iva M. Tolić, Head of Laboratory

Short abstract:
The mitotic spindle, whose formation depends on overlap microtubule bundles, ensures accurate chromosome segregation. In this study, we showed that Aurora B and Borealin localize to overlap bundles in early mitosis, and that PRC1 silencing reduces their colocalization. This leads to decreased CPC accumulation at centromeres, reduced kinetochore phosphorylation, and more frequent chromosome segregation errors. Our results highlight the key role of overlap bundles in CPC regulation and genome stability.

Number of pages: 77 pages
Number of figures: 29 figures
Number of tables: 0 tables
Number of references: 200 references
Original in: English language
Key words: overlap bundles, Aurora B, Borealin, kinetochore phosphorylation, erroneous microtubule attachments

Date of the thesis defense:

Reviewers:
1. dr. sc. Ana Čipak Gašparović, Head of Laboratory (president of the committee)
2. dr. sc. Andreja Ambriović Ristov, Head of Laboratory (committee member)
3. doc. dr. sc. Ivana Škrlec, Assistant professor (committee member)
4. doc. dr. sc. Lidija Milković, Senior research associate (substitute member)

Thesis deposited in: National and University Library in Zagreb, Ul. Hrvatske bratske zajednice 4, Zagreb; City and University Library of Osijek, Europska avenija 24, Osijek; Josip Juraj Strossmayer University of Osijek, Trg sv. Trojstva 3, Osijek

TABLE OF CONTENTS

1. INTRODUCTION

1.1 Cell cycle

The eukaryotic cell cycle is a crucial process that ensures the accurate duplication and distribution of genetic material into two daughter cells, sustaining life in all eukaryotic organisms. This cycle is organized into two main phases: interphase and the M phase (Figure 1.). Interphase is the longer phase and is subdivided into three phases: G1, S and G2. The M phase, on the other hand, consists of nuclear division (mitosis) and cytoplasmic division (cytokinesis). During the interphase, several key events prepare the cell for division. The G1 phase, lasting about 15 hours in human cells, is marked by cell growth and the production of proteins and RNAs required for DNA replication. The G1 checkpoint ensures that the cell is ready to proceed to the next phase. Once the cell passes this checkpoint, it irreversibly commits to division. The next stage is the S phase, which lasts approximately 6 hours, where DNA is replicated, resulting in two identical sister chromatids for each chromosome. The final stage of the interphase, the G2 phase, lasts about 2 hours and involves further cell growth and protein synthesis. During this time, the G2 checkpoint verifies that DNA replication is complete and correct, preventing the cell from entering mitosis if errors are detected. The M phase follows G2 and lasts around 1 hour. Mitosis, the first part of the M phase, ensures that each daughter cell receives an identical set of chromosomes, matching the parental cell. This is followed by cytokinesis, where the cytoplasm is divided, completing the formation of two distinct daughter cells (1).

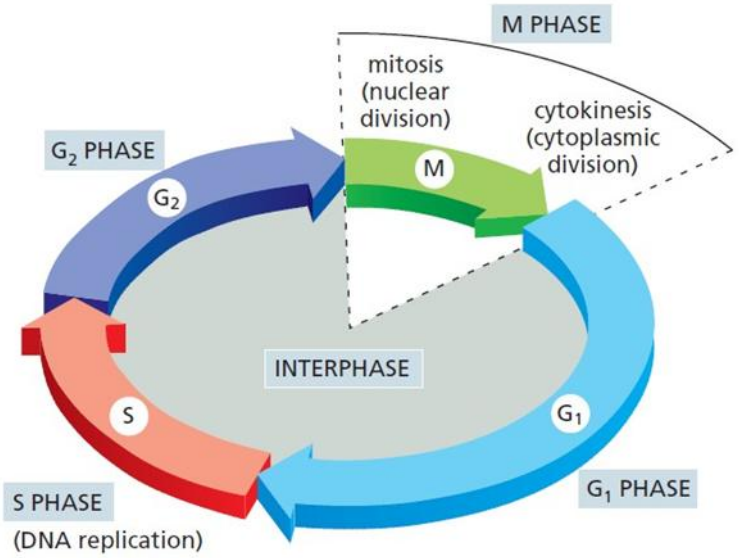

Figure 1. Visual depiction of the eukaryotic cell cycle. The cell cycle is composed of an interphase and the M phase. During interphase, the S phase involves DNA replication, which is then followed by the G2 phase, characterized by protein synthesis and cell growth. The onset of mitosis is indicated by the breakdown of the nuclear envelope (NEBD), leading into mitosis and concluding with cytokinesis. After the M phase, the cycle proceeds with the G1 phase, where protein synthesis occurs. Taken from Alberts et al., 2022

Mitosis must be highly precise; any errors can lead to aneuploidy. Aneuploidy is a condition where cells have an abnormal number of chromosomes, often associated with cancers, miscarriages, and genetic disorders like Down syndrome (2–4). To maintain accuracy, cells use several regulatory mechanisms known as checkpoints, which monitor and control the progression of the cell cycle (Figure 2.). These include the G1 checkpoint, which prevents the transition to the S phase under unfavorable conditions, the S phase checkpoint, which ensures DNA is correctly replicated, and the G2 checkpoint, which stops the cell from entering mitosis if DNA damage is detected (5). Additionally, during mitosis, the spindle assembly checkpoint (SAC) ensures proper attachment of chromosomes to the spindle, halting cell cycle progression if errors are present (6).

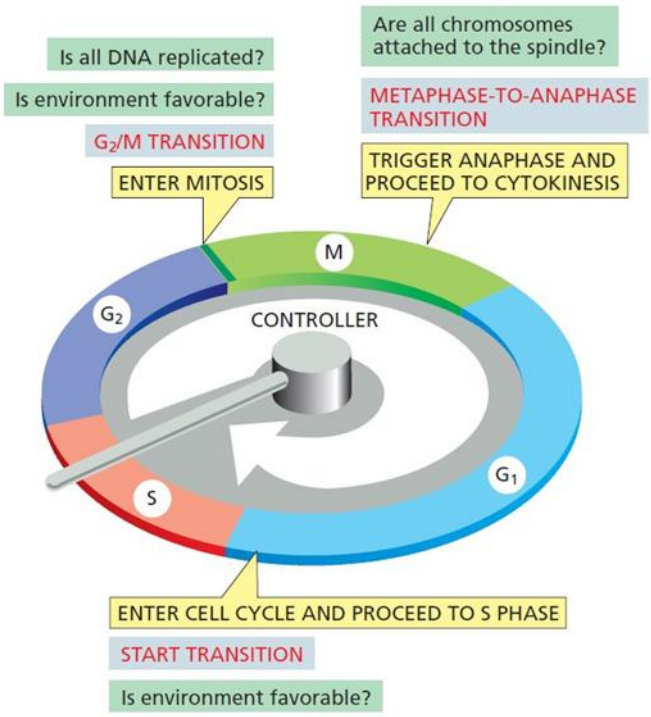

Figure 2. The cell cycle control system initiates essential processes such as DNA replication, mitosis, and cytokinesis. In this illustration, the control system is represented as a central rotating arm called the controller, which moves in a clockwise direction and activates key processes when it aligns with specific transition points on the surrounding dial, indicated by yellow boxes. Feedback on the successful completion of cell cycle events, as well as

environmental signals, can cause the control system to pause progression at these checkpoints. Taken from Alberts et al., 2022

The regulation of these checkpoints is primarily controlled by cyclin-dependent kinases (CDKs) and their regulatory partners, cyclins. Cyclin-dependent kinase (CDK) levels remain relatively stable throughout the cell cycle, but cyclin levels fluctuate between phases, thereby controlling CDK activity. These cyclin-CDK complexes play a crucial role in regulating key checkpoints, such as the transitions from the G1 to S phase and from the G2 to M phase. This regulation is primarily achieved through the phosphorylation of specific proteins at designated regulatory sites, which can either activate or inhibit proteins within complex signaling networks. Notably, CDKs themselves are also regulated through phosphorylation(5). Additionally, the cell cycle is further controlled by the regulated degradation of proteins within proteasomes. This degradation is irreversible, ensuring that the cell cycle progresses in a unidirectional manner from the G1 phase to the M phase. Different types of CDKs are produced by cells, each initiating specific events in particular phases of the cycle (such as G1 CDKs, G1/S CDKs, S phase CDKs, and mitotic CDKs). Importantly, CDKs that drive a particular phase are only active during that specific phase (7).

1.2 M phase

To ensure proper distribution of the genetic material duplicated during the S phase, the cell undergoes substantial structural and molecular rearrangements during the M phase. This phase involves two tightly coordinated processes. First, genetic material is equally divided through mitosis, also known as nuclear division. Second, the cytoplasm and cellular organelles are distributed between two daughter cells in a process called cytokinesis, or cytoplasmic division. The M phase is a continuous process, and there is no distinct microscopic boundary between the end of mitosis and the beginning of cytokinesis (7).

1.2.1 Mitosis

Although mitosis is a continuous process, it is commonly divided into five stages for descriptive clarity: prophase, prometaphase, metaphase, anaphase, and telophase (7) (Figure 3.).

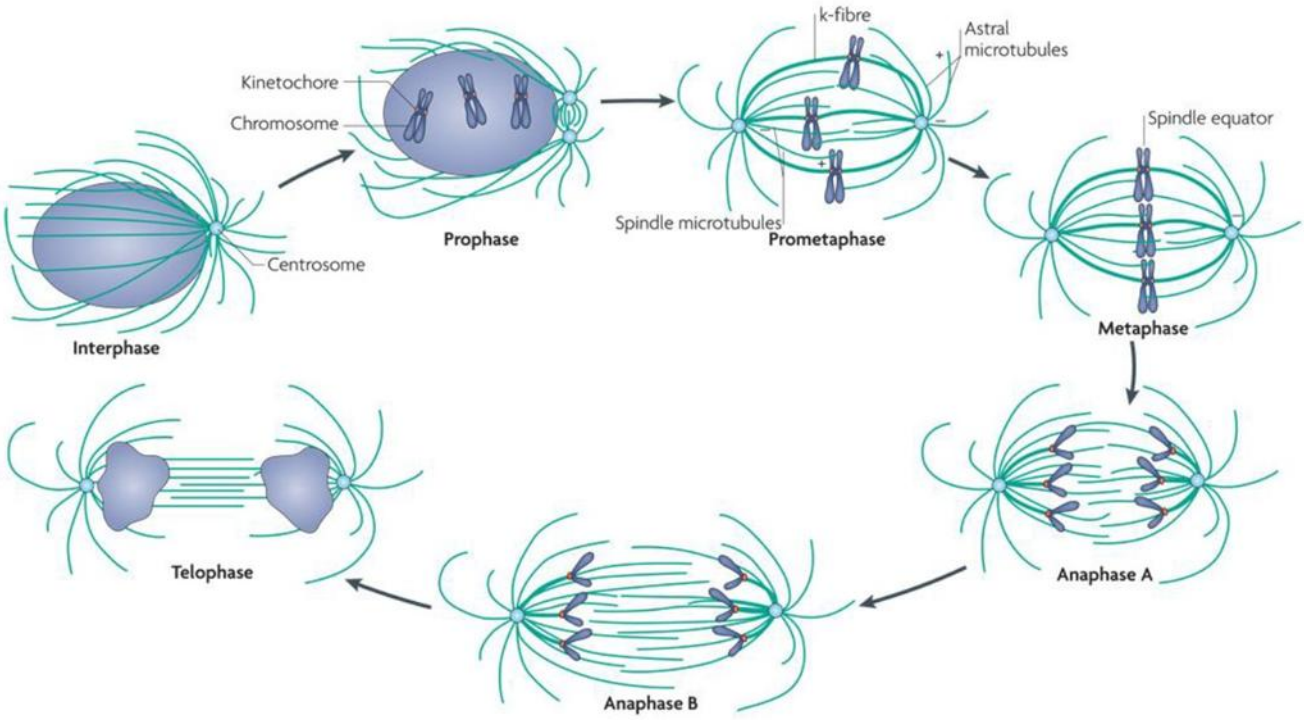

Figure 3. Stages of Mitosis. The process of mitosis is organized into five distinct phases: prophase, prometaphase, metaphase, anaphase, and telophase, which is then followed by the division of the cytoplasm known as cytokinesis. Taken from Walczak et al., 2010

Prophase marks the beginning of mitosis and is characterized by the progressive condensation of chromatin into distinct chromosomes. Each chromosome consists of two identical sister chromatids joined at the centromere, where specialized protein structures called kinetochores begin to assemble to mediate microtubule attachment (8). As condensation advances, the nucleolus disperses while the nuclear envelope remains intact (9). Meanwhile, duplicated microtubule-organizing centers (MTOCs), or centrosomes in animal cells, begin nucleating microtubules to form radial arrays known as mitotic asters (10,11). These centrosomes gradually move apart, driven by motor proteins such as kinesin-5 (Eg5), and establish the two poles of the future mitotic spindle, a process referred to as the prophase pathway of centrosome separation (12). At the same time, condensin complexes mediate chromosome compaction, reducing the length of the DNA more than a thousand-fold (13).

Prometaphase begins with the disassembly of the nuclear envelope, a process known as nuclear envelope breakdown (NEBD), which allows spindle microtubules to interact with chromosomes (14). Microtubules search for and attach to kinetochores in a dynamic process that enables chromosome capture. Once sister chromatids are attached to opposite spindle poles, they become bi-oriented and begin moving toward the cell's equator in a process known as chromosome congression (15). In some cells, centrosome separation may also occur at this stage, a variation known as the prometaphase pathway (12). At the same time, endocytic and exocytic trafficking is paused, and cortical actin reorganizes to facilitate mitotic cell rounding (13). During metaphase, all chromosomes align at the metaphase plate, situated at the central

axis of the spindle. The tension generated by microtubules pulling on kinetochores indicates that proper bipolar attachment has been achieved (16). The spindle assembly checkpoint (SAC) monitors these attachments and delays anaphase onset until all chromosomes are correctly aligned and under tension. Despite the inherent microtubule dynamics, metaphase represents a biophysical steady state in which the overall structure and positioning of the spindle remain constant over time (17).

Once all SAC requirements are fulfilled, the cell proceeds into anaphase, which involves two overlapping processes. In anaphase A, separase cleaves the cohesin complexes that link sister chromatids, triggering their separation. The chromosomes are then drawn toward opposite spindle poles through microtubule depolymerization at both ends of the kinetochore fibers (18,19). During anaphase B, the spindle elongates as antiparallel microtubules slide apart, further increasing the distance between the separating chromosome sets (20,21).

Telophase marks the conclusion of mitosis. The separated chromatids arrive at the spindle poles, and the nuclear envelope begins to re-form around each set of chromosomes. Chromosomes gradually decondense, and the cell membrane starts to invaginate at the equator, giving rise to the cleavage furrow. The final step, cytokinesis, completes cell division. A contractile ring composed of actin and myosin filaments constricts the cytoplasm, ultimately severing the intercellular bridge between the two emerging daughter cells. This terminal event, known as cytokinetic abscission, marks the end of the M phase of the cell cycle (7,22).

1.3 Mitotic spindle

The mitotic spindle, a sophisticated micro-machine composed of microtubules and various associated proteins, assembles during each cell cycle. During mitosis, the primary role of the mitotic spindle is to ensure the equal distribution of chromosomes between two daughter cells (13). The mitotic spindle is composed of microtubules and numerous associated proteins. Its formation typically begins when microtubules nucleate from microtubule-organizing centers (MTOCs), or centrosomes in animal cells, which serve as spindle poles during cell division (23) (Figure 4.).

1.3.1 Centrosomes

The centrosome, essential for mitotic spindle assembly, duplicates once per cell cycle. In newly born cells, a pair of centrioles constitutes the centrosome. These centrioles, initially orthogonally engaged, disengage during the early G1 phase and become loosely connected by a fibrous attachment, allowing them to move apart as they progress through the G1 phase. The assembly of new centrioles, known as procentrioles, begins in the G1/S phase and continues through G2 until they reach full length. This process allows the centrosomes to separate and migrate to opposite sides of the cell, forming the spindle poles necessary for mitosis (24).

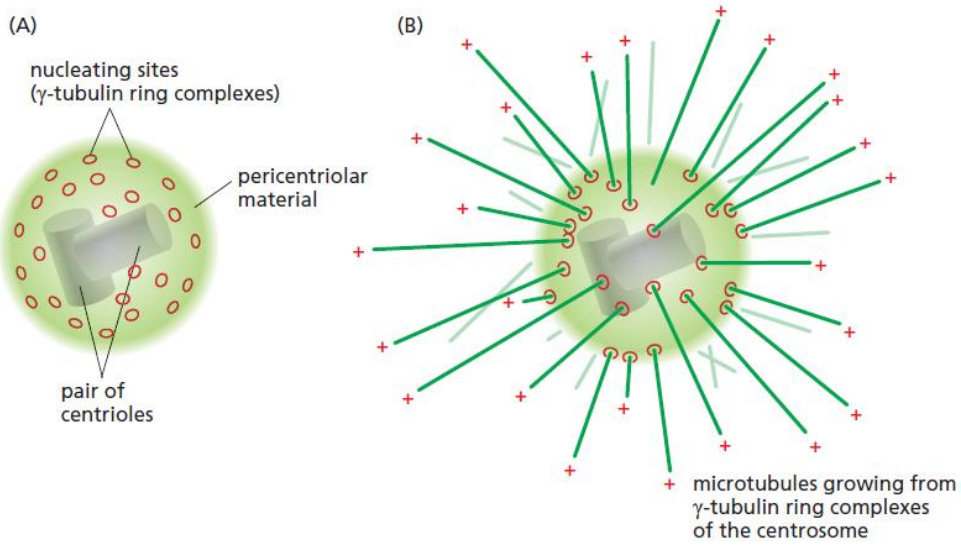

Figure 4. The Centrosome. (A) The centrosome is the main microtubule-organizing center (MTOC) in animal cells. It is located in the cytoplasm near the nucleus and is composed of a pair of centrioles surrounded by the pericentriolar material, a fibrous protein matrix that contains γ-tubulin ring complexes essential for microtubule nucleation. (B) A centrosome with associated microtubules. The minus ends of the microtubules are anchored in the centrosome, having originated from γ-tubulin ring complexes, while the plus ends extend outward into the cytoplasm. Taken from Alberts et al., 2022

1.3.2 Microtubules

Microtubules are the largest cytoskeletal filaments, with a diameter of approximately 25 nanometers. They are constructed from 13 protofilaments composed of αβ-tubulin heterodimers, arranged in a head-to-tail fashion that gives the microtubule its intrinsic polarity (1) (Figure 5.). This polarity results in distinct plus (+) and minus (-) ends, with the plus end exhibiting faster rates of growth and shrinkage due to structural asymmetry between the two ends (25). Microtubules display dynamic instability, a behavior marked by alternating phases of polymerization and depolymerization, driven by the hydrolysis of GTP bound to β-tubulin. As long as a GTP cap remains at the plus end, the microtubule is stabilized and continues to grow; however, loss of this cap triggers rapid disassembly, an event known as catastrophe (26). This dynamic behavior enables rapid remodeling of the microtubule network, which is particularly important during mitosis, where microtubules serve as the main structural and functional elements of the mitotic spindle (27).

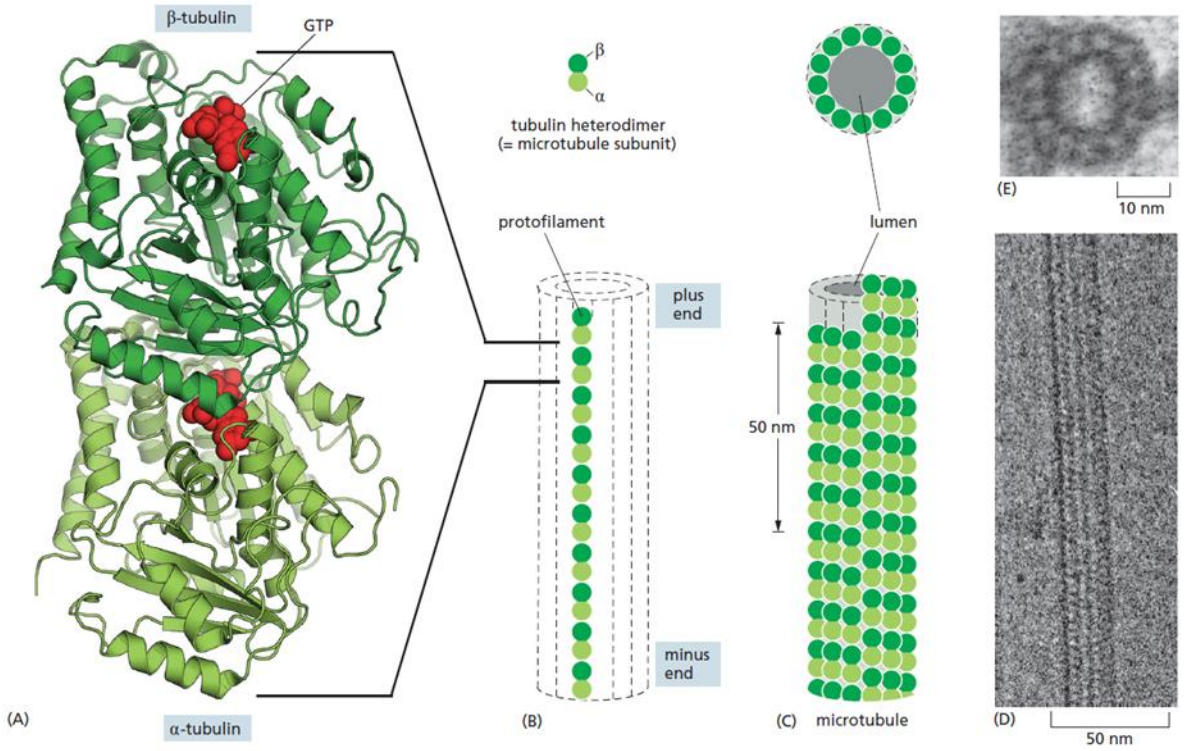

Figure 5. The structure of microtubules A) Tubulin heterodimer formed from tightly linked pair of α- and β- tubulin monomers. B) One tubulin subunit and one profilament. C) A single microtubule consists of 13 protofilaments aligned in parallel. D) Segment of a microtubule viewed in an electron microscope. E) Cross section of a microtubule viewed in an electron microscope. Taken from Alberts et al., 2022

The architecture of the mitotic spindle is composed of distinct classes of microtubule bundles, each with specialized roles in ensuring accurate chromosome segregation. The primary structural components include kinetochore fibers, overlap bundles, polar microtubules, and astral microtubules (28–30) (Figure 6.). Kinetochore fibers (k-fibers) are bundles of parallel microtubules that extend from the spindle poles and attach with their plus ends to the kinetochores, protein complexes located at the centromeric region of chromosomes (8,31). These fibers play a crucial role in exerting pulling forces on sister chromatids, aligning them at the metaphase plate and later segregating them during anaphase. Proper attachment and the tension generated at kinetochores also contribute to silencing of spindle assembly checkpoint (SAC), thus permitting progression into anaphase (32). Overlap microtubules originate from opposite spindle poles and interdigitate in the central region of the spindle to form antiparallel arrays (33,34). Many of these microtubules grow along the surface of k-fibers and connect sister kinetochore fibers, forming structures known as bridging fibers (35–37). These bridging fibers are essential for balancing tension between sister kinetochores and help maintain the characteristic curved shape of the metaphase spindle. They also generate forces that drive spindle elongation during anaphase B (38). Polar microtubules are non-kinetochore microtubules that grow from the spindle poles but do not reach the spindle midzone. Although they do not contribute directly to chromosome movement, they help organize the spindle architecture and stabilize the overall structure (39). Astral microtubules radiate from the

centrosomes toward the cell cortex, forming star-like structures that help position the spindle within the cell and contribute to cleavage furrow placement during cytokinesis (17,40). Altogether, these microtubule classes function in a coordinated manner to support the mechanical and spatial requirements of mitosis.

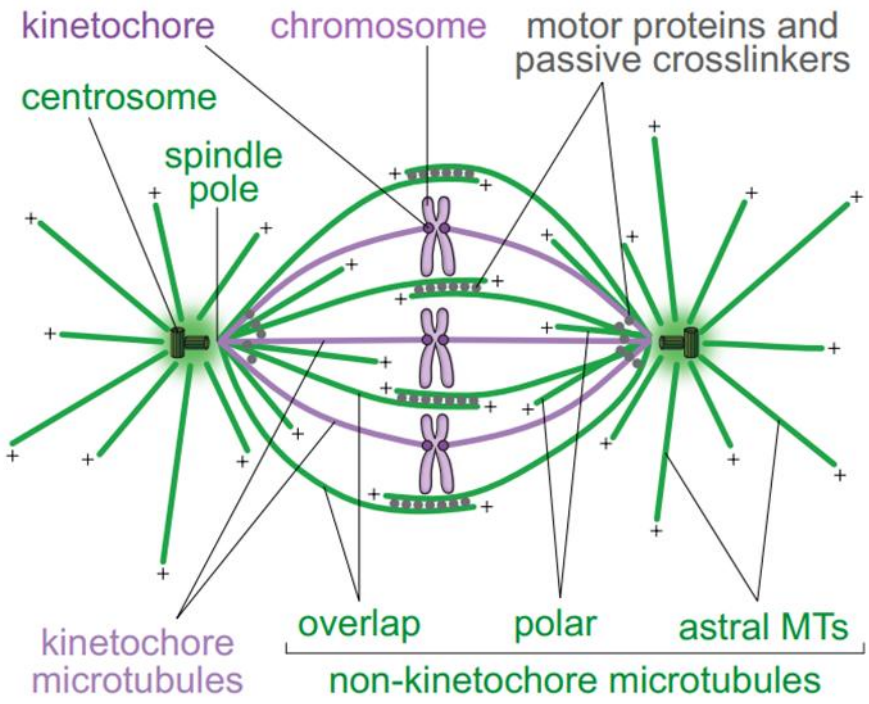

Figure 6. A simplified representation of the mitotic spindle. (Redrawn and modified from (Alberts et al., 2014). Taken from Tolic, 2018.

1.3.3 Overlaping microtubules

As mentioned above, overlap bundles, also referred to as interpolar bundles, are composed of antiparallel microtubules that originate from opposite sides of the spindle (28). While spindle assembly has been thoroughly investigated, particularly in the context of kinetochore behavior and the formation of kinetochore fibers (41–46), the process underlying the formation of overlap bundles remains largely unclear. These structures are crucial for proper spindle assembly. For example, inhibition of the motor protein Eg5/kinesin-5, which separates antiparallel microtubules, results in monopolar spindles (47–50). Although these spindles still contain kinetochore fibers, they lack overlap bundles and are therefore unable to segregate chromosomes, underscoring the essential role of overlap bundles in spindle function. In metaphase, a fully formed spindle contains overlap bundles that span between sister kinetochore fibers, effectively acting as bridging fibers (35). These bundles help to maintain balanced tension at kinetochores (15,35,51–53), support the alignment of chromosomes at the spindle equator (54,55), and contribute to spindle elongation and chromosome segregation during anaphase (21,38,56–58).

The microtubules within bridging fibers are crosslinked by PRC1 (protein regulator of cytokinesis 1) (35,53,59), which shows a strong preference for binding antiparallel

microtubules over parallel ones in vitro (60–63) (Figure 7). PRC1 is a conserved non-motor protein that plays a key role in cytokinesis and in organizing the central region of the mitotic spindle. It acts as a microtubule cross-linker, with its C-terminal domain responsible for microtubule binding, while the N-terminal domain enables dimerization. Positioned between these two ends, the rod domain, along with the N-terminus, mediates interactions with other proteins, such as kinesin-4 (62,64). The bundling activity of PRC1 is tightly controlled by Cdk-mediated phosphorylation: when phosphorylated, PRC1 can still attach to microtubules but loses its ability to cross-link them (65). Dephosphorylation restores this ability, allowing PRC1 to form stable antiparallel bundles (66). This interaction facilitates microtubule sliding and stabilization and promotes the recruitment of central spindle components, including kinesin-4 (KIF4), which is essential for targeting PRC1 to the spindle midzone (67,68). PRC1's ability to cross-link and bundle MTs in an antiparallel orientation is supported by filamentous projections at a fixed angle, enabling precise inter-microtubule linking (67,69,70).

In our study (Matković et al.), we demonstrated that kinetochores and microtubule crosslinkers orchestrate the transformation of the mitotic spindle from a disordered microtubule network into organized overlap bundles, a structural transition essential for accurate chromosome segregation during cell division. Using a combination of super-resolution microscopy, live-cell imaging, and theoretical modeling, we investigated how this transition is regulated, focusing on the roles of kinetochores, chromosomes, and microtubule-associated proteins in promoting the formation and spatial organization of overlap microtubule bundles that support proper spindle assembly and function during mitosis. Our findings reveal that, during early prometaphase, spindle microtubules initially form a dynamic, loosely connected network crosslinked by PRC1. As mitosis progresses, the disordered network is gradually reorganized into distinct, aligned overlap bundles (Figure 7.). This reorganization is driven by the redistribution and bundling activity of PRC1, as well as lateral interactions between kinetochores and microtubules, mediated by the kinesin motor CENP-E and regulated by Aurora B kinase (Figure 8.) (71).

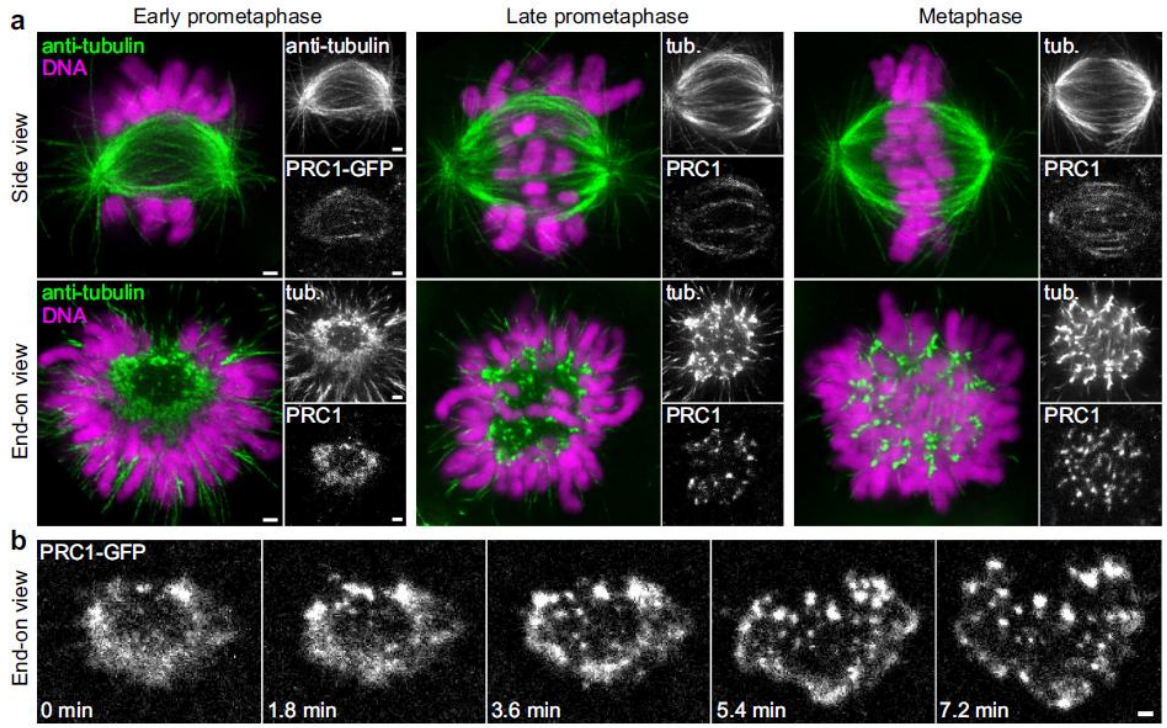

Figure 7. PRC1-crosslinked microtubules progressively reorganize from a loosely arranged network into distinct bundles during mitotic spindle assembly. a) Using STED super-resolution microscopy, we visualized spindles immunostained for α-tubulin in HeLa-Kyoto BAC cells expressing PRC1-GFP, with DNA labeled by DAPI (imaged with confocal resolution). Images captured in early prometaphase, late prometaphase, and metaphase revealed this structural transition. Both parallel and perpendicular spindle orientations relative to the imaging plane were analyzed. b) Additionally, time-lapse imaging of a single z-plane through a vertically oriented prometaphase spindle demonstrated the dynamic reorganization process, starting from the characteristic prometaphase rosette configuration, in cells expressing PRC1-GFP.

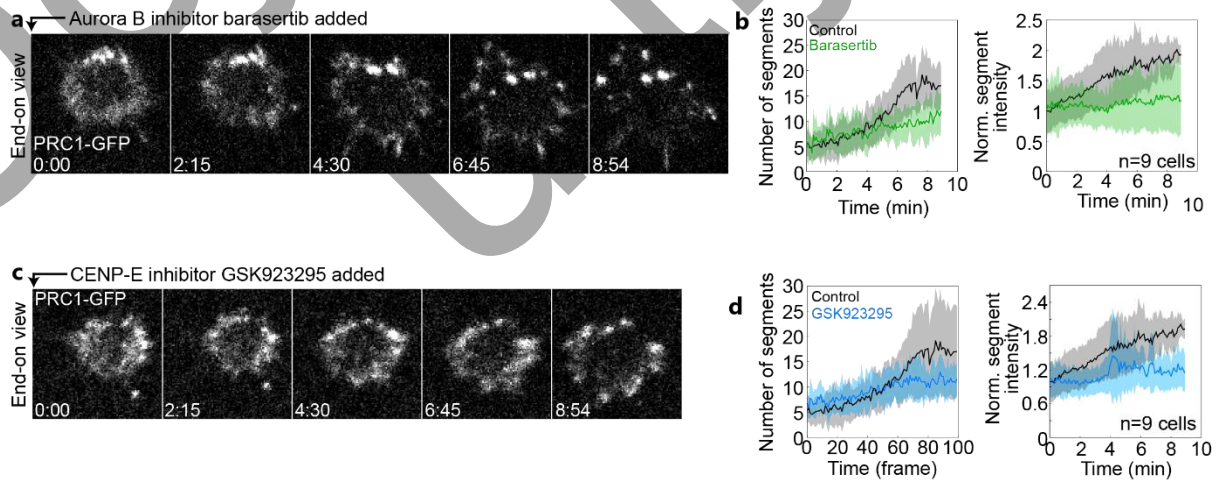

Figure 8. CENP-E promotes overlap bundle formation in an Aurora B-dependent manner. a) Midplane view of a vertically oriented prometaphase spindle in a HeLa-Kyoto cell expressing

PRC1-GFP (white), imaged after treatment with the Aurora B inhibitor Barasertib. b) Quantification of the number of PRC1-positive segments (left) and their normalized mean intensity (right), relative to time point t = 0, using Squassh-based segmentation in both control and Barasertib-treated cells. Shaded areas around the mean lines represent standard deviation; data were collected from 9 cells. c) Time-lapse imaging of the spindle midplane in a vertically oriented prometaphase HeLa-Kyoto cell expressing PRC1-GFP (white), following addition of the CENP-E inhibitor GSK-923295. d) Quantification of the number of PRC1 segments (left) and their normalized mean intensity over time (right), with values normalized to t = 0, in control and GSK-923295-treated cells. Data were obtained using Squassh segmentation. Shaded regions around the average curves indicate standard deviation; measurements represent 9 cells from 9 independent experiments. Inhibition of Aurora B or CENP-E impairs the formation of PRC1-labeled bundles. Specifically, treatment with Barasertib (Aurora B inhibitor) or GSK-923295 (CENP-E inhibitor) at the prometaphase rosette stage resulted in a markedly slower increase in both the number and fluorescence intensity of PRC1-labeled bundles over time, compared to untreated control cells. These findings indicate that both Aurora B kinase activity and CENP-E mediated kinetochore interactions are required for efficient and timely bundling of microtubules during early spindle assembly.

Moreover, we show that chromosomes themselves contribute to bundle architecture. As they congress to the spindle midzone, steric interactions between chromosome arms physically separate bundles, promoting the establishment of a robust bipolar spindle structure. Perturbation of chromosome alignment through the depletion of key components such as Ndc80, Kif18A, or CENP-E leads to a reduction in spindle width, further supporting the role of chromosome crowding in separating overlap bundles (Figure 9.) (71).

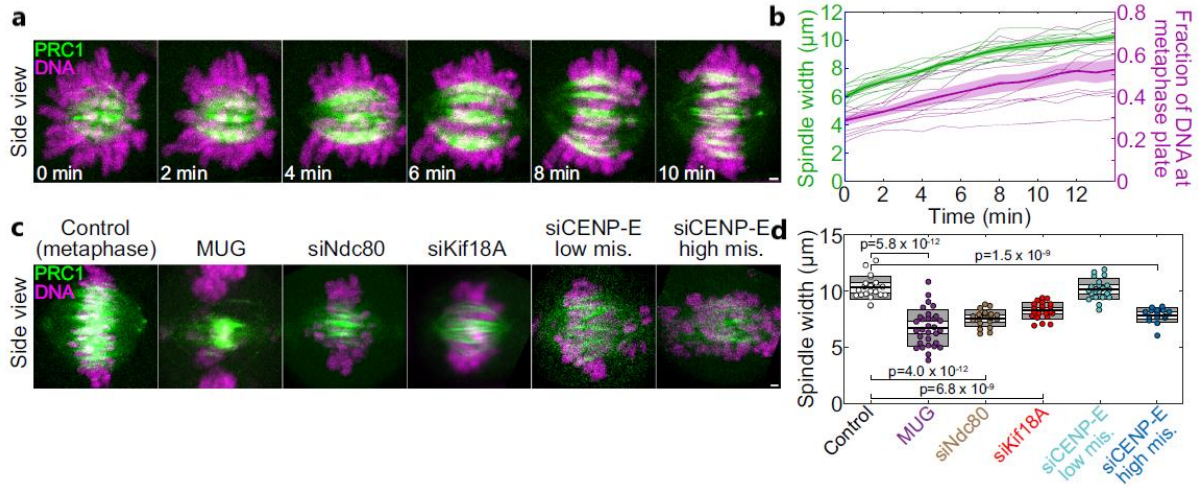

Figure 9. Chromosomes contribute to the separation of microtubule bundles and promote spindle widening. a) Time-lapse imaging (sum projection of 41 z-planes) of a horizontally oriented spindle in HeLa-Kyoto cells expressing PRC1-GFP (green) and labeled with SiR-DNA (magenta) captures spindle dynamics beginning in early prometaphase. b) Quantification of spindle width and the fraction of DNA localized at the metaphase plate over time shows a progressive increase in both parameters. Mean values are shown with shaded areas indicating standard deviation; data represents 10 cells from 10 independent experiments. c) Live-cell

imaging (maximum-intensity projections of 41 planes) was used to visualize metaphase spindles under various experimental conditions. Cells expressed PRC1-GFP (green) and SiR-DNA (magenta) to label DNA. d) Measurements of spindle width across treatments show statistically significant differences compared to control. Mean values are indicated by a black line, with light and dark gray areas representing the 95% confidence interval and standard deviation, respectively. Statistical significance was assessed using one-way ANOVA; each condition included data from 15 to 31 cells.

To mechanistically interpret our experimental findings, we collaborated with the Nenad Pavin group, who developed a one-dimensional theoretical model that integrates the interactions between microtubules, kinetochores, and crosslinking proteins. This model predicts that kinetochores function as sites that attract microtubules, PRC1 promotes local bundling within overlap regions, and steric repulsion between chromosome arms prevents the formation of a single thick central bundle. Instead, this interplay of forces favors the emergence of multiple spatially separated overlap bundles, contributing to proper spindle architecture (71) (Figure 10).

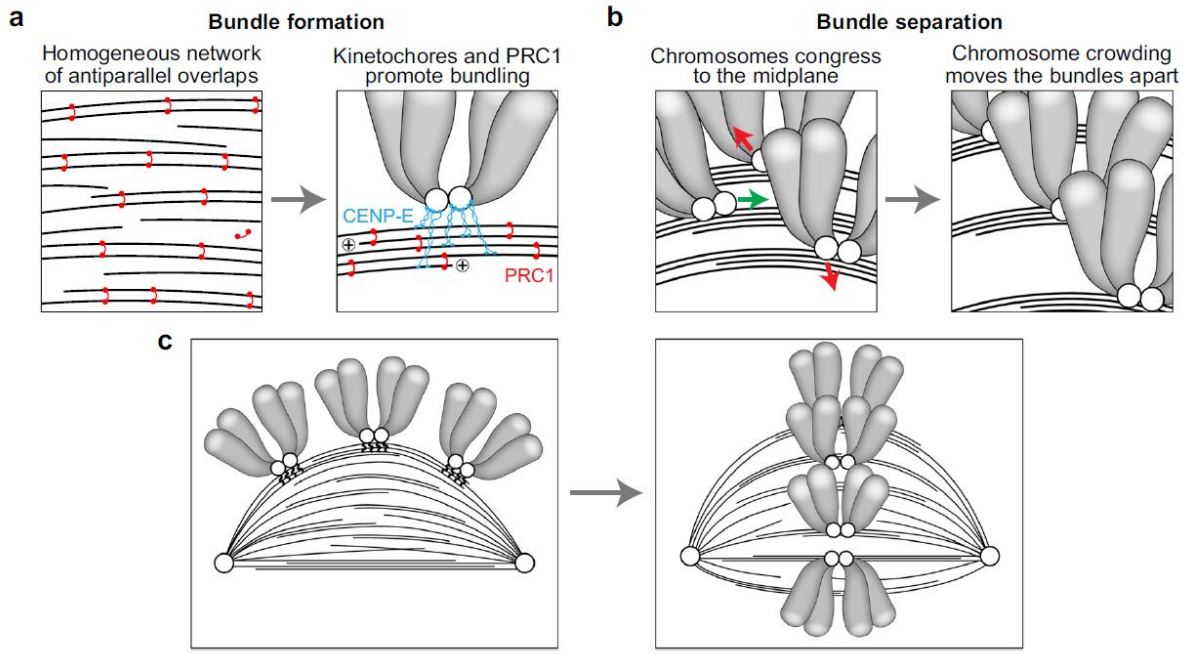

Figure 10. Model of kinetochore-driven formation and separation of overlap bundles. a) Initially, the spindle contains a loose network of microtubules with antiparallel overlaps that are uniformly crosslinked by PRC1 (shown in red). As spindle assembly progresses, lateral microtubule-binding activity of kinetochores, mediated by CENP-E (blue), promotes the formation of tightly packed bundles. b) During chromosome congression toward the spindle midzone (green arrow), steric interactions between chromosome arms contribute to the spatial separation of these bundles (red arrows). c) Together, these mechanisms drive the transition from the early prometaphase rosette configuration, characterized by a disorganized microtubule network and laterally attached chromosomes, to a more mature spindle structure in late prometaphase, in which microtubules are organized into distinct and separated bundles.

1.4 Chromosomes, Centromeres and Kinetochores

As the mitotic spindle assembles in a highly dynamic and spatially coordinated manner, chromosomes must be efficiently captured and incorporated into the spindle to ensure accurate segregation. This process is mediated by kinetochores, specialized multiprotein complexes that form on the centromeric regions of sister chromatids during late prophase. Each chromosome, composed of two sister chromatids, develops two kinetochores located on opposite sides of the centromere, which enable specific and robust interactions with spindle microtubules (Figure 11.) (72,73).

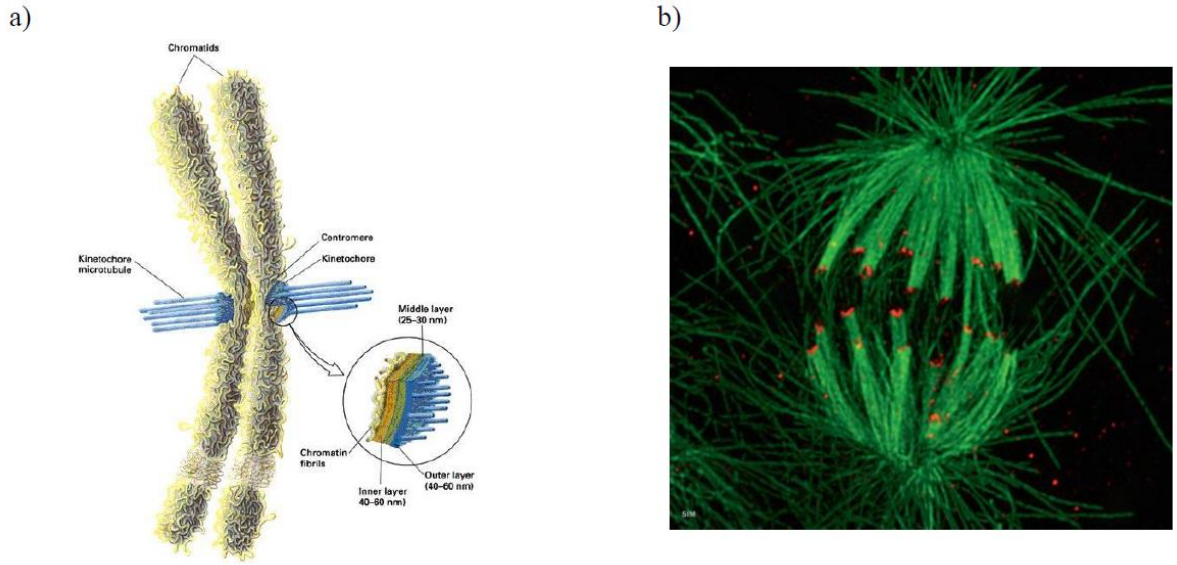

Figure 11. a) Illustration of a mitotic chromosome composed of two sister chromatids, each featuring a kinetochore located in the centromeric region. The kinetochore consists of three layers: the inner layer is anchored to chromatin fibrils, the outer layer is responsible for both microtubule nucleation and attachment, and the middle layer lies between them, serving as a structural interface. Taken from Lodish et al. 2000 b) Fluorescence image of a mitotic cell showing kinetochores in red and microtubules in green. The intense green signal represents kinetochore fibers (k-fibers), which are bundles of microtubules directly attached to kinetochores. Taken from https://www.sciencenews.org/article/view-cell

Structurally, the kinetochore consists of two principal regions: the inner kinetochore, which is tightly bound to centromeric chromatin and persists throughout the cell cycle, and the outer kinetochore, a dynamic domain that mediates microtubule attachment (Figure 11.). A key component of the inner kinetochore is the centromere-specific histone H3 variant CENP-A, which is essential for kinetochore identity and proper assembly (74,75). The outer kinetochore, on the other hand, contains numerous binding sites for microtubule plus ends, approximately 20 per kinetochore in vertebrate cells (76), and is also the site of active force generation during chromosome movement.

Upon the establishment of a bipolar microtubule array, the next major step in spindle formation is the capture of sister chromatids by spindle microtubules. In metaphase, the plus ends of kinetochore microtubules insert directly into specialized attachment sites within the outer kinetochore, forming stable end-on attachments. The number of microtubules attached per kinetochore varies between species, ranging from a single microtubule in budding yeast to 10-40 in animal cells. A key mediator of these attachments is the Ndc80 complex, a rod-like structure anchored in the kinetochore that engages the sides of microtubules near their plus ends. This configuration enables persistent attachment while still allowing microtubule dynamics, which are crucial for regulated chromosome movement during mitosis (1,8,77,78).

Importantly, initial kinetochore-microtubule interactions are often lateral rather than end-on. After nuclear envelope breakdown, kinetochores are exposed to microtubule plus ends emanating from opposite spindle poles. Rather than immediate stable capture, kinetochores first form transient lateral attachments to the microtubule wall, often facilitated by dynein motors localized to the outer kinetochore (77,79,80). These lateral interactions are later converted into stable end-on attachments through coordinated microtubule dynamics and motor activity. In addition to serving as passive microtubule anchors, kinetochores can act as microtubule nucleation centers. This has been demonstrated both in vitro on isolated human mitotic chromosomes (81) and in vivo (82,83), and is thought to accelerate spindle assembly by facilitating kinetochore capture (84,85). During prometaphase, microtubules nucleated at centrosomes undergo rapid polymerization and depolymerization, dynamically exploring the cytoplasm. These search-and-capture movements, including rotational pivoting around the centrosome (86), enhance the probability of kinetochore encounter. Once both sister kinetochores are attached to microtubules emanating from opposite spindle poles, the chromosome becomes properly aligned, which is a prerequisite for entry into anaphase (72,87).

The transition to anaphase is tightly regulated by the spindle assembly checkpoint (SAC), which monitors the attachment status of all kinetochores. If even a single kinetochore remains unattached, SAC activation prevents cell cycle progression. One of the central proteins involved in this checkpoint is Mad2, which localizes to unattached kinetochores and inhibits the activity of Cdc20 (88). Cdc20 is a co-activator of the anaphase-promoting complex/cyclosome (APC/C), a large E3 ubiquitin ligase that triggers the degradation of key mitotic regulators. As long as Mad2 remains active at kinetochores, Cdc20 is sequestered and APC/C is inhibited, thereby delaying the onset of anaphase. The APC/C, once activated by Cdc20, targets two critical substrates: S/M cyclins and securin. The degradation of S/M cyclins leads to inactivation of cyclin-dependent kinases (Cdks), promoting mitotic exit. Securin inhibits separase, a protease responsible for cleaving cohesin, the protein complex that holds sister chromatids together. Upon securin degradation, separase is activated and cleaves cohesin, allowing sister chromatid separation and anaphase progression. Importantly, the activation of APC/C by Cdc20 is itself regulated by phosphorylation events mediated by Cdks, establishing a tightly controlled feedback system that coordinates chromosome attachment status with cell cycle progression (89).

1.4.1 Mechanisms of Erroneous Kinetochore-Microtubule Attachment Correction

Accurate chromosome segregation during mitosis is critically dependent on the formation of correct attachments between kinetochores and spindle microtubules. Errors in these attachments, if left uncorrected, can lead to chromosome missegregation and aneuploidy, a hallmark of many cancers (90–93). Cells have evolved multiple surveillance and correction mechanisms to avoid and rectify erroneous kinetochore-microtubule (KMT) attachments, which can be broadly classified into tension-dependent and tension-independent processes (94–97). The correct configuration, known as amphitelic attachment, occurs when each sister kinetochore is attached to microtubules emanating from opposite spindle poles. This arrangement generates tension across the centromere and ensures that sister chromatids will be pulled to opposite sides of the dividing cell during anaphase (98,99). In contrast, cells often transiently form incorrect attachments that must be corrected to avoid errors in chromosome segregation. These include syntelic, merotelic, and monotelic attachments (Figure 12.). In syntelic attachments, both sister kinetochores are connected to microtubules from the same spindle pole. This configuration fails to generate the necessary tension and is typically recognized and destabilized by tension-sensitive error correction pathways (95,100–102). Merotelic attachments, where a single kinetochore is simultaneously attached to microtubules from both poles, are more problematic. Because they can generate some tension, they may escape detection and persist into anaphase, often resulting in lagging chromosomes and chromosomal instability (103–109). Monotelic attachments occur when only one of the sister kinetochores is attached to microtubules, while the other remains unattached. These configurations are common in early mitosis and are typically corrected as the unattached kinetochore becomes captured by microtubules from the opposite pole (96).

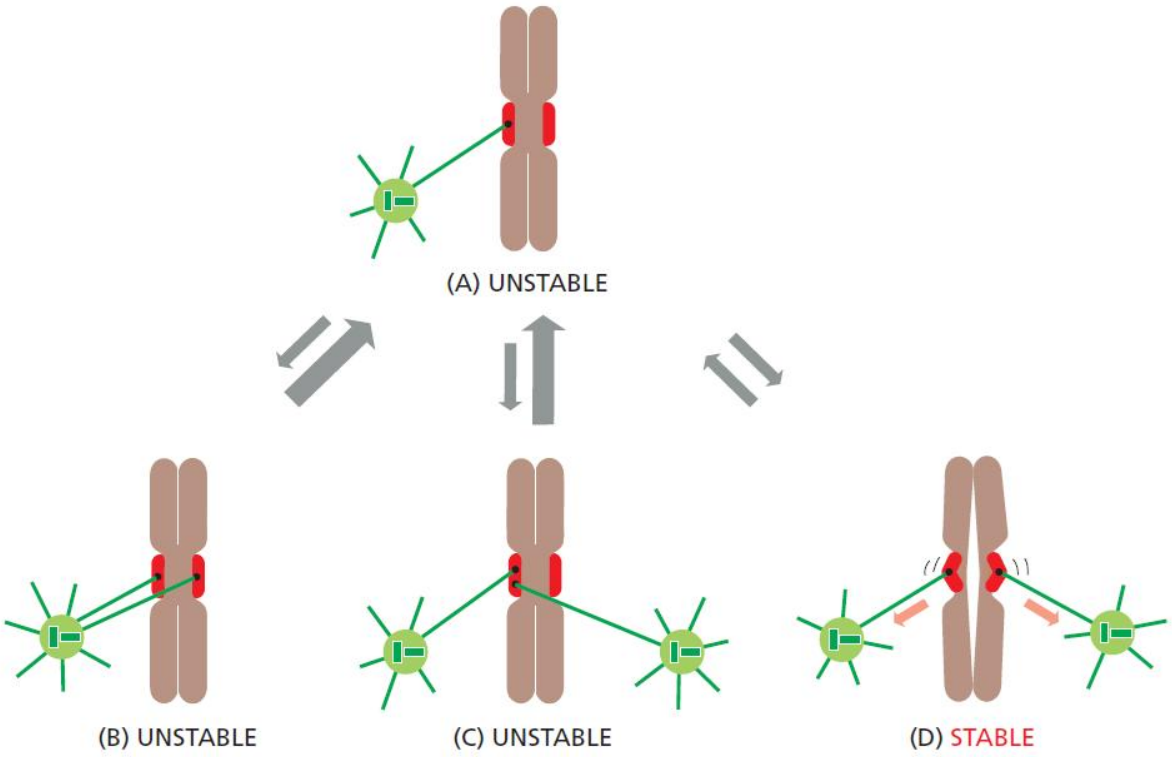

Figure 12. Kinetochore-microtubule attachments (A) The initial attachment of a chromosome typically begins with a monotelic attachment, when a single microtubule from one spindle pole binds to one of the kinetochores in a sister chromatid pair. As additional microtubules associate, various attachment configurations can occur. (B) One possibility is that a second microtubule from the same spindle pole attaches to the other sister kinetochore, forming a syntelic attachment. (C) Alternatively, microtubules from both spindle poles may bind to the same kinetochore, resulting in a merotelic attachment. These aberrant connections are generally unstable, and one of the microtubules usually detaches spontaneously. D) Correct amphitelic attachment is established when a microtubule from the opposite pole binds to the second kinetochore, generating tension across the centromere. Taken from Alberts et al. 2022.

Tension-dependent mechanisms play a central role in recognizing and correcting such errors. When correct amphitelic attachments form, the opposing forces exerted by spindle microtubules generate tension across sister kinetochores. This mechanical tension strengthens the microtubule-kinetochore interface and reduces the phosphorylation activity of Aurora B kinase, a key regulator of attachment stability (110–119). Aurora B resides in the inner centromere and phosphorylates kinetochore substrates to destabilize incorrect attachments (119,120). The spatial separation model posits that when tension pulls kinetochores away from the inner centromere, Aurora B can no longer efficiently reach its substrates, leading to stabilization of proper attachments (111,116,118,119,121). In this way, tension-dependent correction acts as a dynamic feedback system: incorrect attachments fail to generate sufficient tension, allowing Aurora B to promote detachment and facilitate repeated rounds of attachment until proper biorientation is achieved (Figure 13.) (95,111,122–125). Moreover, the microtubule-kinetochore interface exhibits catch bond behavior, whereby tension can paradoxically stabilize attachments by promoting stronger binding at intermediate force levels (126–128).

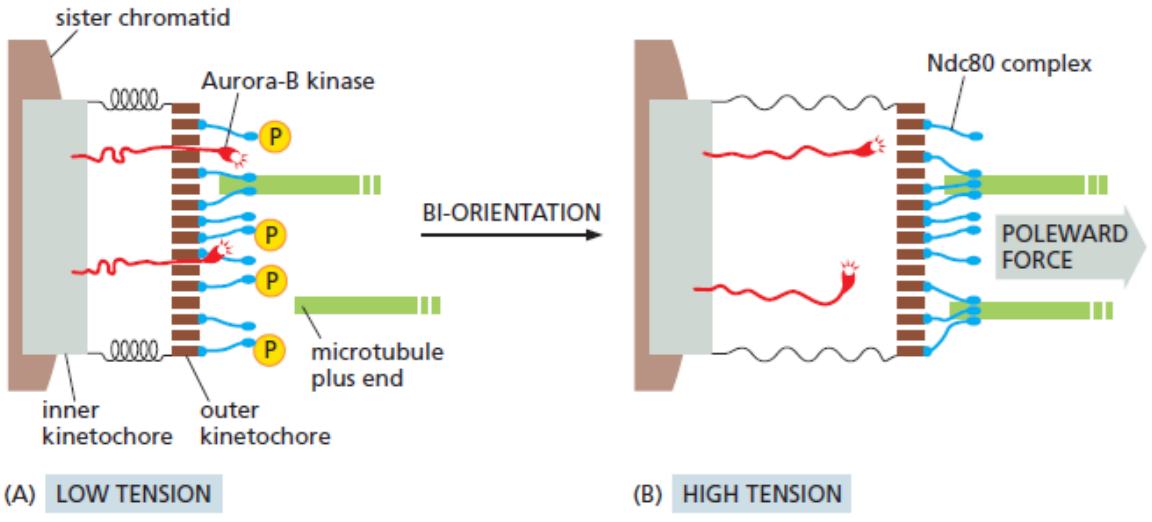

Figure 13. Mechanism by which tension may stabilize kinetochore-microtubule attachments. This figure illustrates a proposed model explaining how tension generated by proper chromosome bi-orientation could enhance the stability of kinetochore-microtubule interactions. For simplicity, only a single kinetochore is shown, with the spindle pole positioned

to the right. (A) In the absence of microtubule attachment or when a sister chromatid pair is connected to only one spindle pole, the kinetochores experience little to no tension. Under these conditions, the protein kinase Aurora B, which is localized to the inner kinetochore, phosphorylates outer kinetochore components such as the Ndc80 complex (depicted in blue). This phosphorylation reduces the affinity of the outer kinetochore for microtubules, resulting in unstable, dynamic attachments characterized by frequent association and dissociation. (B) Once proper bi-orientation is achieved, microtubules from opposite spindle poles exert opposing forces on sister kinetochores. This generates tension across the centromere, physically pulling the outer kinetochore away from the inner kinetochore and, consequently, away from Aurora B kinase. As a result, the phosphorylation of microtubule-binding components is reduced or prevented. The absence of phosphorylation enhances the binding affinity for microtubules, leading to the formation of stable attachments involving multiple microtubules. Taken from Alberts et al. 2022

While tension-dependent mechanisms are highly effective, especially in correcting syntelic errors (95,100–102), tension-independent processes also contribute significantly to ensuring accurate chromosome segregation (96,129–132). These mechanisms rely on the geometric configuration of sister kinetochores and the dynamic nature of microtubule turnover. In metaphase, the back-to-back orientation of sister kinetochores geometrically favors attachment to opposite spindle poles, reducing the likelihood of initial errors (131). Additionally, KMTs are continuously replaced through dynamic instability, allowing for the gradual correction of erroneous attachments over time without the need for tension cues (96,132). This mechanism is particularly relevant for resolving merotelic errors, which often persist undetected by tension-based surveillance (103,107–109,129). During prometaphase, kinetochores exhibit specific adaptations that enhance microtubule capture. At this stage, the geometric constraints are relaxed, and approximately 10% of chromosomes exhibit side-by-side kinetochore orientation, which facilitates the formation of multiple merotelic attachments (133). Despite the increased risk of erroneous attachments, this relaxed configuration enhances the probability of successful microtubule capture, which is a limiting factor during early mitosis (134–136). Prometaphase kinetochores overcome these challenges by expanding their outer corona and adopting a more curved architecture, thereby increasing their surface area for microtubule interactions. Although this increases susceptibility to incorrect attachments, it accelerates the capture process, which is otherwise inefficient under conditions of high chromosomal density and limited space. As cells transition from prometaphase to metaphase, kinetochores become more compact, reducing the likelihood of improper attachments, although the molecular details of this transition remain incompletely understood (135–137).

The dynamics of KMT turnover also shift during mitotic progression. In prometaphase, the half-life of KMTs is approximately 2-3 minutes, reflecting rapid turnover that facilitates error correction. By metaphase, KMT stabilization increases modestly, with half-lives extending to 4-6 minutes (138–140). Importantly, efficient error correction does not require that turnover slows in metaphase; rather, the increased dynamics in early mitosis allow for faster elimination of incorrect attachments and more rapid achievement of amphitelic configurations (96,106,108,129). Aurora B kinase remains a central player throughout these processes. Its

activity is tightly regulated by both centromeric localization and mechanical tension (110–113,113–121,141–151). Aurora B forms a gradient across the centromere, phosphorylating substrates based on their proximity, which directly influences the stability of KMT attachments (56, 62–67, 89). Although its role in destabilizing incorrect configurations is well established, the precise molecular mechanisms by which Aurora B discriminates between correct and incorrect attachments are still being clarified (129,152–157). Moreover, the full extent of the interplay between tension-dependent and tension-independent mechanisms remains an area of active research(96,158–161).

Physiologically, cells must balance the need for stable kinetochore fibers with the necessity of correcting erroneous attachments in a timely manner. This balance is achieved through regulated KMT turnover and the complementary action of multiple error-correction pathways (96,138–140,162). Notably, cells can tolerate a limited number of merotelic attachments, relying on additional corrective mechanisms during anaphase to prevent aneuploidy (152,163–165). From a clinical perspective, defects in these correction systems can lead to persistent attachment errors, chromosomal instability, and ultimately tumorigenesis (90–93,103,108,164,165). Understanding how cells detect and resolve erroneous kinetochore-microtubule attachments is therefore crucial for elucidating the mechanisms of mitotic fidelity and offers potential therapeutic avenues for targeting aneuploidy in cancer.

1.4.2 Chromosome Passenger Complex

The Chromosome Passenger Complex (CPC) is a central orchestrator of mitosis, composed of Aurora B kinase and the regulatory subunits INCENP, Survivin, and Borealin (Figure 14.). This complex dynamically localizes to different regions of the chromosomes during mitosis, with its kinase activity concentrated at the inner centromere during prometaphase and metaphase. This localization is driven by specific histone phosphorylation marks, H3-pT3, catalyzed by Haspin, and H2A-pT120, phosphorylated by Bub1, which facilitate CPC recruitment to the centromere (145,146,148,149,166,167).

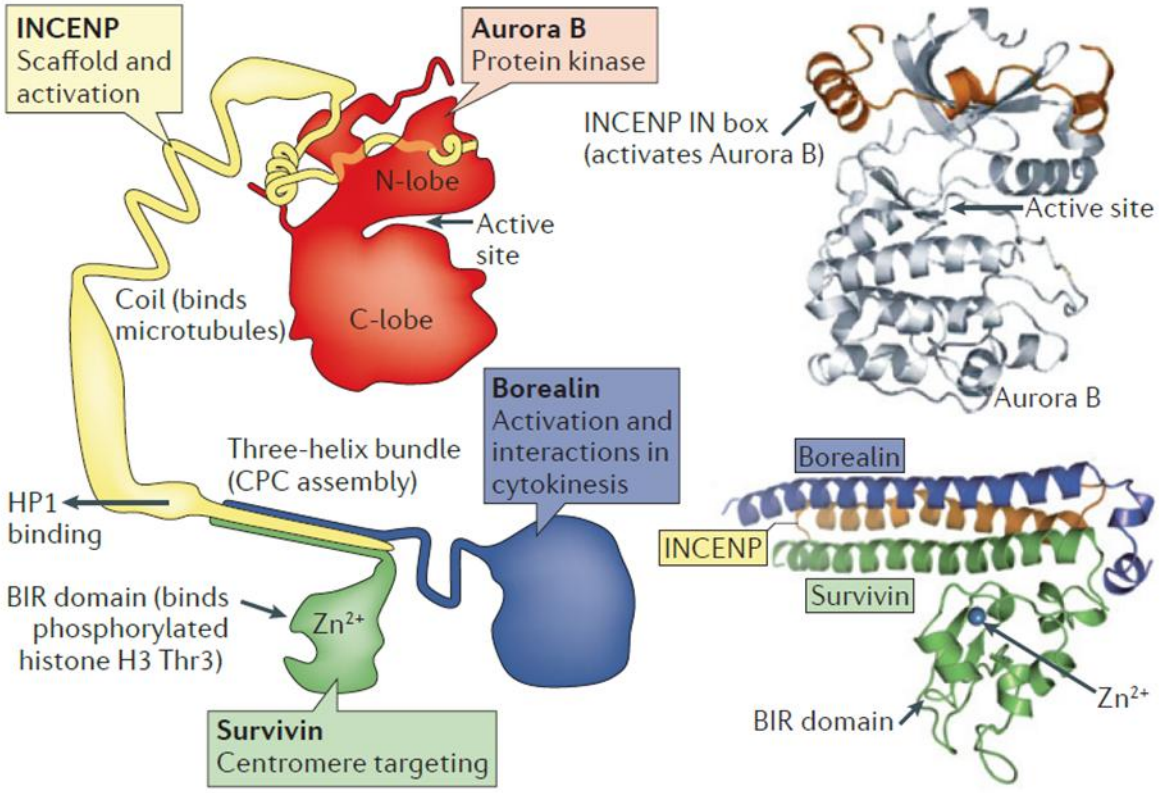

Figure 14. The Chromosome Passenger Complex (CPC) consists of two main functional units: a localization module and a kinase module, which are connected via the central region of INCENP. The kinase module includes Aurora B, which interacts with the highly conserved IN box located at the C terminus of INCENP. The localization module is formed by the N-terminal region of INCENP, along with Survivin and Borealin, which assemble into a three-helix bundle. This structural arrangement connects the BIR (baculovirus IAP repeat) domain of Survivin with the C-terminal region of Borealin, both of which are essential for targeting the CPC to the centromere during mitosis. Taken from Carmena et al. 2012

Aurora B kinase is part of a highly conserved family of serine/threonine kinases (168), which also includes Aurora A, active at the mitotic spindle poles, and Aurora C, which resembles Aurora B in function and is involved in meiosis as well as early stages of mitosis (169). Together with cyclin-dependent kinases (CDKs) and Polo-like kinases (PLKs), Aurora kinases act as central regulators that coordinate specific processes during cell division with the checkpoints that control the overall progression of mitosis and meiosis (169,170). At the centromere, the CPC plays essential roles in several mitotic processes. Aurora B kinase phosphorylates multiple kinetochore substrates, including components of the KMN network such as Ndc80, KNL1, and Dsn1, thereby modulating microtubule-binding activity and promoting the correction of improper kinetochore-microtubule attachments (112,121,138,144,163,171,172). Through this activity, the CPC ensures accurate chromosome bi-orientation, enabling sister kinetochores to attach to microtubules emanating from opposite spindle poles (99). Additionally, it contributes to the maintenance of centromeric cohesion in early mitosis, ensuring sister chromatids remain connected until the appropriate stage of cell

division (173–175) and is crucial for generating the spindle assembly checkpoint (SAC) signal, which delays anaphase onset until all chromosomes are properly attached to the mitotic spindle (112,115,141,163,176,177).

Aurora B also acts as a tension sensor, responding to changes in interkinetochore tension by dynamically regulating the phosphorylation of kinetochore substrates. Under low tension, phosphorylation levels are high, promoting correction of faulty attachments; as tension increases, phosphorylation decreases, stabilizing proper attachments (Figure 15.) (111,114,121,178). Notably, Aurora B generates graded rather than binary changes in microtubule-binding activity, allowing for precise fine-tuning of kinetochore function throughout mitosis (121). Furthermore, its activity is spatially regulated: substrates located closer to the inner centromere receive stronger phosphorylation signals under low-tension conditions (116,121). Interestingly, CPC-mediated kinetochore phosphorylation can occur independently of tension, guided instead by the local centromeric microtubule environment (97).

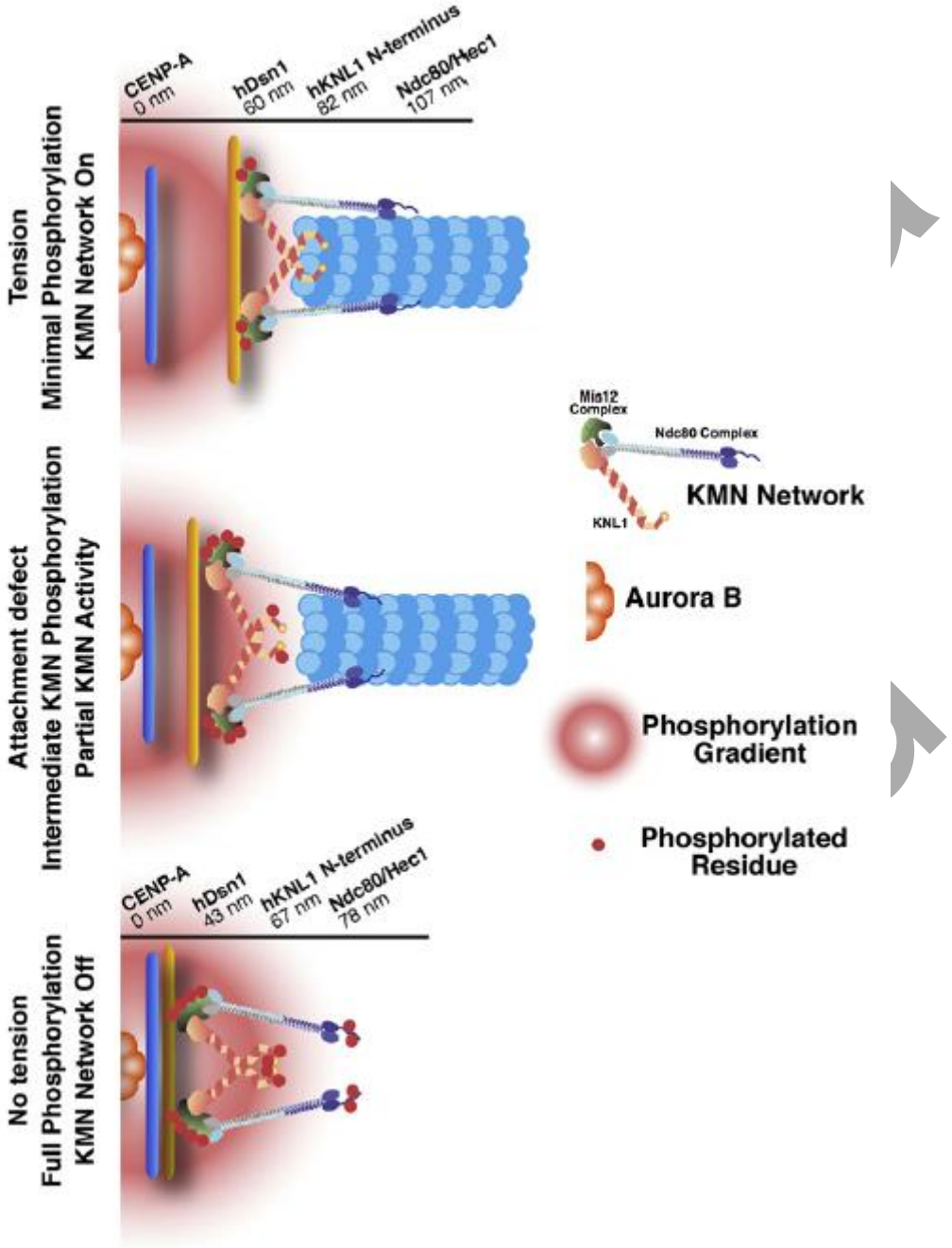

Figure 15. Aurora B Kinase Regulation of Kinetochore-Microtubule Attachments via the KMN Network. This schematic illustrates how Aurora B kinase regulates kinetochore-microtubule attachment through differential phosphorylation of the KMN network components: KNL1, the Mis12 complex, and the Ndc80 complex, under varying tension states at the kinetochore. Aurora B forms a phosphorylation gradient originating from the inner centromere. When kinetochores are under tension, structural stretching positions the Ndc80 complex further from Aurora B, resulting in reduced phosphorylation and stable microtubule attachment. In the absence of tension, the kinetochore remains compact, placing the Ndc80 complex closer to the inner centromere and subjecting it to higher Aurora B activity, which weakens microtubule binding. Taken from Welburn et al. 2010

Aurora B does not act as a simple on/off switch but fine-tunes attachment stability through combinatorial phosphorylation. It targets multiple subunits within the KMN network, specifically Ndc80, KNL1, and Dsn1. Full phosphorylation of these subunits can abolish microtubule binding, whereas partial phosphorylation generates intermediate binding states. This mechanism enables dynamic control of kinetochore activity during error correction and chromosome alignment (121).

In the framework proposed by Trivedi et al. (2016) (163), the CPC operates within the Centromere Signaling Network (CSN), a regulatory circuit that integrates multiple mitotic processes including spindle checkpoint signaling, kinetochore-microtubule attachment regulation, and sister chromatid cohesion. According to this model, the CSN uses positive feedback mechanisms to amplify and spatially restrict CPC activity to the inner centromere, ensuring robust and localized regulation. The integration of the CPC into the CSN enables efficient coordination of error correction, SAC activation, and cohesion maintenance, all of which are essential for high-fidelity chromosome segregation. Dysregulation of CPC function or CSN integrity contributes to chromosomal instability (CIN), a hallmark of many cancers, underscoring the importance of this complex in both normal mitotic progression and tumorigenesis (117).

Aurora B activation is tightly linked to CPC formation and spatial localization. Initially, Aurora B binds to the IN box of INCENP, which triggers a low level of kinase activity. This allows Aurora B to phosphorylate the conserved TSS motif in the C-terminal region of INCENP and Thr232 in its own activation loop, leading to full kinase activation (179–181). Both phosphorylation events are believed to occur in trans, requiring close proximity between neighboring CPC complexes (182). This mechanism explains why Aurora B activity increases with local CPC concentration, e.g. by increasing chromatin density in Xenopus laevis egg extracts (183), by targeting INCENP to ectopic chromosomal loci (184), or along spindle microtubules (183–187). The small GTPase TD60 can also promote activation (186), and full activity additionally requires phosphorylation of Ser311 by the checkpoint kinase 1 (Chk1) (188) near kinetochores, influencing its activity and potentially its role in Plk1 activation and microtubule attachment (189). Plk1 itself enhances Aurora B activity through phosphorylation of Survivin (190). Post-translational modifications, such as monoubiquitylation by CUL3 (191) and sumoylation within the kinase domain (192,193), modulate Aurora B localization and activity. During mitotic exit, Aurora B is degraded by the proteasome, terminating its function (194,195).

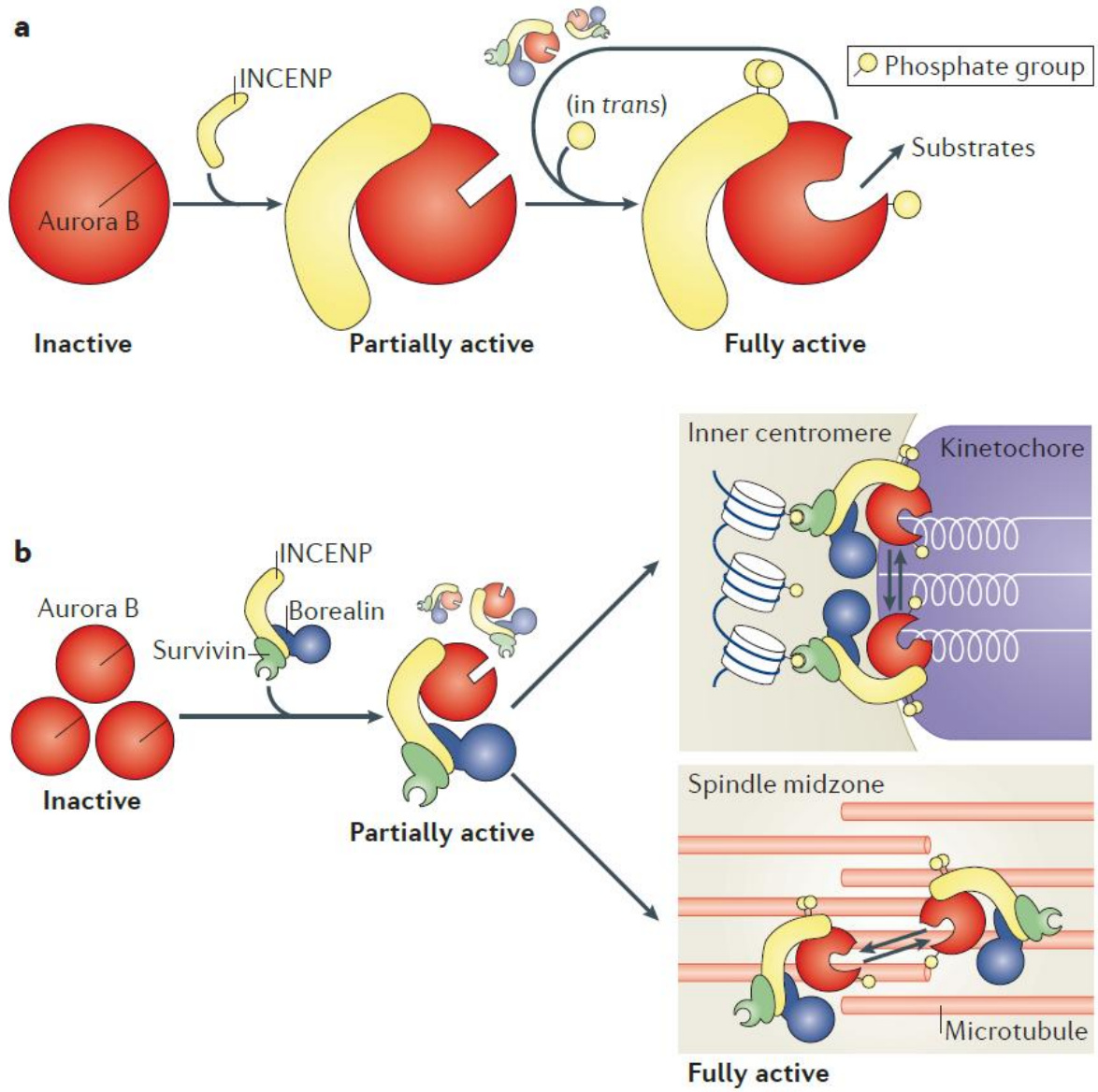

Figure 16. Aurora B kinase activation and localization through the Chromosomal Passenger Complex (CPC). a) Aurora B kinase becomes fully activated through its interaction with inner centromere protein (INCENP) and through phosphorylation events that occur in trans. These modifications are part of a positive feedback mechanism, in which one Aurora B molecule phosphorylates another to amplify activation. b) In living cells, Aurora B activation is tightly coupled to the localization of the chromosomal passenger complex (CPC). The CPC localization module, composed of INCENP, survivin, and borealin, targets the complex to specific structures during mitosis. In early mitosis, it localizes to histones at the inner centromere, while in late mitosis it accumulates at the spindle midzone. This targeted enrichment promotes trans-autophosphorylation of Aurora B, enabling full activation in a spatially regulated manner. Taken from Carmena et al. 2012

Borealin, another core component of the Chromosomal Passenger Complex (CPC), plays a crucial role in ensuring accurate chromosome segregation during mitosis (163). Its N-terminal microtubule-binding domain enables CPC interaction with microtubules, which is critical for inner centromere localization, kinetochore substrate phosphorylation, error correction, and

spindle assembly checkpoint (SAC) function. Borealin mutants lacking this domain show reduced CPC localization, impaired phosphorylation of kinetochore targets such as DSN1, KNL1, CENP-A, and Hec1, and diminished ability to correct erroneous attachments (Figure 17.). Even when Aurora B is targeted to the centromere, Borealin's microtubule-binding remains necessary for full CPC activity, highlighting its role in linking local microtubule structures to kinase regulation and mitotic fidelity (97).

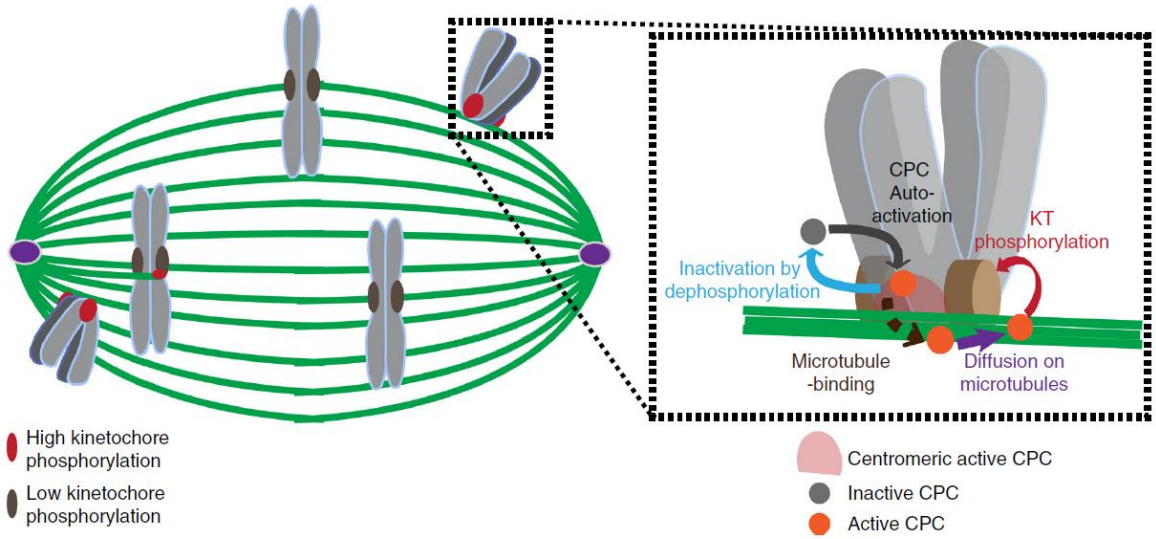

Figure 17. Model of CPC-Mediated Kinetochore Phosphorylation. Schematic representation of how the Chromosomal Passenger Complex (CPC) phosphorylates laterally attached kinetochores. An inactive pool of CPC located outside the centromere (shown in gray) becomes activated through interaction with the centromeric CPC pool (red). Once activated, the non-centromeric CPC (orange) diffuses along microtubules near the centromere (green) and reaches laterally attached kinetochores (brown), where it mediates phosphorylation to support error correction and spindle checkpoint signaling. Taken from Trivedi et al. 2019

2. AIMS OF RESEARCH

The aim of this study is to investigate how overlap microtubule bundles contribute to the spatial and functional regulation of the Chromosomal Passenger Complex (CPC) during mitosis, with a particular focus on their role in the correction of erroneous kinetochore-microtubule attachments. While the importance of kinetochores and k-fibers in chromosome segregation is well established, the contribution of overlap bundles, also known as interpolar or bridging microtubules, remains less understood. These antiparallel bundles, crosslinked by PRC1 and positioned between sister kinetochore fibers, play critical roles in balancing forces across the spindle, maintaining spindle architecture, and enabling proper chromosome alignment. Our central hypothesis is that overlap bundles are not merely structural elements but actively facilitate the error correction process by providing tracks along which the CPC, and specifically its kinase subunit Aurora B, can be spatially distributed toward kinetochores. This localization is essential for phosphorylating key kinetochore substrates involved in detaching improperly attached microtubules, such as those in syntelic or merotelic configurations.

Using a combination of super-resolution microscopy, confocal imaging and functional perturbations, this study aims to answer two key questions:

1. How does the presence and organization of overlap bundles influence CPC localization and activation?
2. How does the disruption of these bundles affect the CPC's ability to correct erroneous kinetochore-microtubule attachments?

These objectives aim to clarify the mechanistic link between spindle architecture and the regulation of mitotic fidelity, highlighting overlap bundles as essential elements in the spatial coordination of CPC activity. These findings may offer new perspectives on how cells maintain chromosome segregation accuracy, with potential implications for understanding mechanisms underlying genome maintenance.

3. MATERIALS AND METHODS

3.1 Cell lines and culture

Experiments were done on human HeLa cells from the High-Throughput Technology Development Studio (Max Planck Institute of Molecular Cell Biology and Genetics, Dresden, Germany). Both cell lines were grown in flasks in Dulbecco's Modified Eagle's Medium with 1 g/L D-glucose, pyruvate and L-glutamine (DMEM, Lonza, Basel, Switzerland), supplemented with 10% (vol/vol) heat-inactivated Fetal Bovine Serum (FBS, Sigma Aldrich, St. Louis, MO, USA) and penicillin (100 IU/mL)/streptomycin (100 mg/mL) solution (Lonza, Basel, Switzerland). The cells were maintained in a humidified incubator at 37°C with 5% CO2 (Galaxy 170S CO2, Eppendorf, Hamburg, Germany) and were regularly subcultured when reaching 70-80% confluence. All cell lines used in the study were confirmed to be mycoplasma-free through testing with the MycoAlert Mycoplasma Detection Kit (Lonza), along with routine checks during imaging experiments using DNA labelling stains.

3.2 Sample preparation, siRNAs, and drug treatments

When the cell confluence reached 80%, the DMEM medium was aspirated from the flask, and the cells were rinsed with 5 ml of phosphate buffered saline (PBS). Afterward, 1 ml 1% trypsin/ethylenediaminetetraacetic acid (EDTA, Biochrom AG, Berlin, Germany) was introduced into the flask, and cells underwent a 5-minute incubation at 37°C in a humidified incubator with 5% CO2.

Following the incubation, trypsin was blocked by the addition of 2 ml of DMEM medium. In RNAi experiments, the cells were seeded to attain 60% confluence the following day before transfection. The cells were cultured on 35 mm uncoated dishes with a glass thickness of 0.17 mm (MatTek Corporation, Ashland, MA, USA), using 1 ml of DMEM medium with the previously mentioned supplements. On the next day, the cells underwent transfection with either targeting or non-targeting siRNA constructs. These constructs were diluted in OPTI-MEM medium (Life Technologies, Waltham, MA, USA) to achieve a final concentration of 100 nM in the medium with cells. Transfections were carried out using Lipofectamine RNAiMAX Reagent (Life Technologies, Waltham, MA, USA) following the manufacturer's instructions, 24 hours before live imaging or 48 hours before fixation. To reduce endogenous PRC1, cells were transfected with human ON-TARGET PRC1 siRNA (L-019491-00-0020, Dharmacon) and control siRNA (D-001810-10-05, Dharmacon, Lafayette, CO, USA). To test the role of overlap bundles in chromosome segregation fidelity, we used Monastrol (HY-101071A/CS-6183, MedChemExpress, Monmouth Junction, NJ, USA) to block the spindles in a monopolar state with a high incidence of syntelic attachments. A Monastrol working solution (100 μM) was added to the dish with untransfected HeLa cells at a final concentration of 100 mM.

3.3 Immunocytochemistry

Untransfected HeLa cells were grown on glass-bottom dishes (14 mm, No. 1.5, MatTek Corporation, Darmstadt, Germany) and fixed by 1 ml of ice-cold methanol for 1 min at -20°C or fixed by 1 ml of 4 % PFA (paraformaldehyde) (Biognost, Zagreb, Croatia) for 15 min at room temperature. After fixation, cells underwent three 5-minutes washes with 1 ml of PBS (phosphate-buffered saline). To block unspecific binding of antibodies and enable permeabilization, cells were incubated in 1 ml of blocking/permeabilization buffer (2% normal goat serum (NGS) and 0.5% Triton-X-100) for 1 hour at room temperature. Cells were then incubated with 500 µl of primary antibody solution overnight at 4°C. The following primary antibodies were used: mouse monoclonal PRC1 (sc-376983, Santa Cruz Biotechnology), diluted 1:300, human anti-CREST (15-235, Antibodic sinc), diluted 1:300, rabbit anti-Aurora B (ab239837, Abcam), diluted 1:500, rabbit anti-Borealin (ABE 1961,EMD Milipore) diluted 1:1000, and rabbit anti-phospho-CENP-A (Ser7) (07-232, Sigma-Aldrich), diluted 1:500. Following the primary antibody treatment, cells were washed with PBS and then incubated in 500 µL of secondary antibody solution for 1 hour at room temperature covered with aluminum foil. The following secondary antibodies were used: donkey anti-mouse IgG Alexa Fluor 488 (ab150105, Abcam, Cambridge, UK), diluted 1:500, donkey anti-mouse IgG Alexa Fluor 594 (ab150112, Abcam, Cambridge, UK), diluted 1:500, Abberior STAR RED goat anti-rabbit IgG (STRED-1002-500UG, Abberior Instruments, Göttingen, Germany), diluted 1:500, donkey anti-rabbit IgG Alexa Fluor 488 (ab150061, Abcam, Cambridge, UK), diluted 1:500, and goat anti-human IgG 594 (ab96909, Abcam, Cambridge, UK), diluted 1:500. Finally, cells were washed with 1 mL of PBS, 3 times for 5 min. In all fixations, DAPI (1 µg/mL) was used for chromosome visualization.

3.4 Imaging

3.4.1 STED microscope system (Abberior Instruments).

Stimulated Emission Depletion (STED) microscopy is an advanced fluorescence imaging technique that surpasses the resolution limits of conventional confocal microscopy. This improved resolution is achieved by selectively deactivating fluorescent dye molecules at the periphery of the excitation spot using high-intensity laser light, which induces stimulated emission. As a result, most of the excited fluorophores outside the central focal region are driven back to their ground state, effectively preventing them from emitting fluorescence. Only the centrally located dye molecules remain fluorescent, enabling the acquisition of high-resolution images with enhanced spatial detail (196). STED microscopy was performed using the Expert Line easy3D STED microscope system (Abberior Instruments) with a 100x/1.4 UPLSAPO100x oil objective (Olympus), avalanche photodiode (APD) detector, and Imspector software to acquire supperresolution images of CPC components in different stages of mitosis of HeLa cells, immunostained with previously mentioned antibodies, with CREST and PRC1 in confocal mode. STED images of CPC components were acquired with a 41 plane Z-stack to cover the whole spindle in a STAR RED channel with the excitation laser power at 15% and depletion laser power at 10%, and pixel size set at 40 nm. Confocal images of CREST and PRC1 were acquired with a 41 plane Z-stack in an Alexa 488 channel with the excitation laser

power at 15 % for PRC1 and an Alexa 594 channel with the excitation laser power at 10 % for CREST, both with pixel size set at 40 nm.

Confocal mode was also used to image fixed HeLa cells stained with anti-phospho-CENP-A and in experiments analyzing lagging chromosomes. Imaging was performed using Alexa 488 and 594, depending on the secondary antibody used and DAPI excitation laser to visualize DNA. The laser power was set to 10%. Pixel size was 50 nm for all imaging. Z-stacks consisted of 41 focal planes spaced 0.5 μm apart to cover the entire spindle, except in experiments focused on lagging kinetochores, where 20 focal planes were acquired.

3.4.2 LSM 800 with Airyscan microscope system (Zeiss).

Confocal microscopy was performed on an Airyscan Zeiss LSM800 confocal scanning microscope equipped with a 60× oil immersion objective (Carl Zeiss, Germany) and an LSM 800 camera. Zeiss software was used to acquire confocal images of CPC components, PRC1, and CREST at different stages of mitosis in HeLa cells immunostained with the antibodies described above. For excitation of labeled cellular structures, laser lines at 405 nm, 488 nm, 561 nm, or 640 nm were used. For experiments in which cells were treated with monastrol, Airyscan mode was used. Airyscan is an advanced confocal detection system that captures light typically blocked by the pinhole in conventional confocal laser scanning microscopes. By collecting these additional photons, it enhances image sensitivity, speed, or resolution. The laser power for 640, 561, 488, and 405 nm in Airyscan mode was set to 0.4% with a Master Gain of 700 V. In all other experiments, standard confocal mode was used, with the following settings: for the 561 nm laser, power was 1% with a pinhole size of 54 μm and Master Gain of 600 V; for the 488 nm laser, power was 0.2% with a pinhole size of 45 μm and Master Gain of 550 V; and for the 405 nm laser, power was 0.2% with a pinhole size of 41 μm and Master Gain of 650 V.

3.5 Image processing and data analysis

All images were analyzed in Fiji/ImageJ (National Institutes of Health, Bethesda, MD, USA). Quantification was performed using the raw images, and contrast adjustments were made for improved clarity in the figures. Plots were generated using MatLab (MathWorks, Natick, MA, USA) and Rstudio (R Foundation for Statistical Computing, Vienna, Austria). Data were presented as mean ± SEM, unless otherwise stated. Group means were compared using a two-tailed t-test when two groups were analyzed, whereas one-way ANOVA followed by Tukey's HSD post hoc test was used when more than two groups were compared. To compare proportions between experimental conditions, a z-score test for two population proportions was used. A p-value < 0.05 was considered statistically significant. The numbers of kinetochore pairs, cells, and independent experiments were indicated in the respective figure captions. The final figures were compiled and arranged in Adobe Illustrator CS5 (Adobe Systems, Mountain View, CA, USA).

Protein silencing. The immunofluorescence analysis was conducted on the cumulative signal from all 41 planes. In Fiji, the spindle region was encircled using a segmented line, and the sum intensity within this outlined area was measured.

CPC intensity in prometaphase. To measure the CPC intensity the region on the spindle with centromeric CPC was encircled in Fiji and mean intensity was measured on the sum of all 41 planes in control and PRC1 depleted cells. The mean intensity of CPC in the cytoplasm was subtracted from mean intensity of centromeric CPC. Furthermore, to get the normalized CPC intensity, value after the cytoplasm subtraction was divided by the average control cell value.

CPC line intensity in prometaphase and metaphase. To quantitatively assess the spatial distribution of CPC components in relation to overlap bundles, we measured the fluorescence intensity of Borealin and Aurora B in mitotic HeLa cells. Cells were immunostained for either Borealin or Aurora B (imaged using STED microscopy), PRC1 (imaged using confocal microscopy), and CREST (confocal microscopy), which served as a marker for kinetochores. To analyze signal distribution, we used Fiji software to extract intensity profiles. Line scans were manually drawn across kinetochore pairs in two orientations: vertically, along the inter-kinetochore axis (perpendicular to the spindle axis), and horizontally, parallel to the spindle axis. In both orientations, lines were centered between the sister kinetochores, and the profiles were aligned such that the midpoint corresponded to the center of the kinetochore pair. All measurements were normalized to the maximum signal intensity of each individual cell to account for variability in overall staining efficiency. In experiments involving PRC1 depletion, signal intensities were instead normalized to the mean value obtained from control cells, allowing for accurate comparison between conditions. For each group, mean intensity profiles were calculated, and standard deviation was plotted as shaded areas around the mean. This approach allowed us to compare both the intensity and spatial distribution of CPC components in control and PRC1-depleted conditions, and to evaluate changes in centromeric enrichment and localization patterns during different mitotic stages.

Mitotic phases, chromosome congression errors and segregation errors. To analyze mitotic progression and assess the impact of PRC1 depletion on chromosome alignment, we performed a time-course analysis following monastrol washout. Cells were fixed at multiple time points (15, 30, and 45 minutes) after washout and immunostained for PRC1, CREST, and DNA. Based on these markers, cells were categorized into distinct mitotic phases: early prometaphase, late prometaphase, metaphase, and anaphase. Classification was performed manually using morphological criteria and CREST signal distribution. The percentage of cells in each phase was quantified for both control and PRC1-depleted populations. To further investigate chromosome alignment defects, we examined the presence of unaligned chromosomes in the same dataset. Cells in metaphase or late prometaphase were assessed for chromosomes that failed to align at the metaphase plate. Unaligned chromosomes were identified visually and confirmed by the presence of mispositioned CREST-positive kinetochores and corresponding DAPI signal. Cells were classified into categories based on the number of unaligned chromosomes observed (one, two, three or four, or more than four). This stratification allowed us to evaluate both the frequency and severity of misalignment events across experimental conditions. Additionally, we quantified the occurrence of lagging chromosomes during anaphase as an indicator of unresolved attachment errors. Cells in anaphase were screened for lagging kinetochores, identified as individual CREST-positive signals located between the separating chromosome masses. Lagging chromosomes were scored in fixed samples across

four experimental conditions: control, PRC1 siRNA alone, monastrol washout alone, and combined PRC1 siRNA with monastrol washout. The frequency of lagging chromosomes was calculated as the percentage of anaphases displaying at least one lagging kinetochore. These measurements provided insight into the efficiency of chromosome segregation and the fidelity of error correction mechanisms.

Phosphorylation of outer kinetochore. To assess the activity of Aurora B kinase at the outer kinetochore under conditions of PRC1 depletion, we analyzed the phosphorylation levels of CENP-A at serine 7 (CENP-A-Ser7P), a known Aurora B substrate. Immunostaining was performed using an antibody against phosphorylated CENP-A (CENP-A-Ser7P) in combination with CREST, a marker for kinetochores. Confocal imaging was carried out for prometaphase cells, and a consistent analysis protocol was applied across all samples. The spindle was boxed in a fixed square that was same for all cells. The intensity ratio was expressed by dividing the CENP-A-Ser7P sum intensity by the CREST sum intensity.

4. RESULTS

4.1 Role of Overlap Bundles in CPC Localization

To investigate the tension-independent error correction mechanism and explore the potential role of overlap bundles in this process, we posed two central questions: (1) how do overlap bundles influence the localization of the Chromosomal Passenger Complex (CPC), and (2) how they affect the correction of erroneous kinetochore-microtubule (K-MT) attachments. It has been proposed that CPC, and particularly its catalytic subunit Aurora B, can be guided by microtubule geometry and spatial positioning, independent of interkinetochore tension, to achieve proper phosphorylation of kinetochore substrates (97), raising the possibility that overlap microtubule bundles may contribute to CPC spatial regulation. To address the first question, we used stimulated emission depletion (STED) microscopy to obtain super-resolution images of Aurora B and Borealin, two core CPC components, in relation to overlap bundles, to examine their spatial distribution. PRC1 was used as a marker of antiparallel microtubule bundles due to its preferential binding to such overlaps (36,54,62,63). Cells were immunostained for PRC1, Aurora B or Borealin. At the onset of prometaphase, Aurora B and Borealin begin to interact with a network of antiparallel microtubules linked by PRC1. As mitosis progresses and overlap bundles become more defined, this interaction continues, suggesting a sustained association between CPC components and PRC1-marked microtubule structures (Figure 18a-b.).

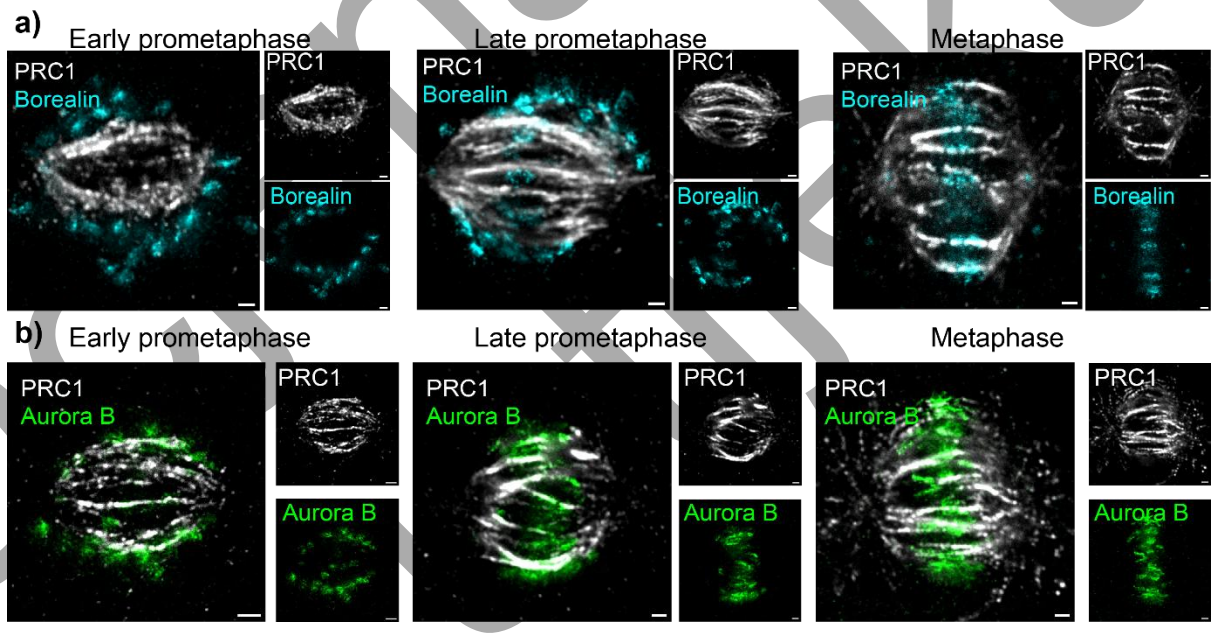

Figure 18. Spatial distribution of CPC components relative to PRC1-labeled overlap bundles during mitosis. **a)** Spindles immunostained for Borealin (cyan, imaged with STED), and for PRC1(white, imaged with confocal microscopy) in HeLa cells during early prometaphase, late prometaphase, and metaphase. **b)** Spindles immunostained for Aurora B (green, imaged with STED), and for PRC1(white, imaged with confocal microscopy) in HeLa cells during early prometaphase, late prometaphase, and metaphase. For each mitotic phase, the large image on the left shows the merged channels of Aurora B or Borealin with PRC1, while the smaller

images on the right present the corresponding individual channels for PRC1 and Aurora B or Borealin. Single imaging planes are shown for each cell. All scale bars: 1 μm.

To further investigate how CPC components interact with overlap microtubule architecture, we analyzed the spatial distribution of Borealin, which contains a microtubule-binding domain (97), in relation to PRC1-labeled antiparallel microtubule overlap bundles and kinetochores in HeLa cells. Cells were immunostained for Borealin (STED), PRC1, and CREST (both confocal resolution), the latter serving as a kinetochore marker (Figure 19a). We performed measurements in both prometaphase and metaphase, stages during which CPC is predominantly localized to the inner centromere. For quantitative spatial analysis, we used Fiji software to measure fluorescence intensity profiles. A line was drawn between the kinetochores, perpendicular to the spindle axis (inter-kinetochore axis), and another line was drawn across the kinetochore pair, parallel to the spindle axis (spindle-parallel axis), allowing us to assess the distribution of Borealin, PRC1, and CREST signals in both dimensions (Figure 19g). The vertical profiling was oriented from the spindle center toward the cytoplasm, while horizontal profiling extended from the metaphase plate toward the spindle pole. In prometaphase, vertical line intensity profiles revealed a clear overlap between Borealin and PRC1, particularly at the central region between kinetochores, corresponding to the inner centromere (Figure 19b). The peak signal of Borealin colocalized with that of PRC1 and partially overlapped with CREST, suggesting that Borealin is positioned at the interface between kinetochores and overlap bundles. In metaphase, this colocalization persisted, although the Borealin signal exhibited a broader distribution, potentially reflecting the redistribution of CPC components as kinetochore-microtubule attachments mature (Figure 19c). Horizontal intensity profiles in prometaphase showed that Borealin was highly enriched at the centromeric region, coinciding with the PRC1 signal and flanked symmetrically by CREST peaks (Figure 19d). In metaphase, although Borealin still colocalized with PRC1, the signal was more diffusely distributed across the centromere-kinetochore axis, consistent with a broader localization pattern as mitosis progresses (Figure 19e). Notably, a comparison of horizontal Borealin profiles between prometaphase and metaphase cells (Figure 19f) demonstrated that the signal was more sharply defined and centromere-concentrated in prometaphase, further supporting the idea that overlap bundles more tightly regulate CPC positioning in early mitosis. Taken together, these data indicate that Borealin is associated with PRC1-labeled antiparallel microtubule overlaps in both prometaphase and metaphase, but that this association is stronger and more spatially confined during prometaphase. This suggests that overlap bundles may play an active role in facilitating Borealin's recruitment or retention at the inner centromere at early mitotic stages, where it contributes to error correction before kinetochore attachments are fully stabilized.

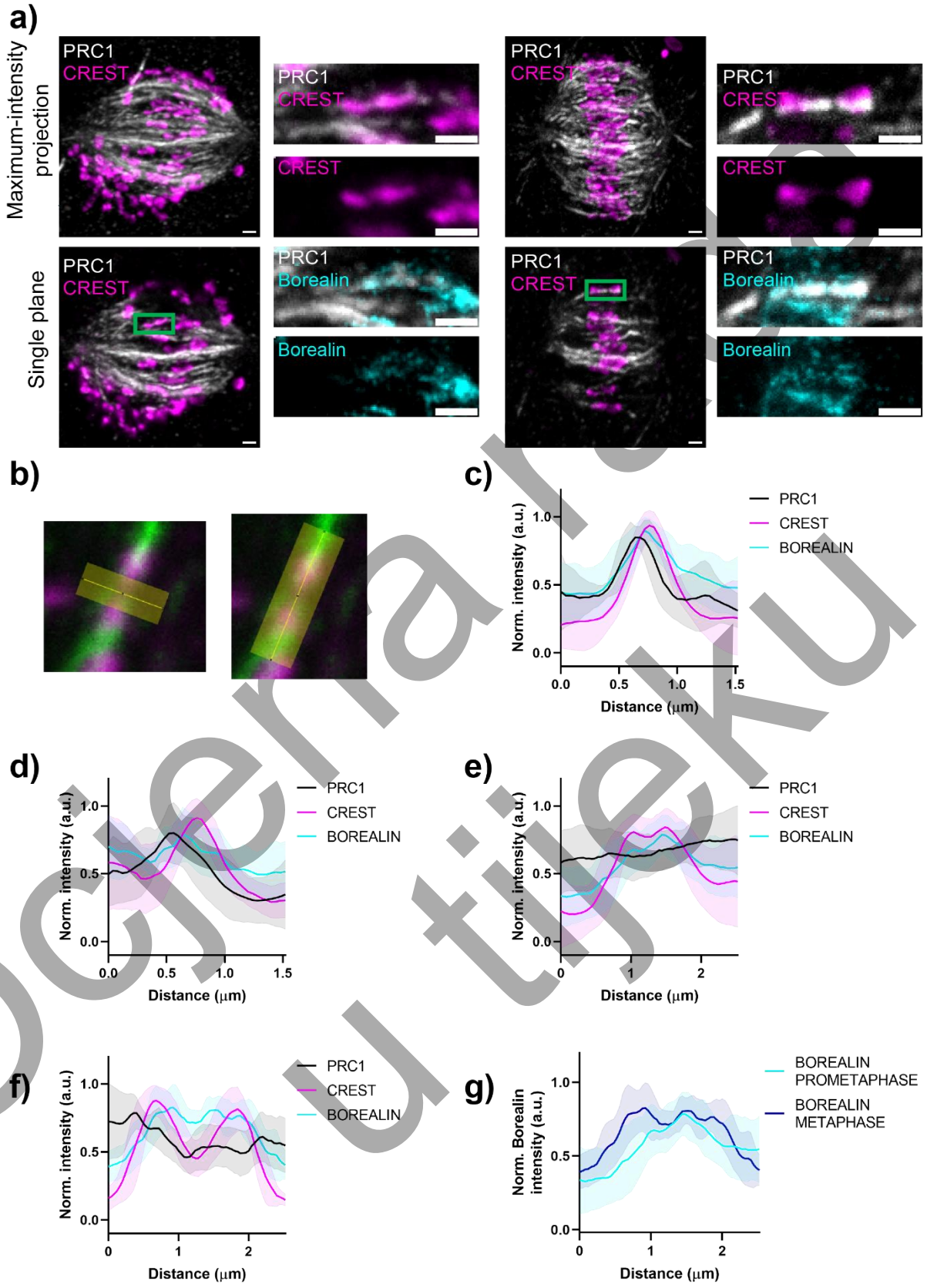

Figure 19. STED imaging shows colocalization of Borealin with PRC1-labeled overlap bundles during mitosis. **a)** Spindles immunostained for Borealin (cyan, imaged with STED), and for PRC1 (white) and CREST (magenta, both imaged with confocal microscopy) in HeLa

cells during prometaphase and metaphase. Close-up of the indicated kinetochore pair is shown on the right side of the spindle image. For both phases, the left side shows maximum-intensity projections and single-plane images of the entire mitotic spindle with merged PRC1 and CREST channels. On the right, for a selected kinetochore pair, merged PRC1 and CREST channels are shown alongside CREST alone, and merged PRC1 and Borealin channels are shown alongside Borealin alone. **b)** Example of line intensity profile measurements across a kinetochore pair: vertical profiling (left) and horizontal profiling (right). Vertical measurements were consistently performed from the spindle centre toward the cytoplasm, while horizontal measurements were taken from the metaphase plate toward the spindle pole **c)** Line intensity profiles of Borealin, PRC1, and CREST in the HeLa cells with panel a) depicting a representative example, measured vertically across kinetochore pairs in prometaphase (n = 18 pairs) **d)** Line intensity profiles of Borealin, PRC1, and CREST measured vertically across kinetochore pairs in metaphase (n = 10 pairs) **e)** Line intensity profiles of Borealin, PRC1, and CREST measured horizontally across kinetochore pairs in prometaphase (n = 18 pairs) **f)** Line intensity profiles of Borealin, PRC1, and CREST measured horizontally across kinetochore pairs in metaphase (n = 10 pairs) **g)** Comparison of horizontal line intensity profiles of Borealin between prometaphase cells (n = 18) and metaphase cells (n = 10). All data were obtained from at least three independent experiments per condition. The central lines represent the mean, and shaded areas represent standard deviation. All measurements were normalized to the maximum intensity value of each individual cell. All scale bars: 1 μm.

Given our hypothesis that Aurora B utilizes overlap microtubule bundles as pathways to efficiently reach its kinetochore targets, we next examined Aurora B localization in relation to both kinetochores and overlap bundles. To explore this spatial relationship, we analyzed HeLa cells in prometaphase and metaphase immunostained for Aurora B, PRC1, and CREST (Figure 20a). For quantitative spatial analysis, we again used Fiji software to measure fluorescence intensity profiles along two axes: vertical and horizontal axis. In both orientations, we observed colocalization between Aurora B and PRC1 in relation to CREST-labeled kinetochores. Vertical line profiles revealed that Aurora B overlapped with PRC1 between kinetochores in both prometaphase and metaphase. This colocalization was more spatially confined and peaked in prometaphase, indicating a stronger spatial relationship with overlap bundles at earlier mitotic stages (Figure 20b). As cells progressed to metaphase, the vertical profile of Aurora B became broader, suggesting a redistribution of the kinase as stable end-on attachments formed (Figure 20c). In horizontal line profiles, Aurora B was sharply concentrated at the inner centromere during prometaphase, coinciding with the PRC1 signal and situated between the CREST-labeled kinetochores (Figure 20d). In metaphase, the Aurora B distribution became more diffuse across the centromeric-kinetochore axis yet still maintained overlap with PRC1 (Figure 20e). This shift may reflect a reduced dependency on overlap bundles for CPC positioning once stable kinetochore-microtubule attachments are established (Figure 20f). Together, these findings suggest that antiparallel microtubule bundles could not only contribute to Aurora B recruitment during early mitosis but may continue to serve as spatial guides or scaffolds that facilitate Aurora B's access to key substrates during the correction of kinetochore-microtubule attachment errors. The prominent overlap in prometaphase is consistent with a model in which

CPC activity is tightly coupled with the early spindle architecture, particularly when lateral attachments dominate and error correction is most active.

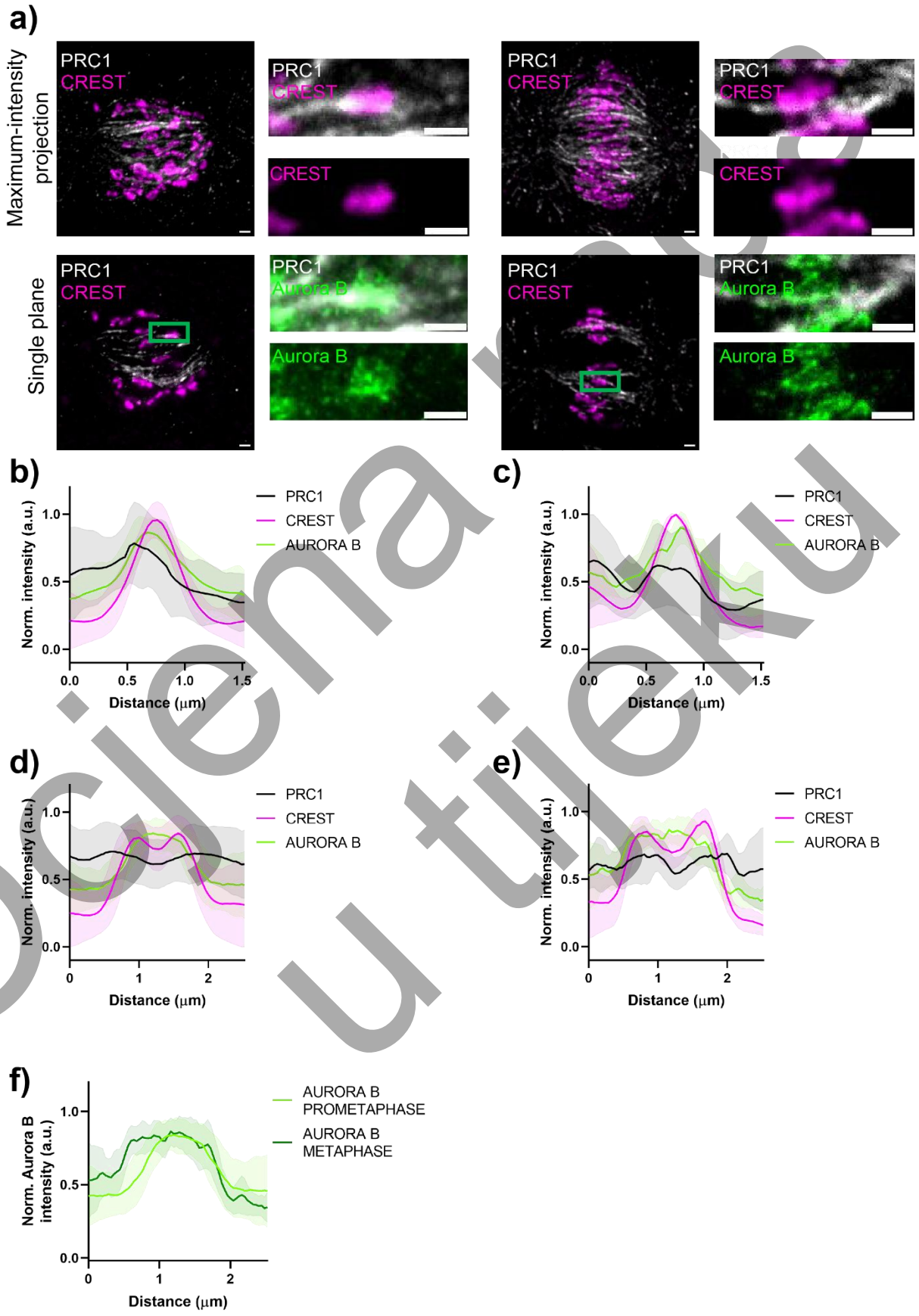

Figure 20. STED imaging shows colocalization of Aurora B with PRC1-labeled overlap bundles during mitosis. a) Spindles immunostained for Aurora B (green, imaged with STED), and for PRC1 (white) and CREST (magenta, both imaged with confocal microscopy) in HeLa cells during prometaphase and metaphase. Close-up of the indicated kinetochore pair is shown on the right side of the spindle image. For both phases, the left side shows maximum-intensity projections and single-plane images of the entire mitotic spindle with merged PRC1 and CREST channels. On the right, for a selected kinetochore pair, merged PRC1 and CREST channels are shown alongside CREST alone, and merged PRC1 and Aurora B channels are shown alongside Aurora B alone. **b)** Line intensity profiles of Aurora B, PRC1, and CREST in the HeLa cells with panel a) depicting a representative example, measured vertically across kinetochore pairs in prometaphase (n = 45 pairs). **c)** Line intensity profiles of Aurora B, PRC1, and CREST measured vertically across kinetochore pairs in metaphase (n = 17 pairs). **d)** Line intensity profiles of Aurora B, PRC1, and CREST measured horizontally across kinetochore pairs in prometaphase (n = 45 pairs). **e)** Line intensity profiles of Aurora B, PRC1, and CREST measured horizontally across kinetochore pairs in metaphase (n = 17 pairs). **f)** Comparison of horizontal line intensity profiles of Aurora B between prometaphase cells (n = 45) and metaphase cells (n = 18). Cells were analyzed as illustrated in Figure 19, panel g). All data were obtained from at least three independent experiments per condition. The central lines represent the mean, and shaded areas represent standard deviation. All measurements were normalized to the maximum intensity value of each individual cell. All scale bars: 1 µm.

4.2 PRC1 depletion impairs centromeric enrichment of CPC components during prometaphase

Previous findings suggested that the CPC associates with spindle microtubules, which may influence its spatial positioning at centromeres and consequently its mitotic functions. The interaction of the CPC with microtubules could potentially regulate either the amount of CPC bound to the inner centromere, the transmission of CPC-mediated signaling to kinetochores, or both (97). This view is supported by the localization pattern of Aurora B and Borealin observed in early mitosis, which closely aligns with antiparallel microtubule overlaps. These overlaps are especially abundant in prometaphase, when the centromere lies near thick bundles of PRC1-crosslinked microtubules (46,71). To test the functional contribution of PRC1-marked overlap bundles to CPC localization, we depleted PRC1 using siRNA. This treatment specifically reduces the population of antiparallel microtubules while preserving the overall spindle structure and k-fiber organization (54). We then analyzed the effect of PRC1 depletion on the localization of the CPC components Aurora B and Borealin during prometaphase. Quantitative measurements of fluorescence intensity at the centromeric region revealed a statistically significant reduction in the accumulation of both proteins in PRC1-depleted cells compared to controls. Aurora B intensity at the centromere decreased by approximately 32%, from a normalized mean value of 1 in control cells to 0.68 in PRC1-depleted cells ($p = 0.0244$, n = 52 control, n = 49 PRC1-depleted, Figure 21a-b). Borealin signal showed an even greater reduction of about 38%, with mean intensity dropping from 1.03 in control to 0.64 in PRC1-depleted cells ($p < 0.0001$, n = 42 per group, Figure 21c-d). These results demonstrate that

overlap bundles facilitate centromeric enrichment of CPC components during early mitosis. To verify the efficiency of PRC1 depletion in this experimental context, we quantified PRC1 signal in prometaphase cells. The intensity of PRC1 was reduced by 98%, confirming successful depletion and supporting the conclusion that the observed effects on CPC localization are due to loss of overlap bundles (Figure 21e, f). Together, these findings provide functional evidence that overlap bundles are essential for proper CPC enrichment at centromeres in prometaphase.

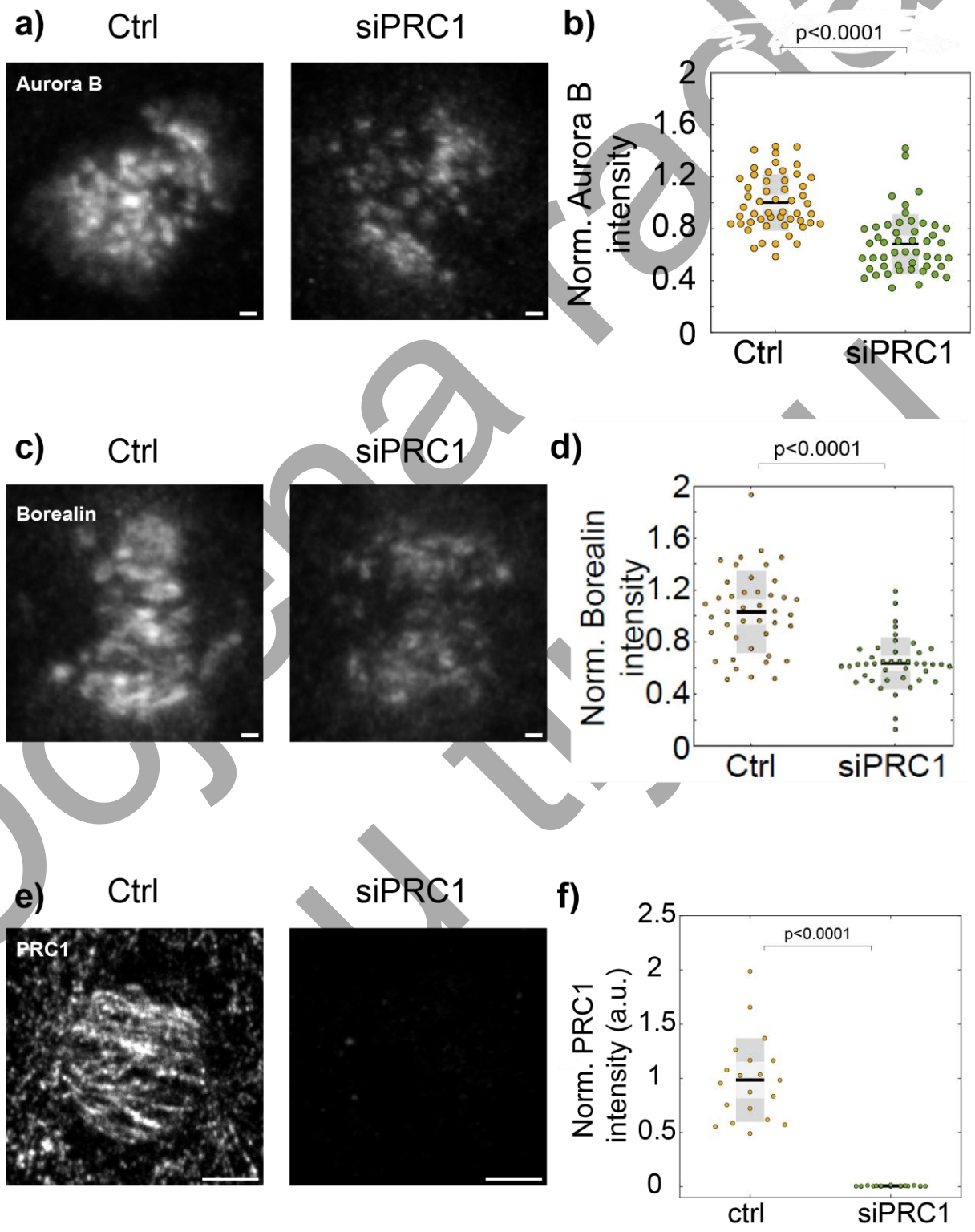

Figure 21. PRC1 depletion reduces centromeric accumulation of Borealin and Aurora B during prometaphase. **a)** Confocal images of maximum-intensity projections of prometaphase spindles in control and PRC1-depleted HeLa cells immunostained for Aurora B (white). **b)** Normalized Aurora B intensity in control cells (n =52) and PRC1-depleted cells (n = 49). **c)** Confocal images of maximum-intensity projections of prometaphase spindles in control and PRC1-depleted HeLa cells immunostained for Borealin (white). **d)** Normalized Borealin intensity in control cells (n =42) and PRC1-depleted cells (n = 42). **e)** Confocal images of maximum-intensity projections of prometaphase spindles in control and PRC1-depleted HeLa cells immunostained for PRC1, illustrating the reduction of PRC1 signal following siRNA treatment used in these experiments. **f)** Normalized PRC1 intensity in control cells (n = 20) and PRC1-depleted cells (n = 20). The graph shows a 98% reduction in PRC1 signal intensity in PRC1-depleted cells. The black line represents the mean, and the light and dark grey areas indicate the 95% confidence interval and standard deviation, respectively, and p values from a two-tailed t-test are given. All data were obtained from at least three independent experiments per condition. All measurements were normalized to the mean intensity obtained from control cells. Scale bars for a) and c): 1 μm. Scale bars for e): 4 μm.

4.3 PRC1 depletion alters Borealin and Aurora B distribution at kinetochores.

To further investigate how PRC1 depletion affects not only the quantity but also the spatial distribution of CPC components at kinetochores, we performed a more detailed analysis of Borealin localization using STED microscopy. High-resolution images of individual kinetochore pairs from control and PRC1-depleted prometaphase cells revealed notable changes in Borealin signal distribution. In control cells, Borealin was sharply enriched at the inner centromere, forming a defined, symmetric signal centered between the CREST-labeled kinetochores. In contrast, PRC1-depleted cells displayed a visibly weaker and more diffuse Borealin signal, often with reduced centromeric concentration (Figure 22a). To quantify this, we measured Borealin intensity profiles along two orthogonal axes, vertically and horizontally (as described before). Both vertical and horizontal analyses showed a clear reduction in Borealin signal in PRC1-depleted cells relative to controls. In the vertical profiles, the central peak corresponding to inner-centromere localization was significantly diminished (Figure 22b), while in the horizontal profiles, the intensity plateau was reduced and more spread out, indicating loss of spatial confinement (Figure 22c). To further dissect this change, we quantified Borealin intensity at three defined positions relative to each kinetochore pair: the peak of the left kinetochore, the midpoint between kinetochores, and the peak of the right kinetochore. In PRC1-depleted cells, signal intensity at all three positions was significantly lower compared to control cells ($p = 0.0001$, $p < 0.0001$, and $p = 0.0058$, respectively) (Figure 22d), confirming a consistent reduction in Borealin localization throughout the inter-kinetochore region.

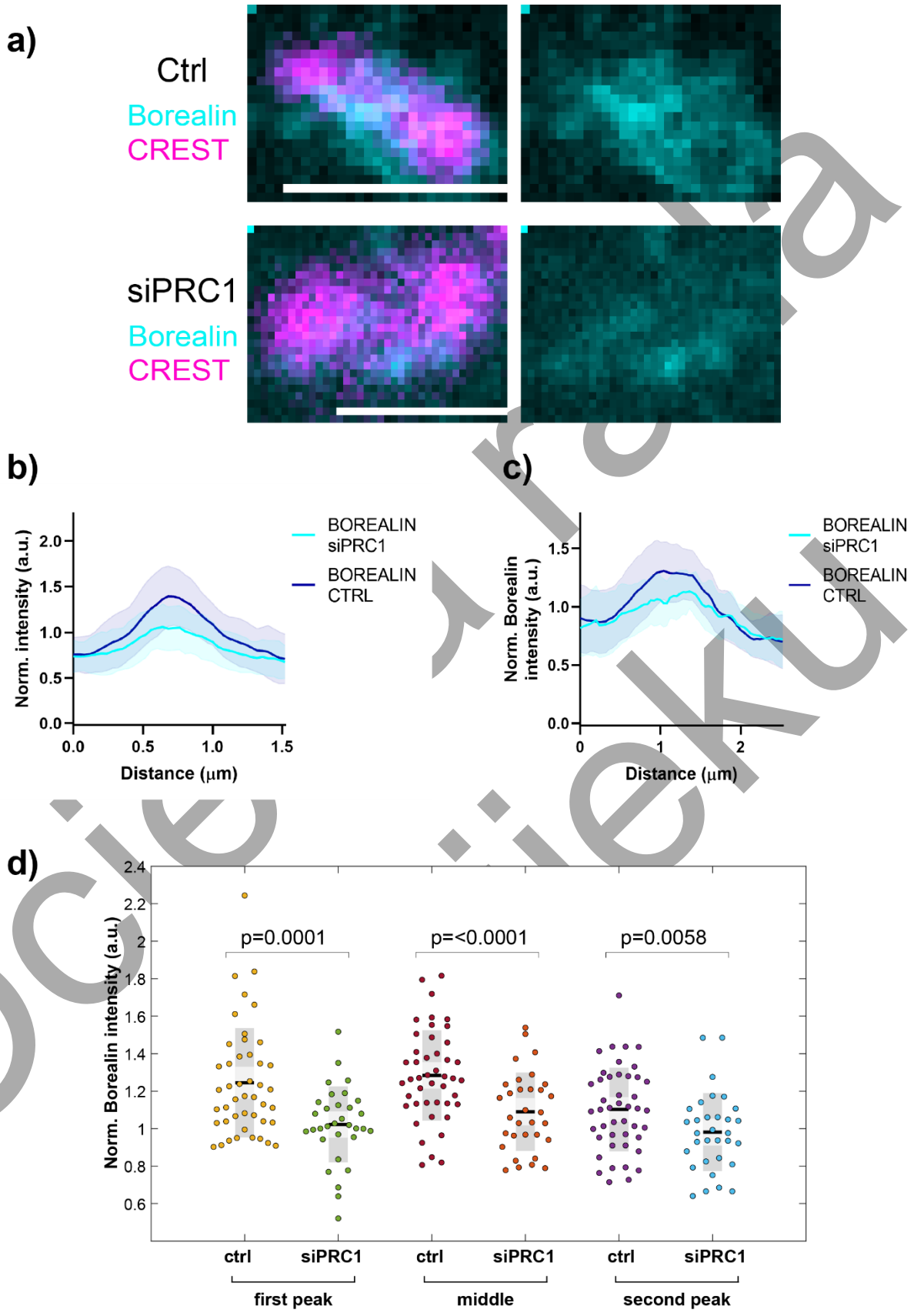

Figure 22. PRC1 depletion alters Borealin distribution at kinetochores. **a)** Representative images of kinetochore pairs from a control cell and a PRC1-depleted HeLa cell, immunostained for Borealin (cyan, imaged with STED) and CREST (magenta, imaged with confocal

microscopy). Merged channels and only Borealin are shown. **b)** Comparison of vertical line intensity profiles of Borealin between control cells (n = 45) and PRC1-depleted HeLa cells (n = 32). **c)** Comparison of horizontal line intensity profiles of Borealin between control cells (n = 45) and PRC1-depleted cells (n = 32). **d)** Borealin signal intensity measured at three defined positions: the first point corresponds to the maximum CREST signal of the left kinetochore, the second point to the midpoint between the kinetochores, and the third to the maximum CREST signal of the right kinetochore. Measurements were performed for both control (n = 45) and PRC1-depleted cells (n = 32). In panel d), the black line represents the mean, and the light and dark gray areas indicate the 95% confidence interval and standard deviation, respectively. Statistical analysis was performed using a one-way ANOVA test and Tukey's HSD post hoc test; p-values indicating significant differences are shown. In panels b) and c), central lines represent the mean, and shaded areas represent standard deviation. Cells were analyzed as illustrated in Figure 19, panel g. All data were obtained from at least three independent experiments per condition. All measurements were normalized to the mean intensity obtained from control cells. All scale bars: 1 μm.

To validate the efficiency of PRC1 depletion and ensure that changes in Borealin signal were not due to technical variability or altered kinetochore structure, we performed control experiments presented in Figure 23. Immunostaining confirmed that PRC1 signal was effectively reduced by siRNA treatment, with a 95.09% decrease in PRC1 intensity compared to control cells, verifying successful depletion (Figure 23a-b). In contrast, CREST signal intensity, used to label kinetochores, remained unchanged between control and PRC1-depleted cells, indicating that kinetochore staining was stable and comparable across conditions (Figure 23c-d). These results confirm that the observed reduction in Borealin intensity is specifically due to PRC1 depletion rather than differences in kinetochore staining or global signal variability. Taken together, these results demonstrate that PRC1 depletion not only reduces overall centromeric accumulation of Borealin but also alters its spatial organization at the kinetochore interface. The diminished and dispersed signal suggests that PRC1-labeled antiparallel microtubule bundles not only facilitate CPC recruitment but also help concentrate and maintain Borealin in a spatially restricted domain at the inner centromere. This loss of structural guidance may impair the CPC's ability to efficiently access its kinetochore substrates, thereby compromising its role in error correction.

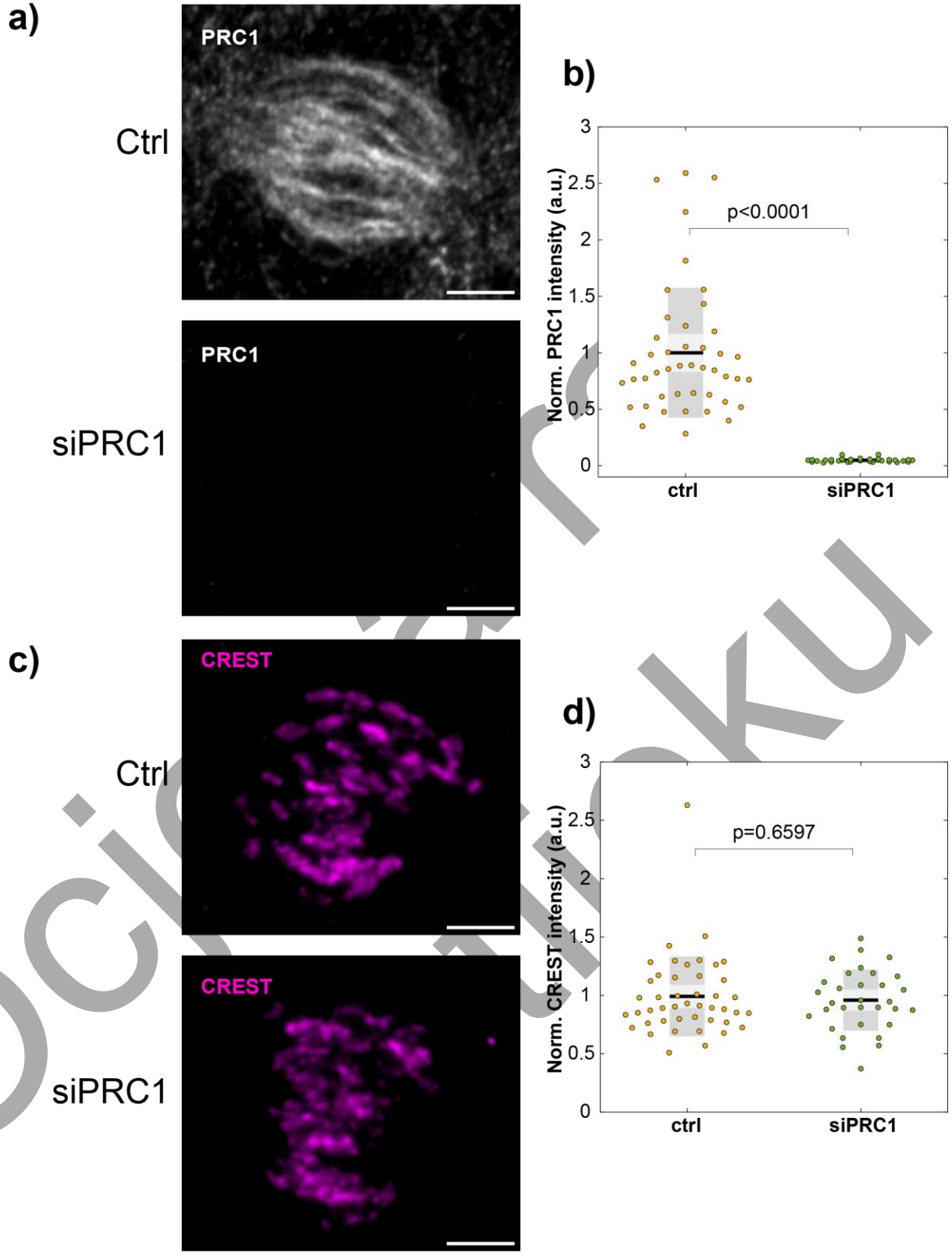

Figure 23. Validation of PRC1 depletion and assessment of CREST signal stability in PRC1-depleted cells used for Borealin intensity analysis. **a)** Confocal images of maximum-intensity projections of prometaphase spindles in control and PRC1-depleted HeLa cells immunostained for PRC1, illustrating the reduction of PRC1 signal following siRNA treatment. **b)** Normalized PRC1 intensity in control cells (n = 45) and PRC1-depleted cells (n = 32). The graph shows a

95.09% reduction in PRC1 signal intensity in PRC1-depleted cells. **c)** Confocal images of maximum-intensity projections of prometaphase spindles in control and PRC1-depleted HeLa cells immunostained for CREST, used to label kinetochores. **d)** Normalized CREST intensity in control cells (n = 45) and PRC1-depleted cells (n = 32). The graph shows that there was no significant change in CREST signal intensity between the two conditions. The black line represents the mean, and the light and dark grey areas indicate the 95% confidence interval and standard deviation, respectively, and p values from a two-tailed t-test are given. All data were obtained from at least three independent experiments per condition. All measurements were normalized to the mean intensity obtained from control cells. All scale bars: 4 μm.

Following the analysis of Borealin distribution, we next examined whether Aurora B exhibits similar changes in localization upon PRC1 depletion. Using STED microscopy, we analyzed Aurora B distribution in control and PRC1-depleted HeLa cells immunostained for Aurora B and CREST. Representative kinetochore pairs from both conditions are shown in Figure 24a. To assess the spatial organization of Aurora B, we conducted both vertical and horizontal analyses. In control cells, vertical line profiles revealed a strong Aurora B signal concentrated between kinetochores. This signal was significantly reduced and dispersed in PRC1-depleted cells (Figure 24b). Horizontal profiles showed that Aurora B was sharply enriched at the inner centromere in control cells, while in PRC1-depleted cells, the signal broadened and declined in intensity, suggesting impaired centromeric targeting (Figure 24c). To quantify this redistribution, we also measured the signal at three defined points along the kinetochore axis, using the same approach as described for Borealin. In PRC1-depleted cells, Aurora B intensity was significantly lower at all three positions compared to controls ($p = 0.0219$, $p = 0.0018$, and $p = 0.0018$, respectively) (Figure 24d). These results indicate that Aurora B, like Borealin, relies on PRC1-labeled overlap bundles for proper enrichment and spatial confinement along the centromere-kinetochore axis.

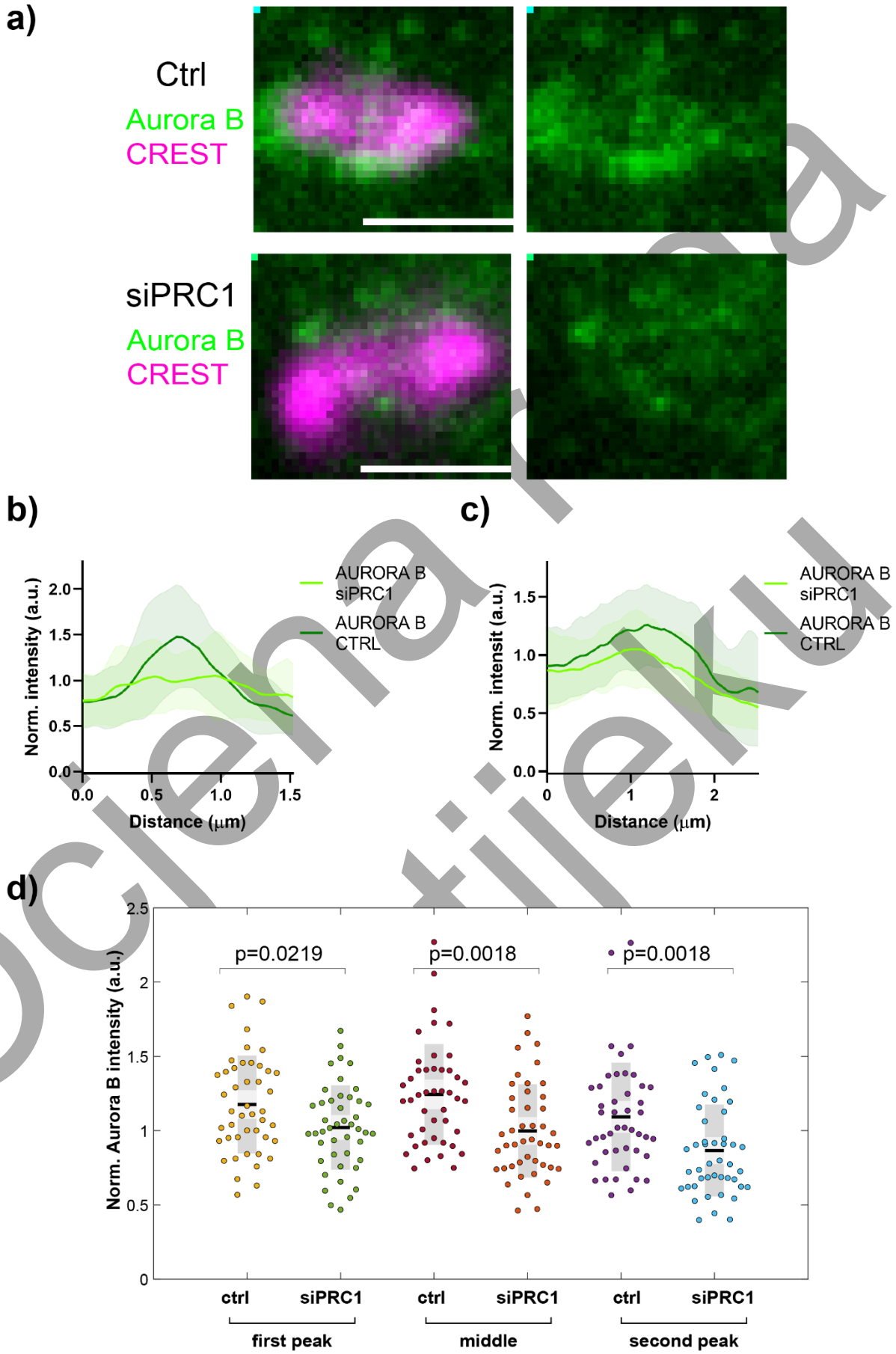

Figure 24. PRC1 depletion alters Aurora B distribution at kinetochores. **a)** Representative images of kinetochore pairs from a control cell and a PRC1-depleted HeLa cell, immunostained for Aurora B (green, imaged with STED) and CREST (magenta, imaged with confocal microscopy). Merged channels and only Aurora B are shown. **b)** Comparison of vertical line intensity profiles of Aurora B between control cells (n = 45) and PRC1-depleted HeLa cells (n = 45). **c)** Comparison of horizontal line intensity profiles of Aurora B between control cells (n = 45) and PRC1-depleted cells (n = 45). **d)** Aurora B signal intensity measured at three defined positions: the first point corresponds to the maximum CREST signal of the left kinetochore, the second point to the midpoint between the kinetochores, and the third to the maximum CREST signal of the right kinetochore. Measurements were performed for both control (n = 45) and PRC1-depleted cells (n = 45). In panel d), the black line represents the mean, and the light and dark gray areas indicate the 95% confidence interval and standard deviation, respectively. Statistical analysis was performed using a one-way ANOVA test and Tukey's HSD post hoc test; p-values indicating significant differences are shown. In panels b) and c), central lines represent the mean, and shaded areas represent standard deviation. Cells were analyzed as illustrated in Figure 19, panel g. All data were obtained from at least three independent experiments per condition. All measurements were normalized to the mean intensity obtained from control cells. All scale bars: 1 μm.

To ensure that the observed changes were specific to Aurora B localization and not due to experimental variability, we validated the efficiency of PRC1 depletion and the stability of the CREST signal (Figure 25). PRC1 intensity was reduced by 97.97% in PRC1-depleted cells relative to controls (Figure 25a-b), confirming efficient depletion. Importantly, CREST intensity remained unchanged between the two conditions (Figure 25c-d), verifying that kinetochore detection was consistent. These controls support the conclusion that the observed redistribution of Aurora B is a direct consequence of PRC1 depletion. Together, our findings reveal that PRC1-mediated antiparallel microtubule overlaps play a role in directing the spatial distribution of the CPC components Borealin and Aurora B during early mitosis. We show that depletion of PRC1 disrupts the centromeric enrichment of both proteins, leading to reduced signal intensity and altered localization patterns at kinetochores. These defects are accompanied by a broader and less confined CPC distribution, suggesting that overlap bundles not only serve as structural elements but also act as scaffolds that promote proper CPC positioning and may be critical for ensuring the fidelity of chromosome segregation during mitosis.

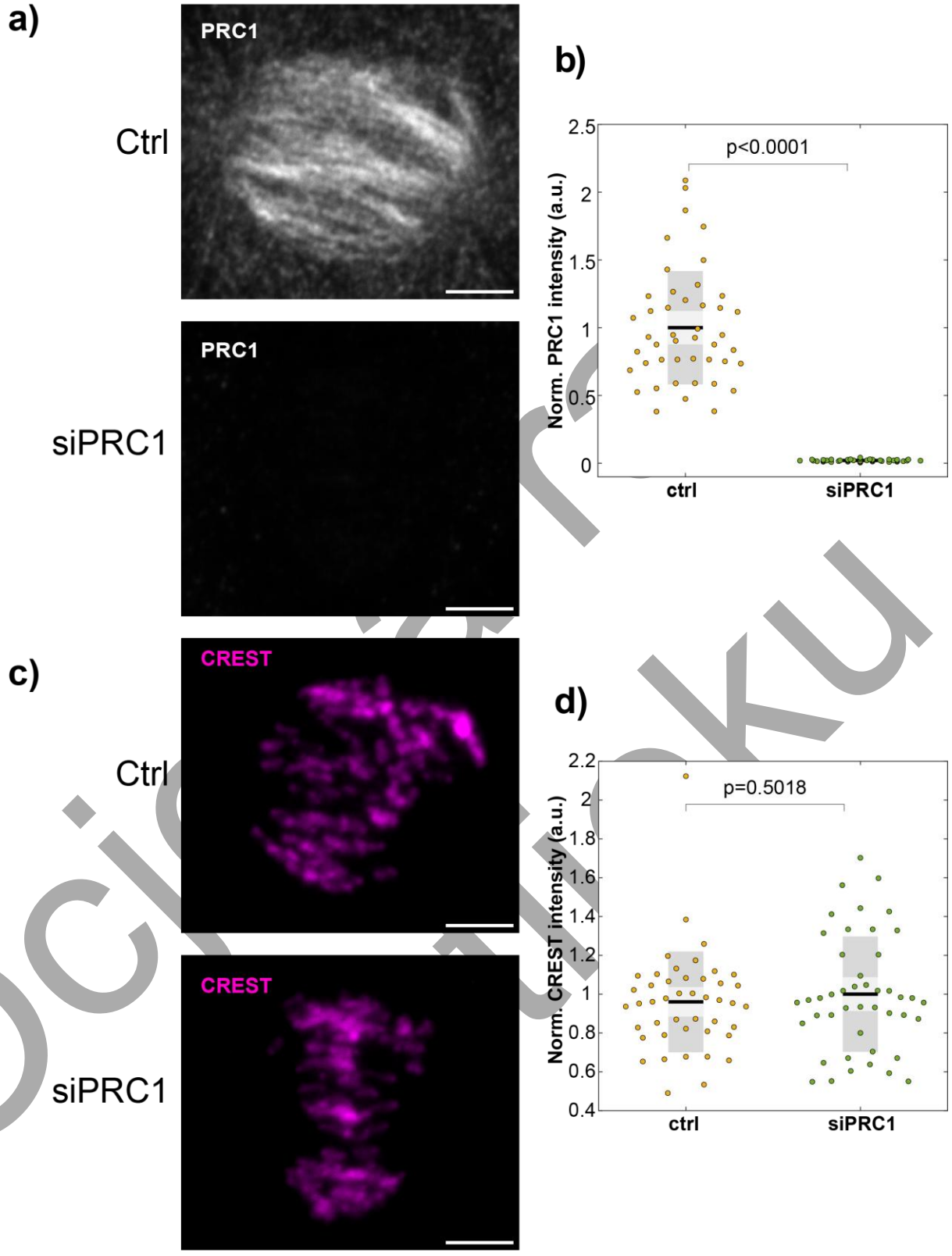

Figure 25. Validation of PRC1 depletion and assessment of CREST signal stability in PRC1-depleted cells used for Aurora B intensity analysis **a)** Confocal images of maximum-intensity projections of prometaphase spindles in control and PRC1-depleted HeLa cells immunostained for PRC1, illustrating the reduction of PRC1 signal following siRNA treatment. **b)** Normalized PRC1 intensity in control cells (n = 45) and PRC1-depleted cells (n = 45). The graph shows a

97.97% reduction in PRC1 signal intensity in PRC1-depleted cells. **c)** Confocal images of maximum-intensity projections of prometaphase spindles in control and PRC1-depleted HeLa cells immunostained for CREST, used to label kinetochores. **d)** Normalized CREST intensity in control cells (n = 45) and PRC1-depleted cells (n = 45). The graph shows that there was no significant change in CREST signal intensity between the two conditions. The black line represents the mean, and the light and dark grey areas indicate the 95% confidence interval and standard deviation, respectively, and p values from a two-tailed t-test are given. All data were obtained from at least three independent experiments per condition. All measurements were normalized to the mean intensity obtained from control cells. All scale bars: 4 μm.

4.4 PRC1-Mediated Overlaps Support Kinetochore Phosphorylation

To further explore the functional significance of overlap bundles, we focused on understanding how overlap bundles influence chromosome segregation fidelity. Previous studies have shown that during prometaphase, microtubules positioned near the centromere region can enhance kinetochore phosphorylation, thereby facilitating the correction of erroneous kinetochore-microtubule attachments. This phosphorylation dependent error correction mechanism is partly mediated by Borealin, a CPC subunit with microtubule-binding activity (93). Based on this, we hypothesized that overlap bundles crosslinked by PRC1 are essential not only for forming the structural scaffold near the centromeres but also for actively supporting the error correction machinery. In this model, Aurora B kinase, not only contributes to the formation of these antiparallel microtubule overlaps (71) but also utilizes them as directional tracks to reach its kinetochore targets. Once localized, Aurora B can phosphorylate specific substrates at kinetochores to destabilize incorrect attachments, thereby promoting accurate biorientation (Figure 26a). To experimentally test this hypothesis, first we depleted PRC1 using siRNA. This allowed us to assess the contribution of overlap bundles independently from the general spindle structure. To assess Aurora B kinase activity at the kinetochore, we measured the phosphorylation of serine 7 (Ser7) on the histone variant CENP-A, a well-established Aurora B substrate (197). Following PRC1 depletion, we observed a marked and statistically significant decrease in Ser7 phosphorylation levels, indicating that the removal of overlap bundles compromises Aurora B-mediated phosphorylation events at kinetochores (Figure 26b-c). These results support our model that PRC1-crosslinked antiparallel microtubule overlaps play an active role in ensuring accurate chromosome segregation by facilitating the localization and accessibility of Aurora B to their kinetochore targets.

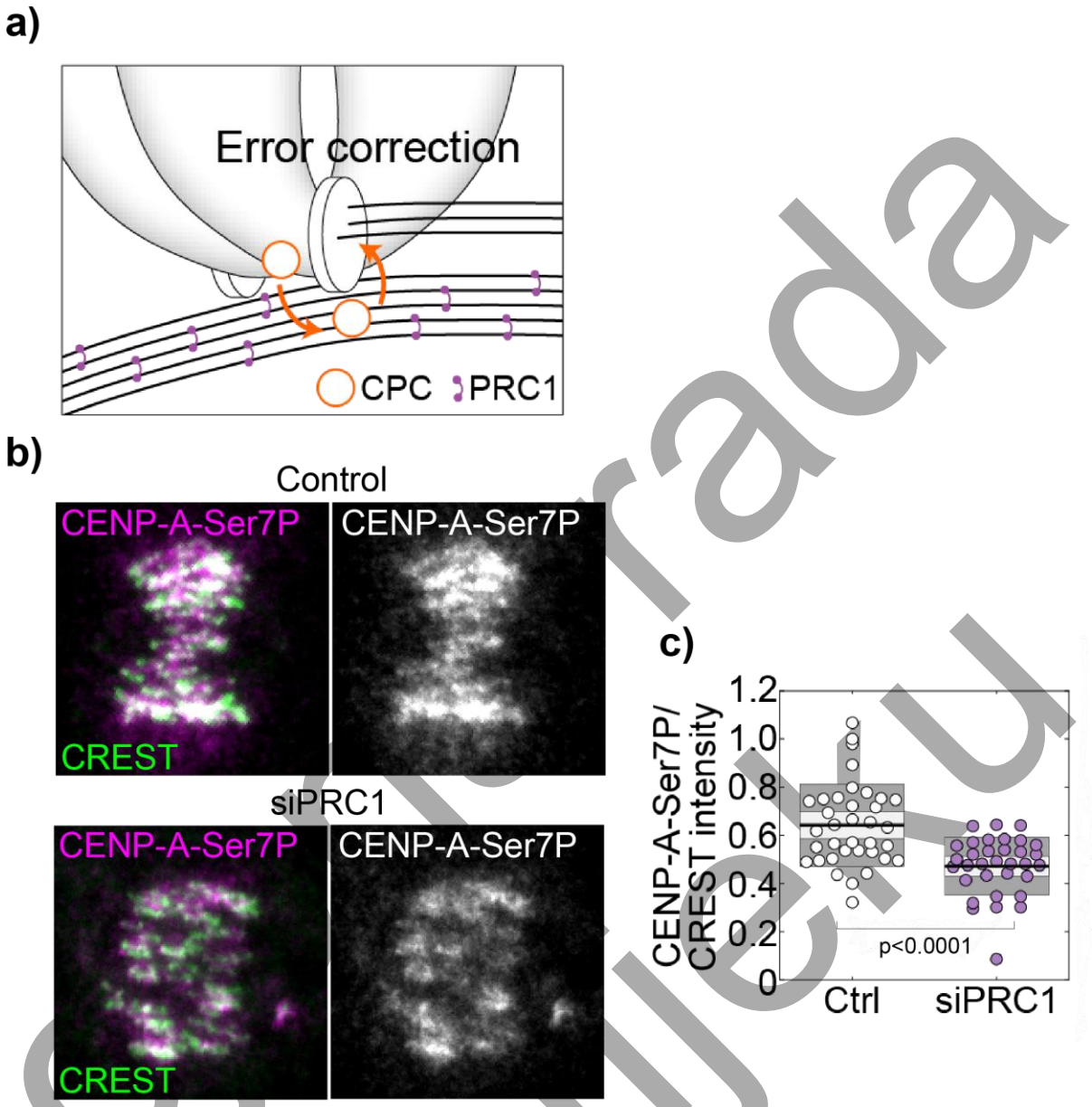

Figure 26. Antiparallel overlaps promote kinetochore phosphorylation by Aurora B **a)** Schematic illustration of the hypothesis that antiparallel overlaps act as tracks facilitating Aurora B access to kinetochore components, enabling their phosphorylation and the correction of erroneous attachments. **b)** Images showing anti-CENP-A-Ser7P (magenta) and CREST (green) in control and PRC1-depleted HeLa cells, merged channels and only anti-CENP-A-Ser7P in white are shown. **c)** Ratio between anti-CENP-A-Ser7P and CREST in control (n=36) and PRC1-depleted cells (n=33). The black line represents the mean, and the light and dark grey areas indicate the 95% confidence interval and standard deviation, respectively, and p value from a two-tailed t-test is given. All data were obtained from at least three independent experiments per condition. All scale bars: 1 µm. *The data were published in Matković et al., 2022.

4.5 Overlap Bundle Disruption Impairs Timely Mitotic Transition

To investigate the functional consequences of impaired CPC localization due to PRC1 depletion, we examined whether overlap bundle disruption impacts mitotic progression following monastrol washout. Monastrol treatment induces the formation of monopolar spindles and stabilizes erroneous kinetochore-microtubule attachments, particularly syntelic ones (49). Upon drug washout, bipolar spindles reform and error correction must occur efficiently for cells to proceed through mitosis. We hypothesized that the disruption of PRC1-crosslinked overlap bundles may interfere with timely error correction and thus delay mitotic progression. To test this, we synchronized HeLa cells using monastrol and fixed them at three defined time points (15, 30, and 45 minutes) after washout, with or without prior PRC1 depletion (Figure 27a). Cells were then classified based on mitotic stage using morphological markers: early prometaphase, late prometaphase, metaphase, and anaphase (Figure 27b). Quantification of mitotic phase distribution at each time point revealed a delay in mitotic progression in PRC1-depleted cells compared to controls. At 15 minutes post-washout, control cells already showed a significant proportion in anaphase (66/356 cells), whereas PRC1-depleted cells had fewer cells in anaphase (23/349) and a higher fraction retained in early prometaphase (118/349 compared to 64/356 in controls) (Figure 27c). This trend continued at 30 minutes, where control cells progressed toward metaphase and anaphase, but PRC1-depleted cells remained largely in late prometaphase (237/392 vs. 193/471 in controls) and displayed reduced transition into anaphase (24/392 vs. 76/471 in controls) (Figure 27d). Even at 45 minutes post-washout, PRC1-depleted cells exhibited delayed mitotic progression, with fewer anaphase figures (53/322) compared to controls (78/352), and a marked increase in late prometaphase figures (105/322 vs. 58/352). The overall mitotic phase distribution was significantly altered between the two conditions, further supporting that PRC1 depletion impairs timely progression through mitosis (Figure 27e). These delays were statistically significant as determined by z-score tests for population proportions. To confirm that PRC1 was effectively depleted in these experiments, we immunostained for PRC1 and observed a strong reduction in signal intensity in PRC1 siRNA-treated cells (Figure 27f). Quantitative analysis revealed a 99.33% decrease in PRC1 intensity compared to controls (Figure 27g), confirming the effectiveness of the siRNA treatment. Together, these data indicate that PRC1 depletion significantly impairs mitotic progression following monastrol washout. The increased retention of cells in prometaphase stages and reduced entry into anaphase suggest that PRC1-crosslinked overlap bundles, through their role in CPC positioning and kinetochore phosphorylation, contribute to the timely correction of erroneous attachments. This supports the model in which microtubule overlap architecture facilitates efficient activation of error correction pathways and proper mitotic timing.

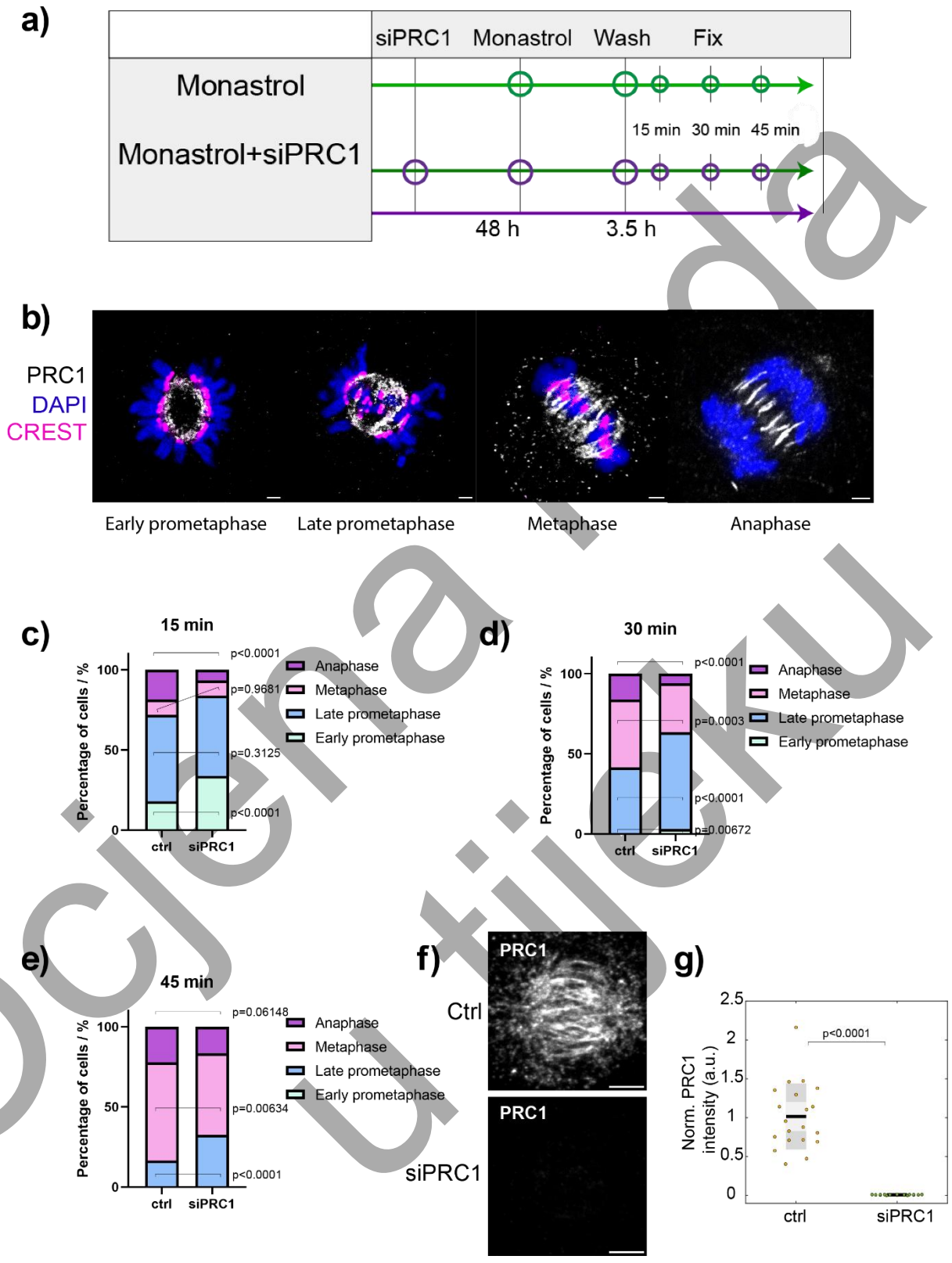

Figure 27. PRC1 depletion delays mitotic progression after monastrol washout. a) Schematic overview of the experimental protocol using monastrol washout to induce an increased frequency of erroneous kinetochore-microtubule attachments during prometaphase. Cells were fixed at multiple time points following washout (15, 30, and 45 minutes). b) Confocal images of HeLa cells at different stages of mitosis (early prometaphase, late prometaphase, metaphase,

and anaphase) used as classification references in this experiment. Single plane images of merged channels are shown. Cells were immunostained for PRC1 (white), CREST (magenta), and DAPI (blue). *In anaphase, only PRC1 and DAPI are shown. c) Quantification of mitotic phase distribution in control (n=356, early prometaphase 64/356, late prometaphase 192/356, metaphase 34/356, anaphase 66/356) and PRC1-depleted (n= 349, early prometaphase 118/349 late prometaphase 175/349, metaphase 33/349, anaphase 23/349) HeLa cells 15 minutes after monastrol washout. d) Quantification of mitotic phase distribution in control (n= 471, early prometaphase 3/ 471, late prometaphase 193/ 471, metaphase 199/ 471, anaphase 76/ 471) and PRC1-depleted (n=392, early prometaphase 12/392, late prometaphase 237/392, metaphase 119/392, anaphase 24/392) HeLa cell 30 min after monastrol washout. e) Quantification of mitotic phase distribution in control (n= 352, late prometaphase 58/352, metaphase 216/352, anaphase 78/352) and PRC1-depleted (n= 322, late prometaphase 105/322, metaphase 164/322 i anaphase 53/322) HeLa cell 45 min after monastrol washout. No early prometaphase cells were observed at this time point. f) Confocal images of maximum-intensity projections of prometaphase spindles in control and PRC1-depleted HeLa cells immunostained for PRC1, illustrating the reduction of PRC1 signal following siRNA treatment used in these experiments. g) Normalized PRC1 intensity in control cells (n = 20) and PRC1-depleted cells (n = 20). The graph shows a 99.33% reduction in PRC1 signal intensity in PRC1-depleted cells. All data were obtained from at least three independent experiments per condition. P-values in panels c), d), and e) were determined using a z-score test for two population proportions. In panel g), the black line represents the mean, and the light and dark grey areas indicate the 95% confidence interval and standard deviation, respectively, and p value from a two-tailed t-test is given. Scale bars for b): 2 μm. Scale bars for f): 4 μm

4.6 PRC1 depletion increases the frequency and extent of chromosome misalignment following monastrol washout

To further examine how overlap bundles contribute to mitotic accuracy, we analyzed the effect of PRC1 depletion on chromosome alignment after monastrol washout, which generates a high frequency of erroneous kinetochore-microtubule attachments in prometaphase. To quantify alignment defects, HeLa cells were classified based on the number of unaligned chromosomes, with representative examples shown in Figure 28a. Immunostaining was performed using antibodies against PRC1 and CREST, with DAPI used to label DNA, and unaligned chromosomes were subsequently manually detected and annotated based on their position outside the metaphase plate. Quantification revealed a significant increase in the percentage of PRC1-depleted cells exhibiting unaligned chromosomes compared to controls. At 30 minutes post-washout, 22.67% (73/322) of PRC1-depleted cells showed misalignment, in contrast to 9.98% (47/471) of control cells (Figure 28b). A similar trend was observed at 45 minutes, where 25.5% (82/322) of PRC1-depleted cells displayed misalignment versus 14.5% (51/352) in controls (Figure 28c), suggesting persistent alignment defects in the absence of PRC1. To better assess the extent of these defects, we further subdivided cells with unaligned chromosomes into four categories based on the number of unaligned chromosomes (1; 2; 3 or 4; or more than 4), as illustrated in Figure 28a. At 30 minutes, most control cells with misalignment had only one or two unaligned chromosomes, whereas PRC1-depleted cells displayed a shift toward more severe misalignment. Specifically, 10.87% of PRC1-depleted cells had three or more

unaligned chromosomes compared to only 3.18% of control cells (Figure 28d). A similar trend was maintained at 45 minutes: 12.42% of PRC1-depleted cells had three or more unaligned chromosomes compared to 6.53% in controls (Figure 28e). Together, these results demonstrate that PRC1 depletion not only increases the frequency of misaligned chromosomes but also leads to more pronounced chromosome misalignment. This supports the model that PRC1-mediated overlap bundles play a critical role in promoting efficient error correction and chromosome congression during mitosis.

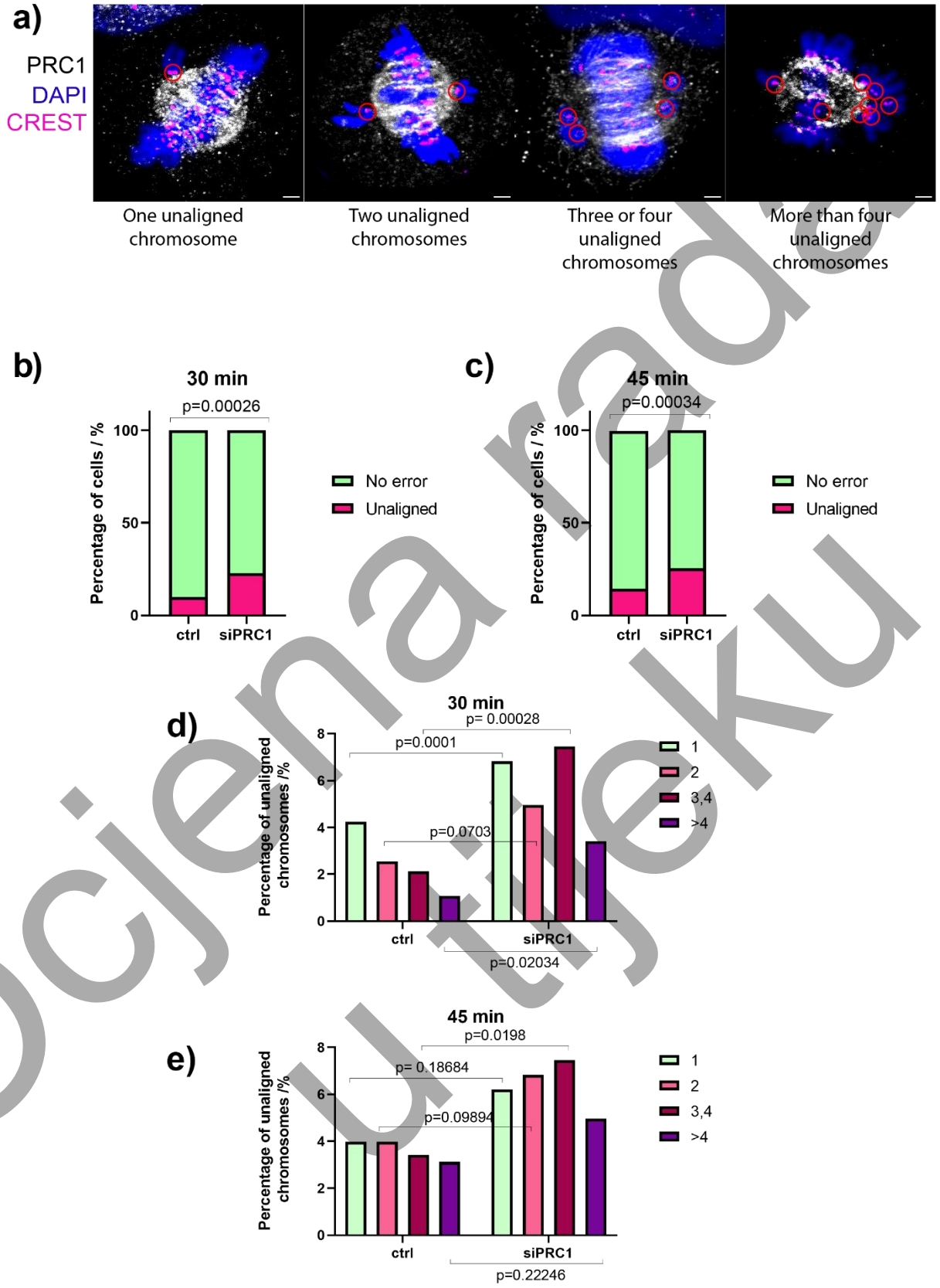

Figure 28. PRC1 depletion increases the frequency and degree of chromosome misalignment following monastrol washout**. a)** Confocal images of HeLa cells with different numbers of unaligned chromosomes, used as classification references in this experiment. Merged channels

are shown. Cells were immunostained for PRC1 (white), CREST (magenta), and DAPI (blue). Unaligned chromosomes are circled. **b)** Quantification of the percentage of cells with unaligned chromosomes in control (n = 47/471) and PRC1-depleted (n = 73/322) HeLa cells 30 minutes after monastrol washout. **c)** Quantification of the percentage of cells with unaligned chromosomes in control (n = 51/352) and PRC1-depleted (n = 82/322) HeLa cells 45 minutes after monastrol washout. **d)** Further classification of cells from panel b) based on the number of unaligned chromosomes, as shown in panel a). Percentages are shown for control (n= 471, one unaligned chromosome 20/471, two 12/471, three or four 10/471, more than four 5/471) and PRC1-depleted (n= 322, one 22/322, two 16/322, three or four 24/322, more than four 11/322) HeLa cells 30 minutes after monastrol washout. **e)** Further classification of cells from panel c) based on the number of unaligned chromosomes, as shown in panel a). Percentages are shown for control (n= 352, one unaligned chromosome 14/352, two 14/352, three or four 12/352, more than four 11/352) and PRC1-depleted (n= 322, one 20/322, two 22/322, three or four 24/322, more than four 16/322) HeLa cells 45 minutes after monastrol washout. All data were obtained from at least three independent experiments per condition. P-values were determined using a z-score test for two population proportions. All scale bars: 2 μm.

4.7 Antiparallel Microtubule Overlaps Are Required for Efficient Correction of Erroneous Attachments

To further investigate the impact of PRC1-mediated overlap bundles on chromosome segregation fidelity, we next focused on analyzing the frequency of lagging chromosomes during anaphase. This analysis followed the previous assessment of unaligned chromosomes and aimed to determine whether impaired overlap bundle formation affects the correction of erroneous K-MT attachments. We performed immunofluorescence staining to visualize kinetochores and DNA in anaphase cells and quantified the incidence of lagging kinetochores across four different experimental conditions: control, PRC1 siRNA, monastrol washout alone, and combined PRC1 siRNA with monastrol washout (Figure 29a). In control cells, lagging chromosomes were rare (1%), while in PRC1-depleted cells this frequency increased slightly to 3.5%, suggesting that the reduction of overlap bundles already compromises segregation fidelity to some extent (Figure 28c). To more rigorously challenge the error correction machinery, we next combined PRC1 depletion with monastrol washout, which generates a high incidence of syntelic attachments that need to be resolved before anaphase onset (49). We then quantified the frequency of lagging kinetochores in anaphase as a readout of error correction efficiency (Figure 28b). In control cells treated with monastrol, only 2.3% of anaphases contained lagging kinetochores, indicating that error correction mechanisms operate efficiently when overlap bundles are intact. However, when PRC1 was depleted in combination with monastrol treatment, the frequency of lagging kinetochores rose significantly to 10.8% (Figure 28c). This pronounced increase strongly supports the notion that PRC1-crosslinked overlap bundles facilitate the correction of erroneous attachments and help maintain chromosome segregation fidelity. Taken together, these findings build on the previous observation that PRC1 depletion increases the number and severity of misaligned chromosomes and establishes a direct functional role for overlap bundles in error correction. Specifically, our data supports a model in which antiparallel overlaps act as spatial organizers that guide Aurora B kinase to kinetochore substrates. By promoting effective kinetochore phosphorylation, these overlap

bundles enable the correction of attachment errors and safeguard genomic stability during mitosis.

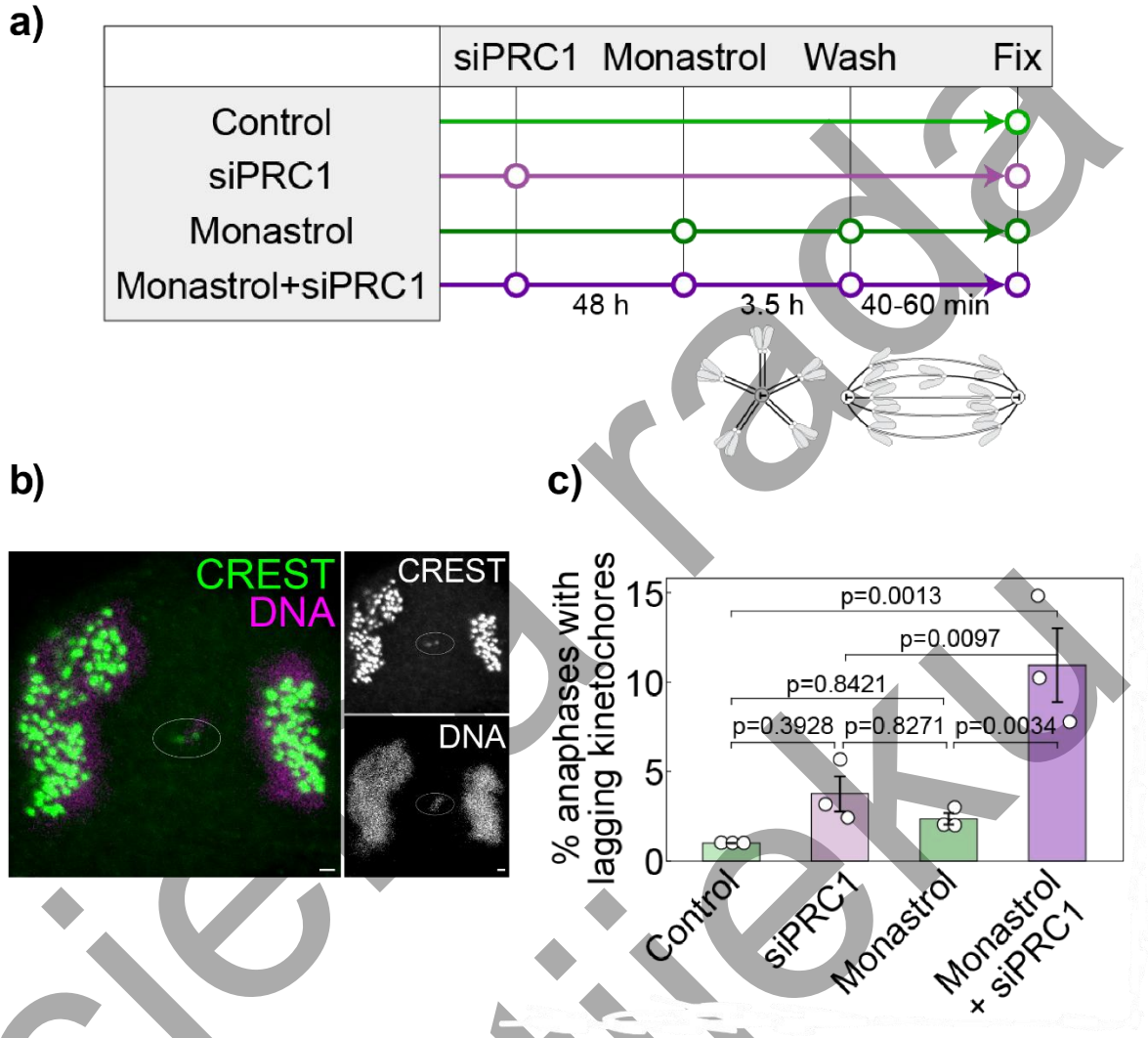

Figure 29. PRC1-mediated overlap bundles contribute to correction of erroneous attachments. **a)** Schematic overview of the experimental protocol using monastrol washout to induce an increased frequency of erroneous kinetochore-microtubule attachments during prometaphase. **b)** Representative image of a lagging chromosome (circled) observed during anaphase in a PRC1-depleted HeLa cell following monastrol washout. The left panel shows a merged image of CREST (green) and DNA (magenta); the right panel displays individual channels in grayscale. **c)** Quantification of lagging kinetochore frequency in four experimental conditions: control (3/299 anaphases), PRC1 siRNA (8/231), monastrol washout (7/298), and combined PRC1 siRNA with monastrol washout (28/259). Data was collected from three independent immunostaining experiments per condition. Statistical analysis was performed using a one-way ANOVA test and Tukey's HSD post hoc test; p-values indicating significant differences are shown. Error bars represent standard error of the mean (s.e.m). Circles represent the means of three independent immunostaining experiments. All scale bars: 1 μm. *The data were published in Matković et al., 2022.

5. DISCUSSION

5.1 1. PRC1-crosslinked Overlap Bundles as Scaffolds for CPC Localization

Our study highlights the essential role of PRC1-crosslinked overlap bundles in guiding the spatial distribution of the Chromosomal Passenger Complex (CPC) during mitosis. These findings are consistent with previous models that emphasize the role of microtubule architecture in supporting regulatory complexes during mitotic progression. Overlap bundles, composed of antiparallel microtubules extending from opposite spindle poles (33,34), are known to support accurate chromosome segregation by contributing to proper spindle architecture and balanced tension at kinetochores (15,35,38,51–53). The microtubules within bridging fibers are crosslinked by PRC1, a conserved non-motor protein that preferentially binds antiparallel microtubules (35,53,59–61,63,66). Inhibition of Eg5/kinesin-5, which separates antiparallel microtubules, results in monopolar spindles that retain kinetochore fibers but lack overlap bundles, demonstrating the essential function of overlap bundles in spindle architecture (47,48,50,50). In our previous work, we demonstrated that kinetochores and microtubule crosslinkers orchestrate the transformation of the mitotic spindle from a disordered microtubule network into organized overlap bundles, a structural transition essential for accurate chromosome segregation during cell division. This reorganization is driven by the redistribution and bundling activity of PRC1, as well as lateral interactions between kinetochores and microtubules, mediated by the kinesin motor CENP-E and regulated by Aurora B kinase. Additionally, steric interactions between chromosomes contribute to the separation of these bundles (71). In addition to their established functions, we propose that overlap bundles also support the localization of CPC components, including Borealin and Aurora B, particularly during prometaphase. This localization is critical, as CPC-driven error correction is most active when kinetochore-microtubule (K-MT) attachments are still forming. Using STED microscopy, we observed Borealin and Aurora B accumulation at the center of kinetochore pairs in prometaphase, where their signals overlapped with PRC1-labeled overlaps. This colocalization was more focused in early mitosis and became broader in metaphase, consistent with the idea that overlap bundles guide CPC recruitment when error correction is most needed. Borealin, which contains a microtubule-binding domain (97), may directly tether the CPC to PRC1-positive regions, reinforcing CPC activity at the inner centromere. The presence of antiparallel microtubules at these sites may provide a localized scaffold that facilitates CPC accumulation and Aurora B kinase activation. Importantly, our findings align with the reaction-diffusion model, which proposes that CPC activity can spread from the inner centromere to kinetochores via microtubules. Trivedi et al. 2019. demonstrated that centromere-proximal microtubules enhance CPC phosphorylation activity at kinetochores even in the absence of interkinetochore tension, supporting our hypothesis that overlap bundles serve as CPC scaffolds independent of mechanical stretch (97). Our results are also consistent with reports showing that Borealin mutants lacking the microtubule-binding domain fail to properly localize CPC and impair its phosphorylation of kinetochore targets (97). Furthermore, CPC enrichment at the centromere is regulated not only by chromatin modifications such as H3T3ph and H2AT120ph (145,146,148,149,166,167) but also by microtubule interactions (172,183,184,186,187). We propose that PRC1-marked overlaps act as structural docking sites

that facilitate CPC accumulation at the inner centromere, enabling rapid response to erroneous attachments. This recruitment mechanism likely acts in parallel with histone modifications and INCENP-HP1 interactions that also contribute to CPC centromeric localization (198–200). To further assess how PRC1 influences the localization of CPC components at kinetochores, we performed spatial analysis of Borealin and Aurora B intensity profiles across kinetochore pairs. In PRC1-depleted cells, both proteins showed reduced signal intensity and broader distribution, particularly in the horizontal axis. These changes suggest that PRC1-crosslinked overlaps help concentrate CPC activity within the narrow centromeric zone between sister kinetochores. This spatial precision is crucial for error correction. In the absence of overlap bundles, Aurora B and Borealin may fail to reach or maintain proximity to their kinetochore substrates, disrupting spatially restricted kinase activity.

5.2 Role of Overlap Bundles in CPC-Driven Correction of Erroneous Attachments

Accurate chromosome segregation relies on the formation of proper kinetochore-microtubule attachments and the efficient correction of errors. The CPC, particularly its kinase subunit Aurora B, is a key player in detecting and correcting incorrect attachments such as syntelic and merotelic configurations (112,121,138,144,163). In our study, we explored whether PRC1-crosslinked overlap bundles contribute to this correction process. To evaluate CPC function under conditions of PRC1 depletion, we measured phosphorylation of CENP-A at Ser7, a direct Aurora B target (197). A significant reduction in CENP-A phosphorylation was observed following PRC1 depletion, indicating compromised Aurora B activity at kinetochores. This supports the model in which overlap bundles facilitate both the spatial positioning and catalytic activation of Aurora B. Without these scaffolds, Aurora B may not accumulate sufficiently at kinetochores to phosphorylate critical substrates involved in attachment correction and checkpoint activation (97,97,121). To functionally assess error correction, we induced syntelic attachment errors using monastrol, followed by drug washout to allow bipolar spindle reformation. We analyzed mitotic progression following monastrol washout. PRC1-depleted cells exhibited delayed transitions from prometaphase to metaphase and from metaphase to anaphase. This delay correlated with increased proportions of cells arrested in prometaphase and reduced numbers entering anaphase. While these results are consistent with impaired CPC activity due to the loss of overlap bundles, we cannot exclude the possibility that PRC1 has additional mitotic roles that independently contribute to the observed delay in mitotic progression. Beyond its role in recruiting and positioning the CPC, PRC1 is also essential for the assembly and maintenance of bridging fibers, key structural elements that stabilize spindle architecture and facilitate chromosome alignment. Disruption of these fibers through PRC1 depletion may compromise the mechanical integrity of the spindle and hinder timely spindle maturation. Thus, delayed formation of bipolar spindles and slower establishment of proper kinetochore-microtubule attachments in PRC1-depleted cells may reflect a combination of perturbed CPC activity and compromised spindle structure. We then quantified chromosome alignment defects and found that PRC1-depleted cells showed both a higher frequency and greater severity of unaligned chromosomes. These defects are consistent with previous models in which CPC mislocalization leads to failed error correction and prolonged checkpoint activation(112,115,121,138,163,176). Our data indicates that proper formation of overlap bundles is a prerequisite for timely mitotic progression and accurate chromosome biorientation.

In control cells, lagging chromosomes during anaphase were rare, but PRC1-depleted cells exhibited a substantial increase in lagging kinetochores. This phenotype became more pronounced under error-prone conditions. These findings suggest that overlap bundles facilitate the correction of error attachments by supporting Aurora B mediated phosphorylation of kinetochore substrates. In the absence of PRC1, Aurora B appears unable to access or phosphorylate its kinetochore targets efficiently, leading to persistent misattachments and segregation errors. This model is further supported by Trivedi et al. 2019, where their simulations and experimental data show that centromere-proximal microtubules enable robust phosphorylation of kinetochore substrates by serving as mediators for active Aurora B, particularly in merotelic attachment configurations. They also showed that the Borealin microtubule-binding domain is critical for this process, as its mutation resulted in both reduced kinetochore phosphorylation and an increase in segregation errors (97). This mechanistic link between CPC-microtubule interactions and the spatial reach of Aurora B activity strengthens the functional significance of PRC1-stabilized overlap bundles observed in our study. In summary, our findings demonstrate that PRC1-crosslinked antiparallel microtubule overlaps function as key scaffolds for the spatial and functional regulation of the CPC during mitosis. These structures support CPC centromeric enrichment, sharpen its spatial distribution, enhance its kinase activity, and promote effective correction of kinetochore-microtubule errors. Loss of overlap bundles via PRC1 depletion results in mislocalized CPC, impaired phosphorylation of substrates, delayed mitosis, and increased chromosome misalignment and segregation errors. Nonetheless, we cannot exclude the possibility that PRC1 contributes to mitotic fidelity through additional functions beyond CPC regulation, such as stabilizing spindle architecture through its role in bridging fiber formation. Thus, our work highlights both the direct regulatory role of microtubule-based architecture in CPC activity and the broader importance of overlap bundles in ensuring the structural and functional integrity of the mitotic spindle.

6. CONCLUSION

In this study, we investigated the role of PRC1-mediated antiparallel microtubule overlaps, also referred to as overlap bundles, in the spatial regulation and functional activity of the Chromosomal Passenger Complex (CPC) during mitosis. Using super-resolution STED microscopy and targeted PRC1 depletion, we demonstrated that these overlap bundles serve as critical scaffolds for the localization and activation of CPC components, particularly Borealin and Aurora B, at the inner centromere. We found that PRC1-labeled overlap bundles colocalize with Aurora B and Borealin during early mitosis, with this spatial association being most pronounced during prometaphase when kinetochore-microtubule (K-MT) attachments are still forming and error correction is most active. This spatial colocalization was disrupted upon PRC1 depletion, resulting in reduced centromeric accumulation of CPC components and broader, mislocalized CPC signal distributions. These findings support a model in which overlap bundles contribute not only to the structural integrity of the spindle but also to the fine-tuned positioning of CPC for effective error correction. Functionally, PRC1 depletion compromised Aurora B kinase activity, as indicated by reduced phosphorylation of CENP-A at Ser7, and led to delays in mitotic progression, increased frequencies of chromosome misalignment, and higher incidence of lagging chromosomes during anaphase. These phenotypes were especially evident under conditions that elevate erroneous attachments, such as monastrol washout, underscoring the importance of overlap bundles in tension-independent error correction pathways. Taken together, our data reveals a dual role for PRC1-crosslinked overlap bundles in mitosis: they provide a spatial framework that concentrates CPC components at the inner centromere and enhance Aurora B's ability to detect and correct K-MT attachment errors. These findings contribute to a deeper understanding of the interplay between spindle architecture and the biochemical regulation of chromosome segregation fidelity. Moreover, they emphasize the importance of microtubule-based scaffolds in coordinating spatial signaling mechanisms during cell division, insights that may have implications for understanding mitotic defects in cancer and for developing targeted therapeutic strategies.

7. REFERENCES

1. Alberts B, Heald R, Johnson A, Morgan D, Raff M, Roberts K, et al. Molecular biology of the cell. Seventh edition, international student edition. New York, NY London: W. W. Norton & Company; 2022. 1404 p.

2. Knouse KA, Davoli T, Elledge SJ, Amon A. Aneuploidy in Cancer: Seq-ing Answers to Old Questions. Annu Rev Cancer Biol. 2017 Mar 6;1(Volume 1, 2017):335–54.

3. Santaguida S, Amon A. Short- and long-term effects of chromosome mis-segregation and aneuploidy. Nat Rev Mol Cell Biol. 2015 Aug;16(8):473–85.

4. Webster A, Schuh M. Mechanisms of Aneuploidy in Human Eggs. Trends Cell Biol. 2017 Jan 1;27(1):55–68.

5. Hochegger H, Takeda S, Hunt T. Cyclin-dependent kinases and cell-cycle transitions: does one fit all? Nat Rev Mol Cell Biol. 2008 Nov;9(11):910–6.

6. Nezi L, Musacchio A. Sister chromatid tension and the spindle assembly checkpoint. Curr Opin Cell Biol. 2009 Dec 1;21(6):785–95.

7. Lodish H; Berk A; Kaiser CA; Krieger M; Bretscher A; Ploegh H; et al. Molecular Cell Biology. 7th ed. New York: W.H. Freeman; 2013.

8. Musacchio A, Desai A. A Molecular View of Kinetochore Assembly and Function. Biology. 2017 Mar;6(1):5.

9. McIntosh JR. Mitosis. Cold Spring Harb Perspect Biol. 2016 Sep 1;8(9):a023218.

10. Mogilner A, Craig E. Towards a quantitative understanding of mitotic spindle assembly and mechanics. J Cell Sci. 2010 Oct 15;123(20):3435–45.

11. Harris N; Oparka KJ. Plant Cell Biology: From Astronomy to Zoology. In Oxford: Oxford University Press; 2009.

12. Kaseda K, McAinsh AD, Cross RA. Dual pathway spindle assembly increases both the speed and the fidelity of mitosis. Biol Open. 2011 Oct 24;1(1):12–8.

13. McIntosh JR, Molodtsov MI, Ataullakhanov FI. Biophysics of mitosis. Q Rev Biophys. 2012 May;45(2):147–207.

14. Kirschner M, Mitchison T. Beyond self-assembly: From microtubules to morphogenesis. Cell. 1986 May 9;45(3):329–42.

15. Maiato H; Gomes AM; Sousa F; Barisic M. Mechanisms of chromosome congression during mitosis. Biology (Basel). 2017;6(1):13.

16. Musacchio A, Salmon ED. The spindle-assembly checkpoint in space and time. Nat Rev Mol Cell Biol. 2007 May;8(5):379–93.

17. Dumont S, Mitchison TJ. Force and Length in the Mitotic Spindle. Curr Biol. 2009 Sep 15;19(17):R749–61.

18. McIntosh JR. Anaphase A: Disassembling Microtubules Move Chromosomes toward Spindle Poles. Biology (Basel). 2017;6(1):15.

19. Mitchison T, Evans L, Schulze E, Kirschner M. Sites of microtubule assembly and disassembly in the mitotic spindle. Cell. 1986 May 23;45(4):515–27.

20. Glotzer M. Anaphase B. Biology (Basel). 2016;5(4):51.

21. Vukušić K, Ponjavić I, Buđa R, Risteski P, Tolić IM. Microtubule-sliding modules based on kinesins EG5 and PRC1-dependent KIF4A drive human spindle elongation. Dev Cell. 2021 May 3;56(9):1253-1267.e10.

22. Glotzer M. Cleavage furrow positioning. Journal of Cell Biology. 2004;164(3):347–51.

23. Lüders J, Stearns T. Microtubule-organizing centres: a re-evaluation. Nat Rev Mol Cell Biol. 2007 Feb;8(2):161–7.

24. Fu J, Hagan IM, Glover DM. The Centrosome and Its Duplication Cycle. Cold Spring Harb Perspect Biol. 2015 Jan 2;7(2):a015800.

25. Akhmanova A, Steinmetz MO. Tracking the ends: a dynamic protein network controls the fate of microtubule tips. Nat Rev Mol Cell Biol. 2008 Apr;9(4):309–22.

26. Mitchison T, Kirschner M. Dynamic instability of microtubule growth. Nature. 1984 Nov;312(5991):237–42.

27. Howard J, Hyman AA. Growth, fluctuation and switching at microtubule plus ends. Nat Rev Mol Cell Biol. 2009 Aug;10(8):569–74.

28. Mastronarde DN, McDonald KL, Ding R, McIntosh JR. Interpolar spindle microtubules in PTK cells. J Cell Biol. 1993 Dec 15;123(6):1475–89.

29. Petry S. Mechanisms of Mitotic Spindle Assembly. Annu Rev Biochem. 2016 Jun 2;85(Volume 85, 2016):659–83.

30. Tolić IM. Mitotic spindle: kinetochore fibers hold on tight to interpolar bundles. Eur Biophys J. 2018 Apr 1;47(3):191–203.

31. McIntosh JR, Grishchuk EL, West RR. Chromosome-Microtubule Interactions During Mitosis. Annu Rev Cell Dev Biol. 2002 Nov 1;18(Volume 18, 2002):193–219.

32. Dumont S; Salmon ED; Mitchison TJ. Deformations within moving kinetochores reveal different sites of active and passive force generation. Science. 2012;337(6092):355–8.

33. McIntosh JR; Cande WZ; Snyder JA. Ultrastructural analysis of mitotic spindle elongation in mammalian cells in vitro. Journal of Cell Biology. 1971;50(2):416–31.

34. Prosser SL, Pelletier L. Mitotic spindle assembly in animal cells: a fine balancing act. Nat Rev Mol Cell Biol. 2017 Mar;18(3):187–201.

35. Kajtez J; Solomatina A; Novak M; Polak B; Vukušić K; Rüdiger J; et al. Overlap microtubules link sister k-fibres and balance the forces on bi-oriented kinetochores. Nature Communications. 2016;7:10298.

36. Polak B, Risteski P, Lesjak S, Tolić IM. PRC1-labeled microtubule bundles and kinetochore pairs show one-to-one association in metaphase. EMBO Rep. 2017 Feb;18(2):217–30.

37. Tolić IM, and Pavin N. Bridging the gap between sister kinetochores. Cell Cycle. 2016 May 2;15(9):1169–70.

38. Vukušić K, Buđa R, Bosilj A, Milas A, Pavin N, Tolić IM. Microtubule Sliding within the Bridging Fiber Pushes Kinetochore Fibers Apart to Segregate Chromosomes. Dev Cell. 2017 Oct 9;43(1):11-23.e6.

39. McIntosh JR, Landis SC. The distribution of spindle microtubules during mitosis in cultured human cells. J Cell Biol. 1971 May 1;49(2):468–97.

40. Urbani L, Stearns T. The centrosome. Curr Biol. 1999 May 6;9(9):R315–7.

41. Nicklas RB; Staehling-Hampton K. Properties of the kinetochore in vitro. I. Microtubule nucleation and tubulin binding. Journal of Cell Biology. 1985;101(3):755–65.

42. Rieder CL, Alexander SP. Kinetochores are transported poleward along a single astral microtubule during chromosome attachment to the spindle in newt lung cells. J Cell Biol. 1990 Jan 1;110(1):81–95.

43. Wollman R, Cytrynbaum EN, Jones JT, Meyer T, Scholey JM, Mogilner A. Efficient chromosome capture requires a bias in the ‘search-and-capture’ process during mitotic-spindle assembly. Curr Biol CB. 2005 May 10;15(9):828–32.

44. O’Connell CB, Loncarek J, Kaláb P, Khodjakov A. Relative contributions of chromatin and kinetochores to mitotic spindle assembly. J Cell Biol. 2009 Oct 5;187(1):43–51.

45. Sikirzhytski V, Renda F, Tikhonenko I, Magidson V, McEwen BF, Khodjakov A. Microtubules assemble near most kinetochores during early prometaphase in human cells. J Cell Biol. 2018 Jun 15;217(8):2647–59.

46. Renda F, Miles C, Tikhonenko I, Fisher R, Carlini L, Kapoor TM, et al. Non-centrosomal microtubules at kinetochores promote rapid chromosome biorientation during mitosis in human cells. Curr Biol CB. 2022 Mar 14;32(5):1049-1063.e4.

47. Sawin KE, LeGuellec K, Philippe M, Mitchison TJ. Mitotic spindle organization by a plus-end-directed microtubule motor. Nature. 1992 Oct;359(6395):540–3.

48. Kapitein LC, Peterman EJG, Kwok BH, Kim JH, Kapoor TM, Schmidt CF. The bipolar mitotic kinesin Eg5 moves on both microtubules that it crosslinks. Nature. 2005 May;435(7038):114–8.

49. Kapoor TM; Mayer TU; Coughlin ML; Mitchison TJ. Probing spindle assembly mechanisms with monastrol, a small molecule inhibitor of the mitotic kinesin, Eg5. Journal of Cell Biology Year: 2000. 2000;150(5):975–88.

50. Blangy A; Lane HA; d'Hérin P; Harper M; Kress M; Nigg EA. Phosphorylation by p34^cdc2^ regulates spindle association of human Eg5, a kinesin-related motor essential for bipolar spindle formation in vivo. Journal of Cell Biology. 1995;129(4):957–68.

51. Milas A, Tolić IM. Relaxation of interkinetochore tension after severing of a k-fiber depends on the length of the k-fiber stub. 2016 [cited 2025 May 28]; Available from: https://sciencematters.io/articles/201603000025

52. Elting MW; Hueschen CL; Udy DB; Dumont S. Mapping Load-Bearing in the Mammalian Spindle Reveals Local Kinetochore Fiber Anchorage that Provides Mechanical Isolation and Redundancy. Current Biology. 2017;27(14):2112-22.e5.

53. Suresh P, Long AF, Dumont S. Microneedle manipulation of the mammalian spindle reveals specialized, short-lived reinforcement near chromosomes. Akhmanova A, Surrey T, Redemann S, Shimamoto Y, editors. eLife. 2020 Mar 19;9:e53807.

54. Jagrić M, Risteski P, Martinčić J, Milas A, Tolić IM. Optogenetic control of PRC1 reveals its role in chromosome alignment on the spindle by overlap length-dependent forces. Akhmanova A, Welburn JP, editors. eLife. 2021 Jan 22;10:e61170.

55. Steblyanko M; Paul R; Magidson V; Khodjakov A. Length-dependent poleward flux of sister kinetochore fibers promotes chromosome alignment: Cell Reports. 2022;40(7):111235.

56. Brust-Mascher I; Scholey JM. Model for anaphase B: Role of three mitotic motors in a switch from poleward flux to spindle elongation. Proc Natl Acad Sci U S A. 2005;102(39):13903–8.

57. Brust-Mascher I, Sommi P, Cheerambathur DK, Scholey JM. Kinesin-5–dependent Poleward Flux and Spindle Length Control in Drosophila Embryo Mitosis. Mol Biol Cell. 2009 Mar 15;20(6):1749–62.

58. Yu CH, Redemann S, Wu HY, Kiewisz R, Yoo TY, Conway W, et al. Central-spindle microtubules are strongly coupled to chromosomes during both anaphase A and anaphase B. Mol Biol Cell. 2019 Sep;30(19):2503–14.

59. Asthana J, Cade NI, Normanno D, Lim WM, Surrey T. Gradual compaction of the central spindle decreases its dynamicity in PRC1 and EB1 gene-edited cells. Life Sci Alliance [Internet]. 2021 Dec 1 [cited 2025 May 28];4(12). Available from: https://www.life-science-alliance.org/content/4/12/e202101222

60. Janson ME; Loughlin R; Loiodice I; Fu C; Brunner D; Nédélec FJ; Tran PT. Crosslinkers and motors organize dynamic microtubules to form stable bipolar arrays in fission yeast. Cell. 2007;128(2):357–68.

61. Kapitein LC, Janson ME, Wildenberg SMJL van den, Hoogenraad CC, Schmidt CF, Peterman EJG. Microtubule-Driven Multimerization Recruits ase1p onto Overlapping Microtubules. Curr Biol. 2008 Nov 11;18(21):1713–7.

62. Subramanian R, Wilson-Kubalek EM, Arthur CP, Bick MJ, Campbell EA, Darst SA, et al. Insights into Antiparallel Microtubule Crosslinking by PRC1, a Conserved Nonmotor Microtubule Binding Protein. Cell. 2010 Aug;142(3):433–43.

63. Bieling P, Telley IA, Surrey T. A Minimal Midzone Protein Module Controls Formation and Length of Antiparallel Microtubule Overlaps. Cell. 2010 Aug 6;142(3):420–32.

64. Kellogg EH, Howes S, Ti SC, Ramírez-Aportela E, Kapoor TM, Chacón P, et al. Near-atomic cryo-EM structure of PRC1 bound to the microtubule. Proc Natl Acad Sci. 2016 Aug 23;113(34):9430–9.

65. Fededa JP, Gerlich DW. Molecular control of animal cell cytokinesis. Nat Cell Biol. 2012 May;14(5):440–7.

66. Subramanian R, Ti SC, Tan L, Darst SA, Kapoor TM. Marking and Measuring Single Microtubules by PRC1 and Kinesin-4. Cell. 2013 Jul 18;154(2):377–90.

67. Zhu C; Lau E; Schwarzenbacher R; Bossy-Wetzel E; Jiang W. Spatiotemporal control of spindle midzone formation by PRC1 in human cells. Proc Natl Acad Sci U S A. 2006;103(16):6196–201.

68. Kurasawa Y, Earnshaw WC, Mochizuki Y, Dohmae N, Todokoro K. Essential roles of KIF4 and its binding partner PRC1 in organized central spindle midzone formation. EMBO J. 2004 Aug 18;23(16):3237–48.

69. Fu C, Yan F, Wu F, Wu Q, Whittaker J, Hu H, et al. Mitotic phosphorylation of PRC1 at Thr470 is required for PRC1 oligomerization and proper central spindle organization. Cell Res. 2007 May;17(5):449–57.

70. Jiang W; Jimenez G; Wells NJ; Hope TJ; Wahl GM; Hunter T; Fukunaga R. PRC1: a human mitotic spindle-associated CDK substrate protein required for cytokinesis. Molecular Cell. 1998;2(6):877–85.

71. Matković J, Ghosh S, Ćosić M, Eibes S, Barišić M, Pavin N, et al. Kinetochore- and chromosome-driven transition of microtubules into bundles promotes spindle assembly. Nat Commun. 2022 Nov 27;13(1):7307.

72. Cheeseman IM, Desai A. Molecular architecture of the kinetochore–microtubule interface. Nat Rev Mol Cell Biol. 2008 Jan;9(1):33–46.

73. Cojoc G, Florescu AM, Krull A, Klemm AH, Pavin N, Jülicher F, et al. Paired arrangement of kinetochores together with microtubule pivoting and dynamics drive kinetochore capture in meiosis I. Sci Rep. 2016 May 11;6(1):25736.

74. Tachiwana H; Kagawa W; Shiga T; Osakabe A; Miya Y; Saito K; et al. Crystal structure of the human centromeric nucleosome containing CENP-A. Nature. 2011;476(7359):232–5.

75. Tachiwana H, Kagawa ,Wataru, and Kurumizaka H. Comparison between the CENP-A and histone H3 structures in nucleosomes. Nucleus. 2012 Jan 1;3(1):6–11.

76. Brinkley BR, Stubblefield E. The fine structure of the kinetochore of a mammalian cell in vitro. Chromosoma. 1966 Mar 1;19(1):28–43.

77. Lampson M, Grishchuk E. Mechanisms to Avoid and Correct Erroneous Kinetochore-Microtubule Attachments. Biology. 2017 Jan 5;6(1):1.

78. Hinshaw SM, Harrison SC. Kinetochore Function from the Bottom Up. Trends Cell Biol. 2018 Jan 1;28(1):22–33.

79. Itoh G, Ikeda M, Iemura K, Amin MA, Kuriyama S, Tanaka M, et al. Lateral attachment of kinetochores to microtubules is enriched in prometaphase rosette and facilitates chromosome alignment and bi-orientation establishment. Sci Rep. 2018 Mar 1;8(1):3888.

80. Magidson V, O'Connell CB, Lončarek J, Paul R, Mogilner A, Khodjakov A. The Spatial Arrangement of Chromosomes during Prometaphase Facilitates Spindle Assembly. Cell. 2011 Aug;146(4):555–67.

81. Telzer BR, Moses MJ, Rosenbaum JL. Assembly of microtubules onto kinetochores of isolated mitotic chromosomes of HeLa cells. Proc Natl Acad Sci. 1975 Oct;72(10):4023–7.

82. Witt PL, Ris H, Borisy GG. Origin of kinetochore microtubules in Chinese hamster ovary cells. Chromosoma. 1980 Dec 1;81(3):483–505.

83. De Brabander M, Geuens G, Mey JD, Joniau M. Nucleated assembly of mitotic microtubules in living PTK2 cells after release from nocodazole treatment. Cell Motil. 1981;1(4):469–83.

84. Maiato H, Rieder CL, Khodjakov A. Kinetochore-driven formation of kinetochore fibers contributes to spindle assembly during animal mitosis. J Cell Biol. 2004 Nov 29;167(5):831–40.

85. Tulu US, Fagerstrom C, Ferenz NP, Wadsworth P. Molecular Requirements for Kinetochore-Associated Microtubule Formation in Mammalian Cells. Curr Biol. 2006 Mar 7;16(5):536–41.

86. Pavin N, Tolić-Nørrelykke IM. Swinging a sword: how microtubules search for their targets. Syst Synth Biol. 2014 Sep;8(3):179–86.

87. Kalinina I, Nandi A, Delivani P, Chacón MR, Klemm AH, Ramunno-Johnson D, et al. Pivoting of microtubules around the spindle pole accelerates kinetochore capture. Nat Cell Biol. 2013 Jan;15(1):82–7.

88. Marques S, Fonseca J, Silva PMA, Bousbaa H. Targeting the spindle assembly checkpoint for breast cancer treatment. Curr Cancer Drug Targets. 2015;15(4):272–81.

89. Yu H. Cdc20: a WD40 activator for a cell cycle degradation machine. Mol Cell. 2007 Jul 6;27(1):3–16.

90. Weaver BAA, Cleveland DW. Does aneuploidy cause cancer? Curr Opin Cell Biol. 2006 Dec;18(6):658–67.

91. Bakhoum SF, Compton DA. Chromosomal instability and cancer: a complex relationship with therapeutic potential. J Clin Invest. 2012 Apr;122(4):1138–43.

92. Nicholson JM, Cimini D. Link between aneuploidy and chromosome instability. Int Rev Cell Mol Biol. 2015;315:299–317.

93. Silk AD, Zasadil LM, Holland AJ, Vitre B, Cleveland DW, Weaver BA. Chromosome missegregation rate predicts whether aneuploidy will promote or suppress tumors. Proc Natl Acad Sci U S A. 2013 Oct 29;110(44):E4134-4141.

94. Walczak CE, Cai S, Khodjakov A. Mechanisms of chromosome behaviour during mitosis. Nat Rev Mol Cell Biol. 2010 Jan 13;11(2):91.

95. Nicklas RB. How cells get the right chromosomes. Science. 1997 Jan 31;275(5300):632–7.

96. Zaytsev AV, Grishchuk EL. Basic mechanism for biorientation of mitotic chromosomes is provided by the kinetochore geometry and indiscriminate turnover of kinetochore microtubules. Mol Biol Cell. 2015 Nov 5;26(22):3985.

97. Trivedi P, Zaytsev AV, Godzi M, Ataullakhanov FI, Grishchuk EL, Stukenberg PT. The binding of Borealin to microtubules underlies a tension independent kinetochore-microtubule error correction pathway. Nat Commun. 2019 Feb 8;10(1):682.

98. Wendell KL, Wilson L, Jordan MA. Mitotic block in HeLa cells by vinblastine: ultrastructural changes in kinetochore-microtubule attachment and in centrosomes. J Cell Sci. 1993 Feb;104 (Pt 2):261–74.

99. McEwen BF, Chan GK, Zubrowski B, Savoian MS, Sauer MT, Yen TJ. CENP-E is essential for reliable bioriented spindle attachment, but chromosome alignment can be achieved via redundant mechanisms in mammalian cells. Mol Biol Cell. 2001 Sep;12(9):2776–89.

100. Skibbens RV, Salmon ED. Micromanipulation of chromosomes in mitotic vertebrate tissue cells: tension controls the state of kinetochore movement. Exp Cell Res. 1997 Sep 15;235(2):314–24.

101. Cane S, Ye AA, Luks-Morgan SJ, Maresca TJ. Elevated polar ejection forces stabilize kinetochore-microtubule attachments. J Cell Biol. 2013 Jan 21;200(2):203–18.

102. Nicklas RB, Koch CA. Chromosome micromanipulation. 3. Spindle fiber tension and the reorientation of mal-oriented chromosomes. J Cell Biol. 1969 Oct;43(1):40–50.

103. Thompson SL, Compton DA. Examining the link between chromosomal instability and aneuploidy in human cells. J Cell Biol. 2008 Feb 25;180(4):665–72.

104. Cimini D. Merotelic kinetochore orientation, aneuploidy, and cancer. Biochim Biophys Acta. 2008 Sep;1786(1):32–40.

105. Cimini D, Fioravanti D, Salmon ED, Degrassi F. Merotelic kinetochore orientation versus chromosome mono-orientation in the origin of lagging chromosomes in human primary cells. J Cell Sci. 2002 Feb 1;115(Pt 3):507–15.

106. Bakhoum SF, Compton DA. Kinetochores and disease: keeping microtubule dynamics in check! Curr Opin Cell Biol. 2011 Dec 21;24(1):64.

107. Cimini D, Howell B, Maddox P, Khodjakov A, Degrassi F, Salmon ED. Merotelic Kinetochore Orientation Is a Major Mechanism of Aneuploidy in Mitotic Mammalian Tissue Cells. J Cell Biol. 2001 Apr 30;153(3):517.

108. Bakhoum SF, Genovese G, Compton DA. Deviant kinetochore microtubule dynamics underlie chromosomal instability. Curr Biol CB. 2009 Dec 1;19(22):1937–42.

109. Bakhoum SF, Silkworth WT, Nardi IK, Nicholson JM, Compton DA, Cimini D. The mitotic origin of chromosomal instability. Curr Biol CB. 2014 Feb 17;24(4):R148.

110. Cheeseman IM, Anderson S, Jwa M, Green EM, Kang J seog, Yates JR, et al. Phospho-regulation of kinetochore-microtubule attachments by the Aurora kinase Ipl1p. Cell. 2002 Oct 18;111(2):163–72.

111. Tanaka TU, Rachidi N, Janke C, Pereira G, Galova M, Schiebel E, et al. Evidence that the Ipl1-Sli15 (Aurora kinase-INCENP) complex promotes chromosome bi-orientation by altering kinetochore-spindle pole connections. Cell. 2002 Feb 8;108(3):317–29.

112. Hauf S, Cole RW, LaTerra S, Zimmer C, Schnapp G, Walter R, et al. The small molecule Hesperadin reveals a role for Aurora B in correcting kinetochore-microtubule attachment and in maintaining the spindle assembly checkpoint. J Cell Biol. 2003 Apr 28;161(2):281–94.

113. Ditchfield C, Johnson VL, Tighe A, Ellston R, Haworth C, Johnson T, et al. Aurora B couples chromosome alignment with anaphase by targeting BubR1, Mad2, and Cenp-E to kinetochores. J Cell Biol. 2003 Apr 28;161(2):267–80.

114. Musacchio A; Salmon ED. Correcting improper chromosome–spindle attachments during cell division. Nature Cell Biology. 2002;4(1):E191-8.

115. Kallio MJ, McCleland ML, Stukenberg PT, Gorbsky GJ. Inhibition of aurora B kinase blocks chromosome segregation, overrides the spindle checkpoint, and perturbs microtubule dynamics in mitosis. Curr Biol CB. 2002 Jun 4;12(11):900–5.

116. Liu D, Vader G, Vromans MJM, Lampson MA, Lens SMA. Sensing chromosome bi-orientation by spatial separation of aurora B kinase from kinetochore substrates. Science. 2009 Mar 6;323(5919):1350–3.

117. Salimian KJ, Ballister ER, Smoak EM, Wood S, Panchenko T, Lampson MA, et al. Feedback control in sensing chromosome biorientation by the Aurora B kinase. Curr Biol CB. 2011 Jul 12;21(13):1158–65.

118. Suzuki A, Badger BL, Wan X, DeLuca JG, Salmon ED. The Architecture of CCAN Proteins Creates a Structural Integrity to Resist Spindle Forces and Achieve Proper Intrakinetochore Stretch. Dev Cell. 2014 Sep 29;30(6):717.

119. Krenn V, Musacchio A. The Aurora B Kinase in Chromosome Bi-Orientation and Spindle Checkpoint Signaling. Front Oncol. 2015;5:225.

120. Sarangapani KK, Asbury CL. Catch and release: How do kinetochores hook the right microtubules during mitosis? Trends Genet TIG. 2014 Mar 13;30(4):150.

121. Welburn JPI, Vleugel M, Liu D, John R Yates III, Lampson MA, Fukagawa T, et al. Aurora B phosphorylates spatially distinct targets to differentially regulate the kinetochore-microtubule interface. Mol Cell. 2010 May 14;38(3):383.

122. Cheeseman IM, Chappie JS, Wilson-Kubalek EM, Desai A. The conserved KMN network constitutes the core microtubule-binding site of the kinetochore. Cell. 2006 Dec 1;127(5):983–97.

123. Tien JF; Umbreit NT; Gestaut DR; Franck AD; Cooper J; Wordeman L; et al. Phosphoregulation and depolymerization-driven movement of the Dam1 complex do not require ring formation. Nature Cell Biology. 2007;9(5):451.

124. Zaytsev AV; Sundin LJ; DeLuca KF; Grishchuk EL; DeLuca JG. Phosphoregulation promotes release of kinetochores from dynamic microtubules via multiple mechanisms. Proc Natl Acad Sci U S A. 2013;110(23):7282–7.

125. Zaytsev AV; DeLuca KF; Grishchuk EL; DeLuca JG. The Ndc80 kinetochore complex directly modulates microtubule dynamics. Proc Natl Acad Sci U S A. 2013;110(23):E4590-9.

126. Grishchuk EL, Molodtsov MI, Ataullakhanov FI, McIntosh JR. Force production by disassembling microtubules. Nature. 2005 Nov 17;438(7066):384–8.

127. Franck AD, Powers AF, Gestaut DR, Gonen T, Davis TN, Asbury CL. Tension applied through the Dam1 complex promotes microtubule elongation: a direct mechanism for length control in mitosis. Nat Cell Biol. 2007 Jun 17;9(7):832.

128. Akiyoshi B, Sarangapani KK, Powers AF, Nelson CR, Reichow SL, Arellano-Santoyo H, et al. Tension directly stabilizes reconstituted kinetochore-microtubule attachments. Nature. 2010 Nov;468(7323):576–9.

129. Cimini D, Moree B, Canman JC, Salmon ED. Merotelic kinetochore orientation occurs frequently during early mitosis in mammalian tissue cells and error correction is achieved by two different mechanisms. J Cell Sci. 2003 Oct 15;116(Pt 20):4213–25.

130. Brinkley BR; Cartwright J Jr. Kinetochore ultrastructure in vincristine-treated mammalian cells. Journal of Cell Science. 1970;7(1):49–64.

131. La Cour L. The mechanism of coordination in bivalents and multivalents: the theory of orientation by pulling. Genetics. 1929;14:1–34.

132. Nicklas RB, Ward SC. Elements of error correction in mitosis: microtubule capture, release, and tension. J Cell Biol. 1994 Sep;126(5):1241–53.

133. Skibbens RV; Skeen VP; Salmon ED. The centromere geometry essential for keeping mitosis error free is controlled by spindle forces. Nature. 2007;450(7172):489–94.

134. Holy TE, Leibler S. Dynamic instability of microtubules as an efficient way to search in space. Proc Natl Acad Sci U S A. 1994 Jun 7;91(12):5682.

135. Hoffman DB, Pearson CG, Yen TJ, Howell BJ, Salmon ED. Microtubule-dependent Changes in Assembly of Microtubule Motor Proteins and Mitotic Spindle Checkpoint Proteins at PtK1 Kinetochores. Mol Biol Cell. 2001 Jul;12(7):1995.

136. Magidson V; O'Connell CB; Lončarek J; Paul R; Mogilner A; Khodjakov A. Adaptive changes in the kinetochore architecture facilitate proper spindle assembly. Nature Cell Biology. 2014;16(11):1247–54.

137. Wynne DJ, Funabiki H. Kinetochore function is controlled by a phospho-dependent coexpansion of inner and outer components. J Cell Biol. 2015 Sep 14;210(6):899–916.

138. Cimini D, Wan X, Hirel CB, Salmon ED. Aurora kinase promotes turnover of kinetochore microtubules to reduce chromosome segregation errors. Curr Biol CB. 2006 Sep 5;16(17):1711–8.

139. Kabeche L, Compton DA. Cyclin A regulates kinetochore microtubules to promote faithful chromosome segregation. Nature. 2013 Oct 3;502(7469):110–3.

140. Zhai Y, Kronebusch PJ, Borisy GG. Kinetochore microtubule dynamics and the metaphase-anaphase transition. J Cell Biol. 1995 Nov;131(3):721–34.

141. Biggins S, Severin FF, Bhalla N, Sassoon I, Hyman AA, Murray AW. The conserved protein kinase Ipl1 regulates microtubule binding to kinetochores in budding yeast. Genes Dev. 1999 Mar 1;13(5):532–44.

142. Chan CS, Botstein D. Isolation and characterization of chromosome-gain and increase-in-ploidy mutants in yeast. Genetics. 1993 Nov;135(3):677–91.

143. Pearson CG; Rieder CL; Tulu US; Salmon ED. Ipl1-dependent phosphorylation of Dam1 is reduced by tension applied on kinetochores. J Cell Sci. 2009;122(Pt 23):4247–55.

144. DeLuca KF, Lens SMA, DeLuca JG. Temporal changes in Hec1 phosphorylation control kinetochore-microtubule attachment stability during mitosis. J Cell Sci. 2011 Feb 15;124(Pt 4):622–34.

145. Kawashima SA, Yamagishi Y, Honda T, Ishiguro K ichiro, Watanabe Y. Phosphorylation of H2A by Bub1 prevents chromosomal instability through localizing shugoshin. Science. 2010 Jan 8;327(5962):172–7.

146. Kelly AE; Ghenoiu C; Xie JZ; Zierhut C; Kimura H; Funabiki H. Survivin reads phosphorylated histone H3 threonine 3 to activate the mitotic kinase Aurora B. Science. 2010;330(6001):235–9.

147. Wang F; Ulyanova NP; van der Waal MS; Patnaik D; Lens SM; Higgins JMG; et al. Histone H3 Thr-3 phosphorylation by Haspin positions Aurora B at centromeres in mitosis. Science. 2010;330(6001):231–5.

148. Yamagishi Y; Honda T; Tanno Y; Watanabe Y. Two histone marks establish the inner centromere and chromosome bi-orientation. Science. 2010;330(6001):239–43.

149. Wang F, Ulyanova NP, Daum JR, Patnaik D, Kateneva AV, Gorbsky GJ, et al. Haspin inhibitors reveal centromeric functions of Aurora B in chromosome segregation. J Cell Biol. 2012 Oct 15;199(2):251.

150. Yamashita Z; Cochran A; Xu Z; Yang X; Chen S; Ruchaud S; et al. Deconstructing Survivin: comprehensive genetic analysis of Survivin function by conditional knockout in a vertebrate cell line. The Journal of cell biology. 2008;183(2):279–96.

151. Hengeveld RC; Krenn V; van der Horst A; Lens SM; Musacchio A. Phosphorylation of the CPC by Cdk1 promotes chromosome bi-orientation. Science. 2010;330(6001):789–93.

152. Cimini D; Cameron LA; Salmon ED. Anaphase spindle mechanics prevent mis-segregation of merotelically oriented chromosomes. Current Biology. 2004;14(23):2149–55.

153. Gregan J, Polakova S, Zhang L, Tolić-Nørrelykke IM, Cimini D. Merotelic kinetochore attachment: causes and effects. Trends Cell Biol. 2011 Jun;21(6):374.

154. Kalantzaki M, Kitamura E, Zhang T, Mino A, Novák B, Tanaka TU. Kinetochore-microtubule error correction is driven by differentially regulated interaction modes. Nat Cell Biol. 2015 Apr;17(4):421–33.

155. Pearson CG, Yeh E, Gardner M, Odde D, Salmon ED, Bloom K. Stable kinetochore-microtubule attachment constrains centromere positioning in metaphase. Curr Biol CB. 2004 Nov 9;14(21):1962–7.

156. McIntosh JR, Hering GE. Spindle fiber action and chromosome movement. Annu Rev Cell Biol. 1991;7:403–26.

157. Kline-Smith SL, Khodjakov A, Hergert P, Walczak CE. Depletion of centromeric MCAK leads to chromosome congression and segregation defects due to improper kinetochore attachments. Mol Biol Cell. 2004 Mar;15(3):1146–59.

158. Campbell CS; Desai A. Tension sensing by Aurora B kinase is independent of survivin-based centromere localization. Nature. 2013;497(7447):118–21.

159. Samejima K, Platani M, Wolny M, Ogawa H, Vargiu G, Knight PJ, et al. The Inner Centromere Protein (INCENP) Coil Is a Single α-Helix (SAH) Domain That Binds Directly to Microtubules and Is Important for Chromosome Passenger Complex (CPC) Localization and Function in Mitosis. J Biol Chem. 2015 Jul 14;290(35):21460.

160. Uchida KSK, Takagaki K, Kumada K, Hirayama Y, Noda T, Hirota T. Kinetochore stretching inactivates the spindle assembly checkpoint. J Cell Biol. 2009 Feb 9;184(3):383–90.

161. Liu ST; Rattner JB; Jablonski SA; Yen TJ. Centromere tension: a divisive issue. Nature Cell Biology. 2010;12(8):919–23.

162. Lampson MA; Grishchuk EL. Regulation of kinetochore–microtubule attachments through homeostatic control during mitosis. Nature Reviews Molecular Cell Biology. 2017;18(2):89–102.

163. Trivedi P, Stukenberg PT. A Centromere-Signaling Network Underlies the Coordination among Mitotic Events. Trends Biochem Sci. 2016 Feb;41(2):160–74.

164. Liu ML; Zhang CZ; Pellman D. Chromothripsis: A New Mechanism for Rapid Karyotype Evolution. Annual Review of Genetics. 2015;49:183–211.

165. Hinchcliffe EH, Day CA, Karanjeet KB, Fadness S, Langfald A, Vaughan KT, et al. Chromosome missegregation during anaphase triggers p53 cell cycle arrest through histone H3.3 Ser31 phosphorylation. Nat Cell Biol. 2016 Jun;18(6):668–75.

166. Boyarchuk Y, Salic A, Dasso M, Arnaoutov A. Bub1 is essential for assembly of the functional inner centromere. J Cell Biol. 2007 Mar 26;176(7):919–28.

167. Ricke RM; Jeganathan KB; Malureanu L; Hwang A; van Deursen JM. Bub1 kinase activity drives error correction and mitotic checkpoint control but not tumor suppression. The Journal of cell biology. 2012;199(6):931–49.

168. Glover DM, Leibowitz MH, McLean DA, Parry H. Mutations in aurora prevent centrosome separation leading to the formation of monopolar spindles. Cell. 1995 Apr 7;81(1):95–105.

169. Carmena M, Ruchaud S, Earnshaw WC. Making the Auroras glow: regulation of Aurora A and B kinase function by interacting proteins. Curr Opin Cell Biol. 2009 Dec;21(6):796–805.

170. Lens SMA, Voest EE, Medema RH. Shared and separate functions of polo-like kinases and aurora kinases in cancer. Nat Rev Cancer. 2010 Dec;10(12):825–41.

171. Knowlton AL, Lan W, Stukenberg PT. Aurora B Is Enriched at Merotelic Attachment Sites, Where It Regulates MCAK. Curr Biol. 2006 Sep 5;16(17):1705–10.

172. Lan W, Zhang X, Kline-Smith SL, Rosasco SE, Barrett-Wilt GA, Shabanowitz J, et al. Aurora B phosphorylates centromeric MCAK and regulates its localization and microtubule depolymerization activity. Curr Biol CB. 2004 Feb 17;14(4):273–86.

173. Tanno Y, Kitajima TS, Honda T, Ando Y, Ishiguro KI, Watanabe Y. Phosphorylation of mammalian Sgo2 by Aurora B recruits PP2A and MCAK to centromeres. Genes Dev. 2010 Oct 1;24(19):2169–79.

174. Dai J, Sullivan BA, Higgins JMG. Regulation of mitotic chromosome cohesion by Haspin and Aurora B. Dev Cell. 2006 Nov;11(5):741–50.

175. Resnick TD, Satinover DL, MacIsaac F, Stukenberg PT, Earnshaw WC, Orr-Weaver TL, et al. INCENP and Aurora B promote meiotic sister chromatid cohesion through localization of the Shugoshin MEI-S332 in Drosophila. Dev Cell. 2006 Jul;11(1):57–68.

176. Santaguida S, Vernieri C, Villa F, Ciliberto A, Musacchio A. Evidence that Aurora B is implicated in spindle checkpoint signalling independently of error correction. EMBO J. 2011 Apr 20;30(8):1508–19.

177. Matson DR, Demirel PB, Stukenberg PT, Burke DJ. A conserved role for COMA/CENP-H/I/N kinetochore proteins in the spindle checkpoint. Genes Dev. 2012 Mar 15;26(6):542–7.

178. Biggins S; Severin F; Bhalla N; Sassoon I; Hyman A; Murray AW. The Ipl1-Aurora protein kinase activates the spindle checkpoint by creating unattached kinetochores. Nature Cell Biology. 2004;6(1):55–61.

179. Honda R, Körner R, Nigg EA. Exploring the functional interactions between Aurora B, INCENP, and survivin in mitosis. Mol Biol Cell. 2003 Aug;14(8):3325–41.

180. Bishop JD, Schumacher JM. Phosphorylation of the carboxyl terminus of inner centromere protein (INCENP) by the Aurora B Kinase stimulates Aurora B kinase activity. J Biol Chem. 2002 Aug 2;277(31):27577–80.

181. Carmena M, Wheelock M, Funabiki H, Earnshaw WC. The chromosomal passenger complex (CPC): from easy rider to the godfather of mitosis. Nat Rev Mol Cell Biol. 2012 Dec;13(12):789–803.

182. Sessa F, Mapelli M, Ciferri C, Tarricone C, Areces LB, Schneider TR, et al. Mechanism of Aurora B activation by INCENP and inhibition by hesperadin. Mol Cell. 2005 Apr 29;18(3):379–91.

183. Kelly AE, Sampath SC, Maniar TA, Woo EM, Chait BT, Funabiki H. Chromosomal enrichment and activation of the aurora B pathway are coupled to spatially regulate spindle assembly. Dev Cell. 2007 Jan;12(1):31–43.

184. Wang E, Ballister ER, Lampson MA. Aurora B dynamics at centromeres create a diffusion-based phosphorylation gradient. J Cell Biol. 2011 Aug 15;194(4):539–49.

185. Fuller BG, Lampson MA, Foley EA, Rosasco-Nitcher S, Le KV, Tobelmann P, et al. Midzone activation of aurora B in anaphase produces an intracellular phosphorylation gradient. Nature. 2008 Jun 19;453(7198):1132–6.

186. Rosasco-Nitcher SE, Lan W, Khorasanizadeh S, Stukenberg PT. Centromeric Aurora-B Activation Requires TD-60, Microtubules, and Substrate Priming Phosphorylation. Science. 2008 Jan 25;319(5862):469–72.

187. Tseng BS, Tan L, Kapoor TM, Funabiki H. Dual Detection of Chromosomes and Microtubules by the Chromosomal Passenger Complex Drives Spindle Assembly. Dev Cell. 2010 Jun 15;18(6):903.

188. Petsalaki E, Akoumianaki T, Black EJ, Gillespie DAF, Zachos G. Phosphorylation at serine 331 is required for Aurora B activation. J Cell Biol. 2011 Oct 31;195(3):449–66.

189. Maciejowski J; Hatch EM; Willems A; Gerlich DW; Cleveland DW. The chromosomal passenger complex activates Polo kinase at centromeres. PLoS Biology. 2013;11(1):e1001250.

190. Chu Y, Yao PY, Wang W, Wang D, Wang Z, Zhang L, et al. Aurora B kinase activation requires survivin priming phosphorylation by PLK1. J Mol Cell Biol. 2011 Aug;3(4):260–7.

191. Sumara I, Quadroni M, Frei C, Olma MH, Sumara G, Ricci R, et al. A Cul3-based E3 ligase removes Aurora B from mitotic chromosomes, regulating mitotic progression and completion of cytokinesis in human cells. Dev Cell. 2007 Jun;12(6):887–900.

192. Fernández-Miranda G, Pérez de Castro I, Carmena M, Aguirre-Portolés C, Ruchaud S, Fant X, et al. SUMOylation modulates the function of Aurora-B kinase. J Cell Sci. 2010 Aug 15;123(Pt 16):2823–33.

193. Ban R, Nishida T, Urano T. Mitotic kinase Aurora-B is regulated by SUMO-2/3 conjugation/deconjugation during mitosis. Genes Cells Devoted Mol Cell Mech. 2011 Jun;16(6):652–69.

194. Stewart S, Fang G. Destruction box-dependent degradation of aurora B is mediated by the anaphase-promoting complex/cyclosome and Cdh1. Cancer Res. 2005 Oct 1;65(19):8730–5.

195. Nguyen HG, Chinnappan D, Urano T, Ravid K. Mechanism of Aurora-B degradation and its dependency on intact KEN and A-boxes: identification of an aneuploidy-promoting property. Mol Cell Biol. 2005 Jun;25(12):4977–92.

196. Hein B, Willig KI, Hell SW. Stimulated emission depletion (STED) nanoscopy of a fluorescent protein-labeled organelle inside a living cell. Proc Natl Acad Sci U S A. 2008 Sep 16;105(38):14271.

197. Zeitlin SG; Shelby RD; Sullivan KF. CENP-A is phosphorylated by Aurora B kinase and plays an unexpected role in completion of cytokinesis. Journal of Cell Biology. 2001;155(7):1147–57.

198. Wheatley SP; Carvalho A; Vagnarelli P; Earnshaw WC. INCENP centromere and spindle targeting: identification of essential conserved motifs and involvement of heterochromatin protein HP1. Current Biology. 1999;(21):114–24.

199. Klein UR, Nigg EA, Gruneberg U. Centromere targeting of the chromosomal passenger complex requires a ternary subcomplex of Borealin, Survivin, and the N-terminal domain of INCENP. Mol Biol Cell. 2006 Jun;17(6):2547–58.

200. Nozawa RS, Nagao K, Masuda HT, Iwasaki O, Hirota T, Nozaki N, et al. Human POGZ modulates dissociation of HP1α from mitotic chromosome arms through Aurora B activation. Nat Cell Biol. 2010 Jul;12(7):719–27.

8. SUMMARY

Mitotic spindles are essential for accurate chromosome distribution between daughter cells. Spindle formation relies on microtubule bundles that extend from opposite poles and overlap in the middle. In metaphase, these bundles act as bridges between sister kinetochore fibers, maintaining tension, aligning chromosomes, facilitating spindle elongation, and supporting chromosome segregation in anaphase. The protein PRC1 links microtubules within these bridging fibers. Previous research has shown that during prometaphase, microtubules near centromeres trigger kinetochore phosphorylation, which is crucial for correcting improper attachments between kinetochores and microtubules. We proposed that overlap bundles are essential for this error correction mechanism and that Aurora B kinase, a catalytic component of the Chromosome Passenger Complex (CPC), utilizes these structures to reach and modify kinetochore substrates.

To test this hypothesis, we used confocal and super-resolution STED microscopy in combination with PRC1 depletion to investigate the spatial relationship between overlap bundles and CPC components. Our results revealed that both Aurora B and Borealin localize to PRC1-labeled overlap bundles during early mitosis, particularly in prometaphase when kinetochore-microtubule attachments are still forming. This colocalization was significantly reduced upon PRC1 depletion, leading to diminished CPC accumulation at the inner centromere, impaired phosphorylation of kinetochore substrates, delayed mitotic progression, increased chromosome misalignment, and a higher frequency of lagging chromosomes in anaphase.

These findings demonstrate that PRC1-crosslinked antiparallel microtubule bundles serve not only as structural elements of the spindle but also as spatial and functional scaffolds for CPC localization and activity. Overlap bundles promote accurate chromosome segregation by facilitating the recruitment and activation of Aurora B at sites where error correction is most needed. This work highlights a novel role for spindle architecture in the regulation of mitotic fidelity and suggests that disruption of this microtubule based spatial signaling could contribute to chromosomal instability in disease.

9. SAŽETAK

Diobena vretena ključna su za pravilnu raspodjelu kromosoma između sestrinskih stanica. Formiranje diobenog vretena ovisi o snopovima mikrotubula koji se protežu od suprotnih polova stanice i preklapaju u središnjem dijelu. U metafazi ti snopovi djeluju kao mostovi između sestrinskih kinetohornih vlakana, održavajući napetost, poravnavajući kromosome te omogućujući produljenje vretena i razdvajanje kromosoma tijekom anafaze. Protein PRC1 povezuje mikrotubule unutar tih preklapajućih snopova. Prethodna istraživanja pokazala su da mikrotubuli u blizini centromera tijekom prometafaze potiču fosforilaciju kinetohora, što omogućuje ispravljanje neispravnih vezanja mikrotubula za kinetohore. Glavna hipoteza ovog istraživanja predlaže da su preklapajući snopovi ključni za korekciju pogrešnih vezanja te da kinaza Aurora B, katalitička podjedinica kompleksa CPC-a, koristi te strukture za pristup i modifikaciju kinetohornih supstrata.

Kako bismo testirali ovu hipotezu, koristili smo konfokalnu i superrezolucijsku STED mikroskopiju u kombinaciji s utišavanjem PRC1 proteina za ispitivanje prostornog odnosa između preklapajućih snopova i komponenti CPC-a. Naši rezultati pokazali su da Aurora B i Borealin lokaliziraju s preklapajućim snopovima u ranoj mitozi, osobito tijekom prometafaze, kada se još formiraju kinetohorni snopovi. Ova kolokalizacija bila je značajno smanjena nakon utišavanja PRC1, što je dovelo do smanjenog nakupljanja CPC-a u unutarnjem centromernom području, smanjene fosforilacije kinetohornih supstrata, usporenog napredovanja mitoze, problema u kongresiji kromosoma prema metafaznoj ploči i veće učestalosti zaostalih kromosoma u anafazi.

Naši rezultati pokazuju da preklapajući snopovi mikrotubula ne djeluju samo kao strukturne komponente mitotskog vretena, već i kao prostorne i funkcionalne platforme koje omogućuju pravilnu lokalizaciju i aktivaciju CPC-a. Preklapajući snopovi doprinose točnom razdvajanju kromosoma tako što omogućuju usmjeravanje i djelovanje Aurora B kinaze na mjestima gdje je korekcija pogrešnih vezanja najpotrebnija. Ovo istraživanje otkriva novu ulogu arhitekture vretena u regulaciji mitotske točnosti i upućuje na to da bi narušavanje ovih mikrotubulskih signalnih struktura moglo pridonijeti kromosomskoj nestabilnosti kod bolesti poput raka.

10. AUTOHOR BIOGRAPHY

Mateja Ćosić was born on April 1st, 1993, in Zagreb, Croatia. She completed her elementary and high school education in Zaprešić. In 2012, she enrolled at the Faculty of Agriculture, University of Zagreb, where she graduated in 2019, majoring in Genetics and Animal Breeding. She completed her studies with highest honors (Summa Cum Laude). Her graduate thesis, titled "Evaluation of genetic correlation between binary and normal variables using the GLIMMIX SAS procedure," was successfully defended as part of her degree requirements.

During her studies, she completed a internship at the Ruđer Bošković Institute in the Laboratory of Molecular Genetics under the mentorship of dr. sc. Helena Ćetković. She also received the Dean's List academic award for maintaining a 5.0 GPA.

She continued her education at the Josip Juraj Strossmayer University in Osijek, enrolling in the Postgraduate University Interdisciplinary Doctoral Study of Molecular Biosciences. Since then, she has been working as a research assistant in the Laboratory of Cell Biophysics, Department of Molecular Biology, at the Ruđer Bošković Institute, Zagreb. Her initial mentor was dr. sc. Juraj Simunić, and after his departure she continued her work under the mentorship of dr. sc. Iva M. Tolić. She is the author of two papers and has participated in three conferences and one workshop. One of the papers she co-authored, "Kinetochore- and chromosome-driven transition of microtubules into bundles promotes spindle assembly", received the Ruđer Bošković Institute Award for Best Scientific Papers in 2022.

Publications:

Ćosić M, Petelinec A. The role of 3D cell cultures in understanding mitosis and tissue architecture. Periodicum biologorum. 2024;126(1-2):1-4. https://doi.org/10.18054/pb.v126i1-2.32856

Matković J, Ghosh S, **Ćosić M**, Eibes S, Barišić M, Pavin N, Tolić IM. Kinetochore-and chromosome-driven transition of microtubules into bundles promotes spindle assembly. Nature communications. 2022 Nov 27;13(1):7307. https://doi.org/10.1038/s41467-022-34957-4

Conferences and workshop:

1. **Ćosić M**, Simunić. "The role of small heat shock protein HSP27 in mitotic spindle assembly and architecture." Mitotic spindle: From living and synthetic systems to theory, 28-31 March 2021, Split, Croatia, poster presentatiton

2. **Ćosić M**, Matković J, Ghosh S, Eibes S, Barišić M, Pavin N, Tolić IM. Kinetochore-and chromosome-driven transition of microtubules into bundles promotes spindle assembly. EMBL Symposium: Microtubules: from atoms to complex systems. 08-11 June 2022, Heidelberg, Germany, poster presentatiton

3. **Ćosić M**, Matković J, Ghosh S, Eibes S, Barišić M, Pavin N, Tolić IM. Kinetochore-and chromosome-driven transition of microtubules into bundles promotes spindle

assembly. Mitotic spindle: From living and synthetic systems to theory, 16-19 April 2023, Dubrovnik, Croatia, poster presentation

4. **Ćosić M**, Matković J, Ghosh S, Eibes S, Barišić M, Pavin N, Tolić IM. Kinetochore- and chromosome-driven transition of microtubules into bundles promotes spindle assembly. Biophysics of Spindle Assembly Workshop, 10-11 October 2022, Zagreb, Croatia, oral presentation